

# **SOUTHAMPTON OCEANOGRAPHY CENTRE**

## **CRUISE REPORT No. 54**

### **RRS *DISCOVERY* CRUISE D279**

**04 APR – 10 MAY 2004**

A Transatlantic hydrography section at 24.5°N

*Principal Scientist*

**S A Cunningham**

**2005**

James Rennell Division for Ocean Circulation and Climate  
Southampton Oceanography Centre  
University of Southampton  
Waterfront Campus  
European Way  
Southampton  
Hants SO14 3ZH  
UK

Tel: +44 (0)23 8059 6436  
Fax: +44 (0)23 8059 6204  
Email: scu@soc.soton.ac.uk



# DOCUMENT DATA SHEET

<p><b>AUTHOR</b></p> <p>CUNNINGHAM, S A et al</p>	<p><b>PUBLICATION DATE</b></p> <p>2005</p>
<p><b>TITLE</b></p> <p>RRS <i>Discovery</i> Cruise D279, 04 Apr – 10 May 2004. A Transatlantic hydrographic section at 24.5°N.</p>	
<p><b>REFERENCE</b></p> <p>Southampton Oceanography Centre Cruise Report, No. 54, 198pp.</p>	
<p><b>ABSTRACT</b></p> <p>The cruise report describes the acquisition and processing of transatlantic hydrographic, velocity, chemistry and other measurements made during three cruises in Spring 2004 at 24.5°N. Measurements were made from shallow water near Africa to shallow water just off Palm Springs beach on the eastern seaboard of the USA. During the principal cruise, RRS <i>Discovery</i> Cruise D279 (4 April to 10 May 2004), 125 full depth CTD and lowered acoustic Doppler current profiler (LADP) stations were completed between the USA and Africa and continuous underway observations were made of currents in the upper 1000m using a ship mounted 75kHz ADP and of surface salinity and temperature. At each station up to 24 water samples were captured for the analysis of oxygen, salinity, nitrate, silicate, phosphate, CFC11, 12, 113 and CCl4 (carbon tetrachloride), discrete total inorganic carbon (TCO<sub>2</sub>), discrete total alkalinity (TA) and, discrete partial pressure of CO<sub>2</sub> (discrete pCO<sub>2</sub>). Direct, near real-time measurements were also made of the air-sea turbulent fluxes of momentum and sensible and latent heat in addition to various mean meteorological parameters including testing of a new Licor sensor to determine its suitability for making direct measurements of the air-sea CO<sub>2</sub> flux. Atmospheric dust samples were gathered on a daily basis. Two prior cruises D277 (26 February to 16 March) and D278 (19 to 30 March) completed 33 full depth CTD/LADP stations in the Florida and Deep Western Boundary Currents, including continuous underway observations of currents in the upper 1000m and of surface salinity and temperature. No LADP or chemistry measurements were made during these cruises. The three cruises provide one CTD and one CTD/LADP transect of the Florida Current, two Florida Current transects at 5knots with the shipboard ADP measuring to the bottom for high accuracy well resolved direct velocity measurements, one section of 16 CTD stations across the Deep Western Boundary Current and a 125 station transatlantic section with a full suite of physical and chemical measurements. The principal scientific objective is to estimate the circulation across 24.5°N, using for the first time, LADP profiles at each station as constraints in an inverse study. Using this circulation and the transatlantic distribution of temperature and other properties we will calculate Atlantic heat and property fluxes. We will also define the size and structure of the Atlantic Meridional Overturning Circulation (MOC) to compare to results from a recently deployed transatlantic mooring array designed to continuously measure the size and structure of the MOC. The 24.5°N section has now been occupied five times since 1957 (including the 2004 section reported here). Therefore, we will analyse temporal trends of temperature to see if the widely reported warming of the thermocline and intermediate waters and cooling of deep water is continuing. Carbon measurements were also obtained in 1992 and 1998 so this section provides a unique decadal view of anthropogenic carbon fluxes.</p>	
<p><b>KEYWORDS</b></p> <p>ADCP, Atlantic Ocean, atmospheric chemistry, carbon tetrachloride, carbon, CFC, circulation, cruise D277 2004, cruise D278 2004, cruise D279 2004, CTD, <i>Discovery</i>, Lowered ADCP, Meridional Overturning Circulation, meteorology, MOC, nutrients, Ocean Surveyor, oxygen, shipboard ADCP</p>	
<p><b>ISSUING ORGANISATION</b></p> <p>Southampton Oceanography Centre Empress Dock European Way Southampton SO14 3ZH UK</p>	
<p>Copies of this report are available from: Tel: +44(0)23 80596116</p>	<p>National Oceanographic Library, SOC PRICE: Email: nol@soc.soton.ac.uk</p>





<b>CONTENTS</b>	
<b>SCIENTIFIC PERSONNEL</b>	<b>7</b>
<b>SHIP'S PERSONNEL</b>	<b>11</b>
<b>ACRONYMS</b>	<b>12</b>
<b>ACKNOWLEDGEMENTS</b>	<b>13</b>
<b>1. INTRODUCTION</b>	<b>14</b>
<b>2. SCIENTIFIC BACKGROUND</b>	<b>16</b>
<b>3. OBJECTIVES</b>	<b>19</b>
<b>4. BASIC OBSERVATIONAL STRATEGY</b>	<b>20</b>
<b>5. ITINERARY</b>	<b>21</b>
<b>6. NARRATIVE</b>	<b>23</b>
<b>7. D279 BRIDGE TIMETABLE OF EVENTS</b>	<b>26</b>
<b>8. CTD OPERATIONS – D279</b>	<b>31</b>
<b>9. CTD DATA PROCESSING AND CALIBRATION</b>	<b>42</b>
<b>10. SBE35 DEEP OCEAN STANDARDS THERMOMETER</b>	<b>68</b>
<b>11. WATER SAMPLE SALINITY ANALYSIS</b>	<b>77</b>
<b>12. WINCHES</b>	<b>79</b>
<b>13. ADCP AND BATTERY PACK</b>	<b>82</b>
<b>14. LOWERED ACOUSTIC DOPPLER CURRENT PROFILER</b>	<b>83</b>

<b>15. LOWERED ACOUSTIC DOPPLER CURRENT PROFILER DATA PROCESSING SOFTWARE TEST SUITE</b>	<b>109</b>
<b>16. NAVIGATION AND SHIPBOARD ACOUSTIC DOPPLER CURRENT PROFILER</b>	<b>110</b>
<b>17. ASHTECH 3DF GPS ATTITUDE DETERMINATION</b>	<b>112</b>
<b>18. OCEAN SURVEYOR 75KHZ SHIPBOARD ACOUSTIC DOPPLER CURRENT PROFILER</b>	<b>114</b>
<b>19. 150KHZ SHIPBOARD ACOUSTIC DOPPLER CURRENT PROFILER</b>	<b>121</b>
<b>20. MEASUREMENT OF DISSOLVED OXYGEN</b>	<b>128</b>
<b>21. MEASUREMENT OF NUTRIENTS</b>	<b>131</b>
<b>22. AUTOFLUX – THE AUTONOMOUS AIR-SEA INTERACTION SYSTEM</b>	<b>138</b>
<b>23. SURFACE MET DATA</b>	<b>162</b>
<b>24. SALINITY CALIBRATION OF UNDERWAY DATA</b>	<b>164</b>
<b>25. BATHYMETRY</b>	<b>167</b>
<b>26. SHIPBOARD INSTRUMENTATION AND COMPUTING</b>	<b>170</b>
<b>27. CARBON</b>	<b>175</b>
<b>28. HALOCARBONS</b>	<b>186</b>
<b>29. ATMOSPHERIC SAMPLING</b>	<b>188</b>
<b>30. TRIAL FLOAT DEPLOYMENT</b>	<b>192</b>
<b>31. DISSOLVED OXYGEN MICROELECTRODE SENSOR</b>	<b>193</b>
<b>32. REFERENCES</b>	<b>196</b>

## SCIENTIFIC PERSONNEL

### D277, 26<sup>th</sup> Feb to 16<sup>th</sup> March 2004

Principally a moorings deployment cruise (Cunningham, 2005) but including a CTD/LADP and SADP section across the Florida Current at 27°N between 79° 12.23'W and 79° 51.89'W, and a SADP section across New Providence Channel to measure the transport of water flowing west into the Florida Current.

Table 1: D277 scientific and technical personnel.

Stuart Cunningham	PS (SOC)
Darren Rayner	Scientist (SOC)
Pedro Vélez Belchi	Scientist (IEO)
Stephen Whittle	OED
Ian Waddington	OED
John Wynar	OED
Robert McLachlan	OED
Elizabeth Rourke	OED
Christian Crow	OED
Peter Keen	OED

10 persons

## **D278, 19<sup>th</sup> March to 30<sup>th</sup> March 2004**

Principally a moorings deployment cruise (Cunningham, 2005) but including a CTD/LADP and SADP section along the Abaco Mooring Array at 26.5°N between 71° 58.12'W and 76° 53.67'W to measure properties and transport of the Deep Western Boundary Current.

Table 2: D278 scientific and technical personnel.

Stuart Cunningham	PS, SOC
Darren Rayner	SOC
Harry Bryden	SOC
Marc Lucas	SOC
Jochem Marotzke	MPI
Johanna Baehr	MPI
Clotilde Dubois	MPI
Fiona McLay	MPI
Bill Johns	UoM
Lisa Beal	UoM
Deb Shoosmith	UoM
Mark Graham	UoM
Robert Jones	UoM
Ian Waddington	OED
John Wynar	OED
Robert McLachlan	OED
Christian Crow	OED
Jeffrey Benson	OED
Jeffrey Bicknell	OED
Chris Hunter	OED

20 persons

**D279, 4<sup>th</sup> April to 12<sup>th</sup> May 2004**

Transatlantic hydrography.

Table 3: D279 scientific and technical personnel.

Stuart Cunningham	PS	SOC
Louise Duncan	PI LADP	SOC
Steve Alderson	PI SADP, Nav	SOC
Hannah Longworth	PI CTD, Salts, Samples	SOC
Rachel Hadfield	PI Underway obs	SOC
Amanda Simpson	PI Bathymetry	SOC
Margret Yelland	PI Autoflux	SOC
Robin Pascal	Autoflux	SOC
Richard Sanders	PI Nutrients, Oxygen	SOC
Abigail Pattenden	Oxygen	SOC
Angela Landolfi	Nutrients, Oxygen	SOC
Rhiannon Mather	Oxygen	SOC
Ute Schuster	PI Carbon	UEA
Gareth Lee	Carbon	UEA
Maria Nielsdottir	Carbon	UEA
David Cooper	PI CFC	UoM
Charlene Grail	CFC	UoM
David Teare	PI CTD technical	OED
Peter Keen	CTD	OED
Martin Bridger	TLO	OED
Richard Phipps	Mechanical	OED

21 persons

Table 4: D279 watches (watch leader in bold).

Physics

0800-1600	1600-2400	0000-0800
<b>Louise Duncan</b>	<b>Robin Pascal</b>	<b>Richard Sanders</b>
Hannah Longworth	Margret Yelland	Steven Alderson
	Rachel Hadfield	Amanda Simpson

CTD Technical

1200-1600	1600-0200	0200-1200
Martin Bridger	Peter Keen	<b>David Teare</b>

Oxygen and Nutrients

0800-1600	1600-2400	0000-0800
Angela Landolfi	Abigail Pattenden	<b>Richard Sanders</b>
		Rhiannon Mather

Carbon

0800-1600	1600-2400	0000-0800
Maria Nielsdottir	<b>Ute Schuster</b>	Gareth Lee

CFCs

1400-0200	0200-1400
David Cooper	<b>Charlene Grail</b>

## SHIP'S PERSONNEL

Table 5: Ship's personnel for D277, D278 and D279.

Rank	D277	D278	D279
Master	<i>Roger Chamberlain</i>	<i>Roger Chamberlain</i>	<i>Roger Chamberlain</i>
Chief Officer	Derek Noden	Richard Warner	Richard Warner
2 <sup>nd</sup> Officer	John Mitchell	Phil Oldfield	Phil Oldfield
3 <sup>rd</sup> Officer	Annalaara K-Willis	Darcy White	Darcy White
Chief Engineer	Sam Moss	Sam Moss	Bernard McDonald
1 <sup>st</sup> Engineer	Martin Holt	Stephen Bell	Stephen Bell
2 <sup>nd</sup> Engineer	Antony Healy	John Harnett	John Harnett
3 <sup>rd</sup> Engineer	Gary Slater	Chris Uttley	Chris Uttley
ETO	Dean Hurren	Dennis Jakobaufderstroht	Dennis Jakobaufderstroht
CPO (Deck)	Greg Lewis	Greg Lewis	Iain Thomson
CPO (Scientific)	Stephen Smith	Martin Harrison	Martin Harrison
PO (Deck)	<i>Andy MacLean</i>	<i>Andy MacLean</i>	<i>Andy MacLean</i>
SG1A	Stephen Day	Mark Moore	Gerry Cooper
SG1A	Robert Dickinson	Robert Dickinson	Alan McPhail
SG1A	<i>Robert Spencer</i>	<i>Robert Spencer</i>	<i>Robert Spencer</i>
SG1A	William McLennan	William McLennan	Ian Cantile
MM1A	Donald MacDiarmid	Donald MacDiarmid	John Smyth
SCM	Keith Curtis	Keith Curtis	Edward Staite
Chef	Paul Lucas	Stephen Nagle	John Haughton
Assistant Chef	Walter Link	John Giddings	John Giddings
Steward	John Giddings	Alastair Harkness	Alastair Harkness
Deck Technician	Michael Minnock	-	-
Extra CPO (Scientific)	-	Michael Trevaskis	Simon Avery
Extra SG1A	-	Gerry Cooper	-
<b>Total</b>	<b>22</b>	<b>23</b>	<b>22</b>

## ACRONYMS

---

Acronym	Meaning
CFC	Chlorofluorocarbon
CTD	Conductivity, temperature and depth instrument
EC	Eddy correlation
i/b	In board
ID	Inertial dissipation
IEO	Institutio Espanol de Oceanografia, Tenerife, Spain
JRD	James Rennell Division
LADP	Lowered Acoustic Doppler Current Profiler
MBL	Maximum breaking load
MPI	Max Planck Institute
o/b	Out board
OED	Ocean Engineering Division, SOC
PI	Principal Investigator
PS	Principal Scientist
SADP	Shipboard Acoustic Doppler Current Profiler
SOC	Southampton Oceanography Centre
TLO	Technical Liaison Officer
u/s	Unserviceable
UEA	University of East Anglia
UoM	University of Miami
UPS	Uninterruptible power supply

---



## ACKNOWLEDGEMENTS

Particular thanks go to Captain Roger Chamberlain who participated in cruises 277 to 279. Without the good working relationship we developed through all three cruises not nearly so much scientific work would have been completed. During the cruise there were ongoing worries about the new winch system. Some teething troubles were experienced but Chief Engineer Bernard McDonald on D279 kept us working. As always, the RRS *Discovery* was an excellent ship to work on and the crew were thoroughly professional. The 21 scientists were one of the most relaxed and enthusiastic groups it has been my privilege to lead. Thanks are also due in particular to Brian King, who travelled to the Bahamas to help with mobilisation and so allowed me a few days rest, confident that we would be ready to sail on time.

## 1. INTRODUCTION

The 24.5°N transatlantic section between 69° 9'W and 23° 30'W has been occupied in 1957, 1981, 1992, 1998 and 2004 (reported here), with the western and eastern boundaries being closed at different latitudes (Table 1.1, Figure 1.1).

The 1957 data differ most from the other occupations: the number of stations is much lower and temperature and salinity data were obtained from discrete samples at approximately 25 depths. From 1981, temperature and salinity profiles were obtained by CTD with discrete salinity samples being measured against standard sea-water. Using the linearity of the Eastern basin deep T/S relationship between 2 and 2.5°C ([*Saunders*, 1986], [*Mantyla*, 1994]) and assuming constant deep water characteristics, the 1957 salinities are between 0.004 to 0.006 higher than in subsequent years ([*Bryden et al.*, 1996], [*Arbic and Owens*, 2001]).

Table 1.1: Hydrographic sections along 24.5°N.

Year	Number of Stations	Reference
1957	38	[ <i>Fuglister</i> , 1960]
1981	90	[ <i>Roemmich and Wunsch</i> , 1985]
1992	101	[ <i>Parilla et al.</i> , 1994]
1998	130	[ <i>McTaggart et al.</i> , 1999]
2004	125	[ <i>Cunningham</i> , 2005]

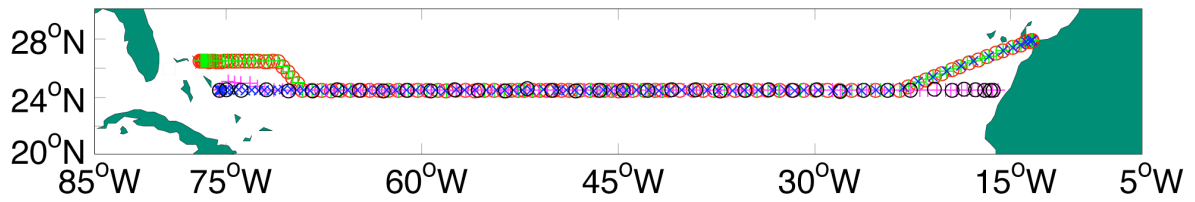


Figure 1.1: CTD stations occupied during RRS *Discovery* Cruise 279 in 2004 (green plus), repeating the 1998 occupation (red circle) except in the eastern basin where there were five fewer CTD stations in 2004. For these two occupations the western boundary is closed at 26.5°N, where long-term current meter arrays have measured the mean southward transport and variability of the Deep Western Boundary Current (DWBC) ([*Lee et al.*, 1990], [*Lee et al.*, 1996], [*Fillenbaum et al.*, 1997], [*Bryden et al.*, 2004]). The 24.5°N transatlantic section has been occupied five times between 69° 9'W and 23° 30'W, with the western and eastern boundaries being closed at different latitudes. In 1957 (black circles) and 1981 (blue cross), the western boundary was approached at 24.5°N, while in 1992 (pink plus) the boundary was closed perpendicular to the continental slope by a small adjustment to the zonal section. In 1975, Spanish responsibilities for Western Sahara were transferred to the joint administration of Morocco and Mauritania. Subsequently, there has been a territorial dispute between the Polisario peoples of Western Sahara and Morocco, with the Polisario seeking to establish an independent state. Permission to work within the disputed territorial waters has not been sought resulting in a northward excursion within Spanish and Moroccan water in 1981, 1998 and 2004.

## 2. SCIENTIFIC BACKGROUND

In the North Atlantic, the wind driven and thermohaline circulations combine in a meridional overturning circulation (MOC) that drives a northward heat transport reaching a maximum of 1.3PW at 24.5°N (~25% of the global net atmosphere-ocean heat flux) ([*Bryden and Imawaki*, 2001]). The ocean heat flux is effected by the temperature difference between a northward transport of very warm water in the Florida Current, cooler Intermediate water and very cold Antarctic Bottom Water (AABW), and the southward transport of warm thermocline and cold North Atlantic Deep Water (Figure 2.1) ([*Hall and Bryden*, 1982], [*Roemmich and Wunsch*, 1985], [*Ganachaud and Wunsch*, 2000], [*Ganachaud*, 2003]. As a consequence of the MOC, northwest Europe enjoys a mild climate for its latitude: however abrupt rearrangement of the Atlantic Circulation has been shown in climate models and paleoclimate records to be responsible for a cooling of the European climate of between 5-10°C ([*Broecker and Denton*, 1989], [*Dansgaard*, 1993], [*Rahmstorf and Ganopolski*, 1999] [*Vellinga and Wood*, 2002],).

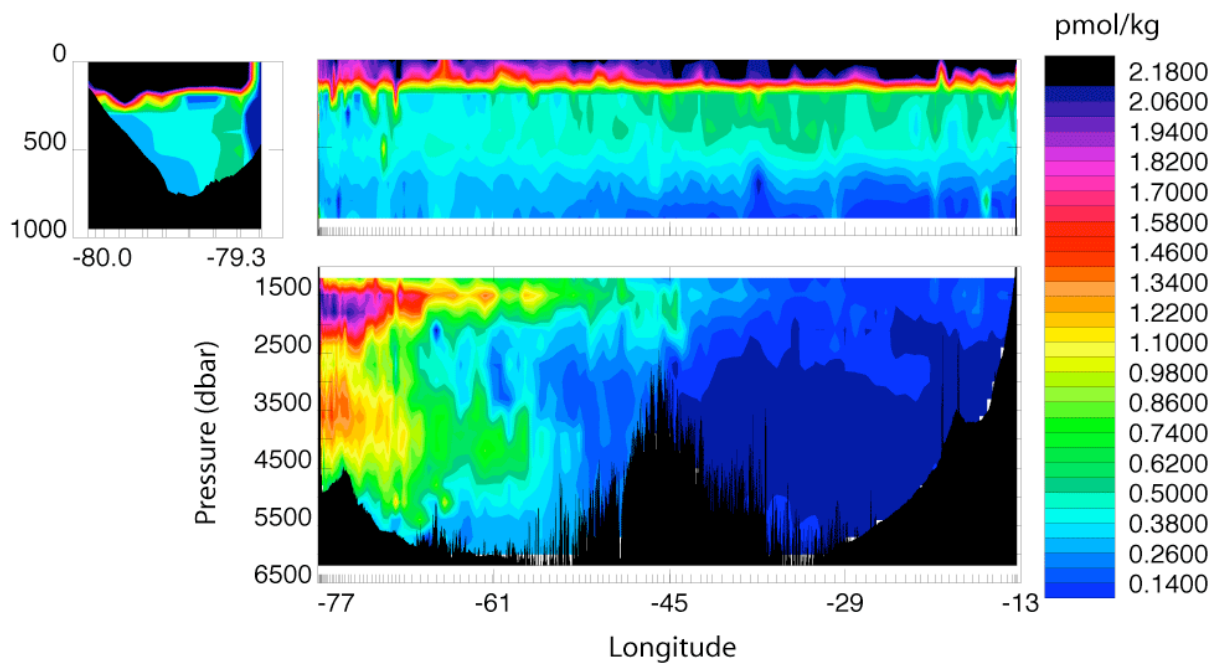
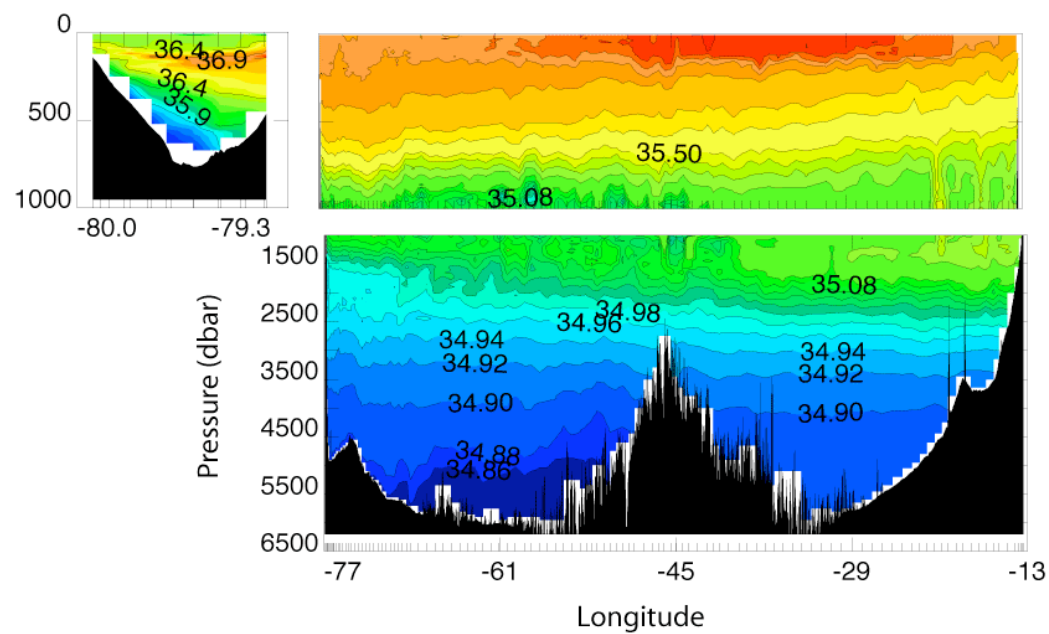
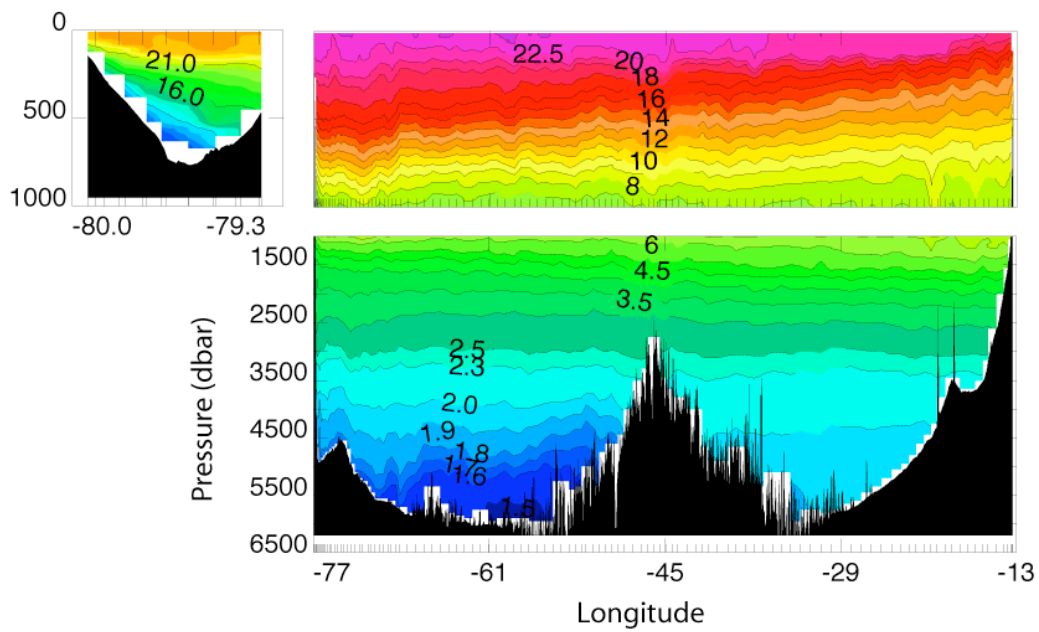


Figure 2.1: CTD temperature (i) and salinity (ii) and from discrete samples carbon tetrachloride ( $\text{CCl}_4$ ) (iii) at a nominal latitude of  $24.5^\circ\text{N}$  measured during RRS *Discovery* Cruise 279, 4<sup>th</sup> April to 10<sup>th</sup> May 2004. The water mass distribution illustrates clearly our a priori view of the circulation at  $24.5^\circ\text{N}$  ([Hall and Bryden, 1982], [Bryden and Imawaki, 2001]). In the upper 150dbar warm, saline surface water is created by excess evaporation over precipitation. The main thermocline between 9–22°C, with isotherms sloping up to the east, contains recently ventilated late winter water, subducting southward under the surface water as part of the Sverdrup circulation. Intermediate water between 4–8°C, with the 4°C isotherm sloping down to the east, consists of two water masses: in the western basin, low salinity water due to the northward penetration of Antarctic Intermediate Water and in the east, high salinities due to the southward and westward spread of Mediterranean Overflow Water. Two cores of North Atlantic Deep Water (NADW) are clearly shown in the  $\text{CCl}_4$  distribution, spreading south in the Deep Western Boundary Current (DWBC). The upper NADW at a pressure of 1500dbar, with a temperature and salinity of about 3.6°C and 34.99 respectively, is formed by deep winter mixing in the Labrador Sea. Lower NADW at about 3500dbar has a core temperature and salinity of 2°C and 34.90 respectively and has its source in the Greenland-Iceland-Norwegian Seas. Southward transport in the DWBC is confined to within 200km of the continental slope, and offshore 200km to 625km (the eastward extent of existing current meter measurements) the DWBC has a broad northward recirculation. The accumulated transport eastward from the continental shelf deeper than 1000m increases rapidly to a maximum of 34.9Sv southward 200km offshore, gradually decreasing to less than 25Sv 625km offshore ([Bryden *et al.*, 2004]). Therefore, the  $\text{CCl}_4$  distribution is the result of a relatively narrow and rapid transport southward close to the continental slope with a broad interior recirculation and isopycnal mixing by eddies, which from the upper NADW  $\text{CCl}_4$  distribution we conclude extends beyond the mid-Atlantic Ridge (MAR). Northward flowing Antarctic Bottom Water with temperatures less than 1.9°C is piled onto the western flank of the MAR. In the eastern basin at depths below the intermediate waters, the NADW is thought to be the oldest and least varying water mass in the North Atlantic, as it has no direct source and is a result of mixing between AABW and NADW as the AABW flows north across a series of sills. This results in a linear and stable relationship between temperature and salinity, which can be used to compare the quality of salinity measurements between cruises ([Saunders, 1986]).

### 3. OBJECTIVES

This cruise is part of the James Rennell Division Core Strategic Programme “Ocean Variability and Climate” and is a contribution to the project “Monitoring the Atlantic Meridional Overturning Circulation at 26.5°N”, which is part of the NERC directed programme RAPID Climate Change. In March and April 2004, 22 moorings were deployed across the Atlantic to continuously measure the size of the overturning [Cunningham, 2005]. The key objectives of this cruise are:

- To measure the circulation across 24.5°N, for the first time including direct top-to-bottom lowered ADP measurements at each station and continuous current measurements in the top 1000m.
- To calculate the transport of heat, freshwater, oxygen, nutrients, CFCs and carbon into the North Atlantic.
- To quantify the size and structure of the Atlantic MOC, for direct comparison with the MOC monitoring array.

#### **4. BASIC OBSERVATIONAL STRATEGY**

Between 4<sup>th</sup> April and 10<sup>th</sup> May 2004, 125 full depth CTD/LADP stations were occupied across the Atlantic at a nominal latitude of 24.5°N, including a section across the Florida Current (Figure 1.1). During two preceding cruises (D277 and D278), sections were also occupied across the Florida and Deep Western Boundary Currents and are reported here. Continuous underway observations were made of currents in the upper 1000m, surface salinity and surface temperature. At each station, up to 24 water samples were captured for the analysis of oxygen, salinity, nitrate, silicate, phosphate [Richard Sanders, Deacon Division SOC], CFC11, 12, 113 and CCl4 (carbon tetrachloride) [David Cooper, University of Miami], discrete total inorganic carbon (TCO<sub>2</sub>), discrete total alkalinity (TA) and discrete partial pressure of CO<sub>2</sub> (discrete pCO<sub>2</sub>) [Ute Schuster, University of East Anglia]. Direct, near real-time measurements were also made of the air-sea turbulent fluxes of momentum and sensible and latent heat, in addition to various mean meteorological parameters including testing of a new Licor sensor to determine its suitability for making direct measurements of the air-sea CO<sub>2</sub> flux [Margaret Yelland, JRD SOC].



## 5. ITINERARY

The main objective of this report is to document transatlantic hydrographic observations made during RRS *Discovery* Cruise 279 (125 CTD stations). Two previous cruises D277 and D278 also led by Stuart Cunningham were principally mooring deployment cruises with related scientific objectives. As part of the moorings deployments, a limited number of hydrographic observations were made in the Florida Current and along the Abaco mooring array (12 and 16 CTD stations respectively). Instrumentation and calibration methods are the same for observations on all three cruises and so they are reported here. Moorings deployments on D277 and D278 are reported in Cunningham (2005).

Table 5.1: Cruise timetable and ports of departure.

Cruise	Sail	Port	Dock	Port	Days at sea	No. CTD stations	Main science tasks
277	26/02/04	Santa Cruz de Tenerife	16/03/03	Freeport, Grand Bahama	19	12	Moorings deployments, Florida Current hydrography and New Providence Channel SADP section
278	19/03/04	Freeport, Grand Bahama	30/03/03	Freeport, Grand Bahama	11	16	Moorings deployments, Abaco mooring array hydrography
279	04/04/04	Freeport, Grand Bahama	10/05/04	Santa Cruz de Tenerife	37	125	Florida Current and transatlantic hydrography and chemistry

### 5.1 D277 Hydrographic Observations of Note

1. Deep CTD station 277003 as test of new winch performance at 24° 25.44'N, 56° 1.38'W. Water depth 6454 m, CTD maximum depth 6419 m (6559 dbar).
2. Florida Current CTD section: CTD stations 277005 to 277012, from 14/03 2016 to 15/03 1222, occupied east to west.

3. Florida Current SADP section: 5 kn steam west to east along the CTD section to obtain direct velocity measurements of the current from the 150kHz and 75kHz shipboard SADPs. The 75kHz obtained bottom track velocities across the whole section. Dates: 15/03 1307 to 2145.
4. New Providence Channel SADP section: 5 kn steam across the channel in the direction 024°T. Dates: 16/03 0554 to 1156.

## **5.2 D278 Hydrographic Observations of Note**

1. CTD stations 278001 to 278016 occupied along the Abaco mooring array. The stations were occupied around mooring operations and the east west station grid was not monotonic in time.

## **5.3 D279 Hydrographic Observations of Note**

1. Florida Current SADP section: 5 kn steam east to west along the CTD section to obtain direct velocity measurements of the current from the 150kHz and 75kHz shipboard SADPs. The 75kHz obtained bottom track velocities across the whole section. Dates: 04/04 2139 to 05/04 0653.
2. Florida Current CTD section at 27°N: CTD stations 2 to 10, from 05/04 0634 to 06/04 0157, occupied west to east.
3. Transatlantic section: stations 12 to 40 along 26.5°N, from 76° 55.6'W to 70° 59.2'W; stations 40 to 45 from 26.5°N to 24.5°N, to 69° 8.8'W; stations 45 to 107 at 24.5°N to 23° 29.7'W; stations 107 to 125 from 24.5°N to 27° 54.9'N, to 13° 22.4'W.
4. Continuous underway observations were made of currents in the upper 1000m, surface salinity and surface temperature. At each station, up to 24 water samples were captured for the analysis of salinity and a variety of other nutrients and gasses.

## 6. NARRATIVE

**D279 Narrative ((Day of year), times in GMT, CTD station numbers given as D279 incremental number, five digit *Discovery station number*)**

**4<sup>th</sup> April (095):** 1630. CTD test station. 2030 Begin 5 kn steam east to west for SADP section across the Florida Current at a latitude of 27°N. Section slightly delayed due to heavy traffic. **5<sup>th</sup> (096):** Begin working a planned nine station CTD section west to east across the Florida Current. First CTD station at approximately 0630. Thereafter, stations worked through the day and night. A succession of problems have delayed the CTD operation: main logging PC is unreliable – keeps crashing. Options: swap with backup pc, reinstall software, get another computer – computers swapped, and there have since been no crashes; Secondary T seems not to be working – after three stations a faulty pump was replaced restoring the secondary temperature and oxygen; Oxygen sensor apparently not working – traced to the configuration file having zeros in every entry; altimeters not working – altimeters and cables swapped. By 2400 we had started station 9 with one more station to complete. The estimated completion time was 1600, so we have lost about 12 hours completing this short section. **6<sup>th</sup> (097):** Station 010, *15314*, last on FC section completed at 0300. Steaming north about Grand Bahama and Abaco to start of main section. Arrived on station at 1800, found a suitable water depth of 300 m after running into 30 m deep water. As the CTD 11, *15315* was being recovered, news came through that the agent had the followers in Freeport. Therefore, we are steaming back to collect them. Two of the scientific party had a reaction to the Scopoderm (hyoscine) patches for motion sickness. In one case this included severe side effects - loss of focus in one eye and abnormal retinal size in that eye. The patches were removed and the retinal size monitored with ophthalmoscope under advice from Haslar. An eye patch was worn to reduce eye strain. Over three days, eye focus was recovered and retinal size returned to normal, matching the unaffected eye. **7<sup>th</sup> (098):** Arrived off Freeport and collected followers by off port transfer (OPT) at 0715. En-route back to start of CTD section. Arrived on station 12, *15316* at 2015 – a repeat of station 11 *15315*. Began working CTD stations eastward along 26.5°N. Station spacing close, so CTD work very intensive. Time limiting factor is the LADP download between stations. **8<sup>th</sup> (099):** Main event of the day was the failure of the winch scrolling gear on station 17, *15321*, CTD o/b 1904. Due to the wear on the scrolling gear follower, it was decided to replace the current follower with one of the new ones picked up in Freeport. On station 17 (at the foot of the continental slope in about 4800 m, 2 miles west of mooring WBH2), the follower sheared with the CTD 26 m off bottom. The depth shallowed and the CTD touched bottom, so we towed 135°T to find deeper water to clear the CTD from the bottom and allow wire to be paid out. Richie Phipps, the ship's engineers and the Captain worked for three hours to replace the follower. This has now been done and we are at 3800 m hauling in at 30 m/min. The diagnosis of what happened is that as the old follower wore down, it caused burrs to turn on the

continuous screw. The new follower carriage seized on one of these and the knife/tooth of the follower sheared off. Fortunately the follower stuck solid in the middle of the screw rather than flying to one end and smashing into the gear case. The follower is under more tension in one direction than the other because as the wire leads outboard from the follower, it turns 90 degrees round a pulley leading to the traction winch. CTD i/b 0300. **9<sup>th</sup> (100) to 12<sup>th</sup> (102)**: Continue working stations eastward across the Deep Western Boundary Current. On station 28, *15332*, the Workhorse battery pack was deployed with the air vent removed. The vent was spotted on the deck lab floor with the CTD at 2500 m, so we recovered the CTD, removed the flooded pack and started a new station 29, *15333*. Deployments of styrene cups on the CTD were halted as one bottle at 2500 m on station 30, *15334* had a dramatic CFC11 contamination. David Cooper suspected that the cups contravened the Montreal Protocol that bans the use of CFCs in such products. **13<sup>th</sup> (103)**: A barbecue was held on the aft deck in celebration of three birthdays. Weather was splendid and we were on station 36, *15341* during most of the barbecue. **14<sup>th</sup> (104)**: Completed 040, *15344* last western boundary station on latitude 26.5°N at 1544. Turned south course 139°T. Weather has turned cooler and wet after the passage of a sharp front during the night. **17<sup>th</sup> (108)**: Murder game started at 0000. To try and recover some contingency, we have relaxed the station positions to be within 0.5nm of the position. This allows the ship to approach at full speed, then come on station faster than coming on station to a precise position. **22<sup>nd</sup> (113)**: Discovery 6 failed. Five hour interlude in data processing while the disks were mounted on Discovery 2. **26<sup>th</sup> (117)**: We reached the MAR station today: station 079, *15381*, completed at 1238. **27<sup>th</sup> (119)**: Workhorse slave unit removed from CTD frame prior to station 087, *15388*. **29<sup>th</sup> (120)**: Deployed Richard Babb's trial Iridium argo float at 1515 at 24° 30.24'N, 38° 32.07'W (24.50407°N, 38.53441°W) after station 090, *15391*. The float is in a grey plastic case and is designed to float on the surface (no buoyancy control) to test the Iridium transmitter/receiver. **30<sup>th</sup> (121)**: A potential winch problem narrowly avoided. Just after the CTD was landed at the end of station 38, *15397*, the Chief Engineer heard the CTD traction winch gear box making an unusual noise. The problem was that the storage drum drive shaft and drive motor shafts had decoupled so that the storage drum was then stationary relative to the traction winch. The drive shaft decoupled because the shaft coupling joint came loose due to poor design. **2<sup>nd</sup> May (123)**: Differential G12 receiver changed region from AM-SAT to EA-SAT at 1415. **6<sup>th</sup> (127)**: Electrical termination started to fail at the end of station 112, cast ended at 1912. After some diagnosis the work of retermination started at 2100. At start of 113, new termination failed as soon as the CTD was deployed. Therefore, a second termination was started. **7<sup>th</sup> (128)**: Second termination complete at 0715. Started station 113 at 0740. Time lost to termination problems about 10 hours. **8<sup>th</sup> (129)**: EB3 satellite buoy. Last reported position (26° 59.86'N, 16° 13.8'W) data from this buoy were received at 1930 on 30<sup>th</sup> March (090). Approach position from the south west along cruise track. Visibility and sea-state good for observations. The buoy could not be located so a box survey of length two cables was completed around this position to

no effect. Steamed for station 118, 6 nm away. **9<sup>th</sup> (130)**: Last station completed at 2100, station 125. Headed for Santa Cruz de Tenerife.

## 7. D279 BRIDGE TIMETABLE OF EVENTS

Date	Time (UT)	Event		
30/03/04	1500	Arrived Freeport - end of Cruise 278		
03/04/04	2000	Familiarisation of newly joined non-RSU personnel		
04/04/04	1330	Emergency and lifeboat muster		
	1455	Pilot embarked		
	1533	Vessel cleared berth		
	1555	Pilot disembarked		
	1600	Full away. Course 117 T		
	1729	PES Fish cast outboard	26 29.8N	079 00.2W
	1746-1842	Station 15305-CTD cast outboard	26 28.7N	079 00.6W
	1842	Set course 340 T		
	2150	Altered course to 270 T onto ADP survey line	26 59.8N	079 11.4W
	2158-0617	Engaged in ADP Survey @ 5 knots	27 00.0N	079 11.8W
05/04/04	0617-46	Station 15306-CTD 46 cast outboard	27 00.3N	079 56.1W
	0801-53	Station 15307-CTD 47 cast outboard	27 01.0N	079 51.4W
	1004-49	Station 15308-CTD 48 cast outboard	27 01.1N	079 46.5W
	1244-1350	Station 15309-CTD 49 cast out to 525 m	27 01.0N	079 40.9W
	1540-1641	Station 15310-CTD 50 cast out to 635 m	27 01.0N	079 37.1W
	1834-1933	Station 15311-CTD 51 cast out to 760 m	27 00.9N	079 30.2W
	2109-2204	Station 15312-CTD 52 cast out to 670 m	27 00.9N	079 23.3W
	2321-0010	Station 15313-CTD 53 cast out to 605 m	27 00.0N	079 16.8W
06/04/04	0136-0220	Station 15314-CTD 54 cast out to 455 m	26 59.9N	079 11.6W
	0220	Set course 336 T full away		
	0300	Altered course to 006 T	27 05.0N	079 15.6W
	0447	Altered course to 090 T	27 26.0N	079 12.0W
	0731	Altered course to 113 T	27 26.0N	078 35.0W
	1237	Altered course to 129 T	27 02.5N	077 30.2W
	1614	Altered course to 180 T	26 36.8N	076 54.1W
	1734-1817	Station 15315-CTD 121 cast out to 340 m	26 30.4N	076 55.6W
	1836	PES inboard – proceeding to Freeport Roads	26 30.3N	076 55.0W
07/04/04	0600	Approaching Freeport Roads		
	0726-33	Agents boat alongside – scroll followers transferred to ship		
	0742	Full away to resume science		
	1954	PES Fish outboard	26 26.5N	076 55.0W
	2047-2121	Station 15316-CTD 121 cast out to 260 m	26 30.5N	076 55.6W
	2234-0040	Station 15317-CTD 120 cast outboard	26 32.0N	076 48.3W

08/04/04	0235-0502	Station 15318–CTD 119 cast out to 2350 m	26 30.7N	076 46.9W
	0700-1022	Station 15319–CTD 118 cast outboard	26 31.4N	076 44.3W
	1243-1701	Station 15320–CTD 117 cast out to 4440 m	26 30.5N	076 41.3W
	1904-0300	Station 15321–CTD 116 cast out to 4595 m	26 30.0N	076 37.6W
	2054	WINCH STOPPED – SCROLLING FAILURE		
	2225	Attempting to tow CTD to deeper water for veering to scroll point		
	2338	Scroll problem fixed – slow hauling and monitoring		
09/04/04	0000	All aspects of winch handed back to lab and winch operator		
	0300	CTD inboard	26 28.5N	076 34.2W
	0628-1103	Station 15322–CTD 115 cast outboard	26 29.1N	076 31.3W
	1325-1748	Station 15323–CTD 114 cast out to 4825 m	26 30.0N	076 25.8W
	1939-2330	Station 15324–CTD 113 cast out to 4825 m	26 29.5N	076 18.1W
10/04/04	0115-0501	Station 15325–CTD 112 cast out to 4805 m	26 29.2N	076 12.6W
	0727-1045	Station 15326–CTD 111 cast outboard	26 29.9N	076 05.6W
	1247-1605	Station 15327–CTD 110 cast out to 4700 m	26 30.1N	075 54.7W
	1750-2100	Station 15328–CTD 109 cast outboard	26 29.4N	075 42.3W
	2315-0240	Station 15329–CTD 108 cast out to 4685 m	26 28.9N	075 30.9W
11/04/04	0433-0745	Station 15330–CTD 107 cast out to 4630 m	26 29.5N	075 18.5W
	0955-1330	Station 15331–CTD 106 cast out to 4895 m	26 30.9N	075 04.7W
	1532-1704	Station 15332–CTD 105 cast but aborted due to battery problems		
	1735-2038	Station 15333–CTD 105 cast out to 4525 m	26 30.6N	074 47.3W
	2332-0302	Station 15334–CTD 104 cast out to 4554 m	26 31.2N	074 29.8W
12/04/04	0439-0807	Station 15335–CTD 103 cast out to 4565 m	26 30.6N	074 14.1W
	0948-1330	Station 15336–CTD 102 cast out to 4750 m	26 30.1N	073 55.8W
	1531-1924	Station 15337–CTD 101 cast out to 4920 m	26 30.6N	073 33.8W
	2106-0100	Station 15338–CTD 100 cast out to 5080 m	26 30.0N	073 11.7W
13/04/04	0313-0701	Station 15339–CTD 99 cast out to 5124 m	26 30.1N	072 50.8W
	1005-1355	Station 15340–CTD 98 cast out to 5188 m	26 30.0N	072 29.1W
	1651-2053	Station 15341–CTD 97 cast out to 5274 m	26 29.3N	072 00.4W
	2255-0250	Station 15342–CTD 96 cast out to 5370 m	26 29.0N	071 45.1W
14/04/04	0539-0938	Station 15343–CTD 95 cast out to 5465 m	26 30.5N	071 20.6W
	1140-1544	Station 15344–CTD 94 cast out to 5495 m	26 29.4N	070 59.2W
	1832-2227	Station 15345–CTD 93 cast out to 5537 m	26 08.0N	070 36.1W
15/04/04	0115-0454	Station 15346–CTD 92 cast out to 5495 m	25 45.9N	070 14.3W
	0750-1208	Station 15347–CTD 91 cast out to 5504 m	25 22.8N	069 52.6W
	1458-1913	Station 15348–CTD 90 cast out to 5590 m	25 00.1N	069 30.4W
	2241-0230	Station 15349–CTD 89 cast out to 5670 m	24 29.6N	069 08.8W

16/04/04	0647-1050	Station 15350-CTD 88 cast out to 5740 m	24 30.5N	068 24.8W
	1455-1841	Station 15351-CTD 87 cast out to 5705 m	24 30.7N	067 40.2W
	2230-0220	Station 15352-CTD 86 cast out to 5730 m	24 29.2N	066 55.4W
17/04/04	0612-0950	Station 15353-CTD 85 cast out to 5260 m	24 30.2N	066 11.5W
	1335-1725	Station 15354-CTD 84 cast out to 5545 m	24 29.7N	065 27.8W
	2130-0130	Station 15355-CTD 83 cast out to 5600 m	24 30.6N	064 39.6W
18/04/04	0516-0905	Station 15356-CTD 82 cast out to 5755 m	24 29.9N	064 00.1W
	1327-1712	Station 15357-CTD 81 cast out to 5785 m	24 30.3N	063 16.1W
	2120-0115	Station 15358-CTD 80 cast out to 5850 m	24 30.2N	062 31.7W
19/04/04	0515-0905	Station 15359-CTD 79 cast out to 5686 m	24 30.5N	061 47.9W
	1300-1653	Station 15360-CTD 78 cast out to 5835 m	24 30.1N	061 03.8W
	2057-0105	Station 15361-CTD 77 cast out to 5880 m	24 30.7N	060 19.4W
20/04/04	0507-0907	Station 15362-CTD 76 cast out to 5820 m	24 30.9N	059 35.5W
	1315-1657	Station 15363-CTD 75 cast out to 5870 m	24 29.9N	058 51.5W
	2047-0045	Station 15364-CTD 74 cast out to 5800 m	24 30.0N	058 08.0W
21/04/04	0435-0835	Station 15365-CTD 73 cast out to 5870 m	24 30.1N	057 23.3W
	1232-1629	Station 15366-CTD 72 cast out to 5870 m	24 29.7N	056 40.0W
	2009-0017	Station 15367-CTD 71 cast out to 5890 m	24 31.1N	055 56.2W
22/04/04	0419-0800	Station 15368-CTD 70 cast out to 5865 m	24 30.3N	055 12.8W
	1210-1548	Station 15369-CTD 69 cast out to 5197 m	24 30.0N	054 28.4W
	1945-2345	Station 15370-CTD 68 cast out to 5870 m	24 29.6N	053 44.2W
23/04/04	0250-0648	Station 15371-CTD 67 cast out to 5325 m	24 29.9N	053 10.7W
	0940-1325	Station 15372-CTD 66 cast out to 5260 m	24 30.2N	052 38.2W
	1603-1926	Station 15373-CTD 65 cast out to 4909 m	24 30.0N	052 09.3W
	2300-0242	Station 15374-CTD 64 cast out to 5280 m	24 30.0N	051 32.3W
24/04/04	0554-0925	Station 15375-CTD 63 cast out to 5422 m	24 30.4N	050 59.8W
	1255-1611	Station 15376-CTD 62 cast out to 4703 m	24 30.3N	050 26.5W
	1915-2235	Station 15377-CTD 61 cast out to 4600 m	24 30.6N	049 52.4W
25/04/04	0142-0532	Station 15378-CTD 60 cast out to 5210 m	24 30.4N	049 20.0W
	0830-1150	Station 15379-CTD 59 cast out to 4400 m	24 29.8N	048 46.4W
	1602-1852	Station 15380-CTD 57 cast out to 3945 m	24 30.3N	047 57.8W
	2320-0205	Station 15381-CTD 56 cast out to 3485 m	24 29.9N	047 07.5W
26/04/04	0459-0740	Station 15382-CTD 55 cast out to 3300 m	24 29.7N	046 34.5W
	1025-1235	Station 15383-CTD 54 cast out to 2765 m	24 29.7N	046 02.1W
	1536-1817	Station 15384-CTD 53 cast out to 3415 m	24 30.3N	045 29.4W



	2117-2400	Station 15385–CTD 52 cast out to 3300 m	24 29.1N	044 56.7W
27/04/04	0323-0610	Station 15386–CTD 51 cast out to 3876 m	24 30.1N	044 23.7W
	0920-1207	Station 15387–CTD 50 cast out to 3770 m	24 30.0N	043 50.6W
	1614-1917	Station 15388–CTD 48 cast out to 4117 m	24 30.6N	043 00.5W
	2330-0253	Station 15389–CTD 47 cast out to 3965 m	24 29.9N	042 11.0W
28/04/04	0600-0910	Station 15390–CTD 46 cast out to 4610 m	24 30.5N	041 38.4W
	1225-1541	Station 15391–CTD 45 cast out to 5130 m	24 30.2N	041 05.5W
	2000-2317	Station 15392–CTD 43 cast out to 4852 m	24 30.7N	040 16.9W
29/04/04	0507-0823	Station 15393–CTD 42 cast out to 5150 m	24 29.9N	039 14.7W
	1230-1526	Station 15394–CTD 41 cast out to 4630 m	24 29.9N	038 31.4W
	1530	Float deployed by Pascal/Yelland	24 30.2N	038 32.1W
	1950-2330	Station 15395–CTD 40 cast out to 5500 m	24 29.9N	037 41.7W
30/04/04	0355-0710	Station 15396–CTD 39 cast out to 5300 m	24 29.4N	036 52.7W
	1130-1502	Station 15397–CTD 38 cast out to 5740 m	24 29.6N	036 02.8W
	1920-2242	Station 15398–CTD 37 cast out to 5040 m	24 30.3N	035 13.7W
01/05/04	0303-0610	Station 15399–CTD 36 cast out to 5030 m	24 29.7N	034 23.4W
	1015-1350	Station 15400–CTD 35 cast out to 5865 m	24 29.9N	033 34.4W
	1833-2209	Station 15401–CTD 34 cast out to 5870 m	24 30.6N	032 39.4W
02/05/04	0301-0637	Station 15402–CTD 33 cast out to 5635 m	24 30.0N	031 43.8W
	1117-1441	Station 15403–CTD 32 cast out to 5695 m	24 29.7N	030 48.7W
	1930-2305	Station 15404–CTD 31 cast out to 5710 m	24 30.1N	029 53.4W
03/05/04	0348-0715	Station 15405–CTD 30 cast out to 5658 m	24 30.5N	028 59.9W
	1200-1522	Station 15406–CTD 29 cast out to 5580 m	24 30.1N	028 04.1W
	2005-2335	Station 15407–CTD 28 cast out to 5531 m	24 30.7N	027 08.9W
04/05/04	0420-0738	Station 15408–CTD 27 cast out to 5370 m	24 29.9N	026 13.9W
	1210-1516	Station 15409–CTD 26 cast out to 5270 m	24 30.1N	025 19.1W
	2005-2328	Station 15410–CTD 25 cast out to 5136 m	24 29.7N	024 24.2W
05/05/04	0421-0735	Station 15411–CTD 22 cast out to 5050 m	24 30.8N	023 29.7W
	1130-1432	Station 15412–CTD 21 cast out to 4880 m	24 44.3N	022 49.3W
	1830-2135	Station 15413–CTD 20 cast out to 4740 m	24 59.1N	022 08.9W
06/05/04	0114-0427	Station 15414–CTD 19 cast out to 4565 m	25 13.3N	021 28.7W
	0815-1125	Station 15415–CTD 18 cast out to 4388 m	25 27.0N	020 48.3W
	1505-20	Station 15416–CTD 17 aborted due to depth	25 41.4N	020 09.1W
	1520-1610	Relocating vessel to desired depth		
	1610-1900	Station 15416–CTD 17 cast out to 4180 m	25 39.0N	020 14.6W

	2236-0736	DOWN TIME for TERMINATION problems		
07/05/04	0736-1020	Station 15417-CTD 16 cast out to 3772 m	25 55.2N	019 29.1W
	1332-1542	Station 15418-CTD 14 cast out to 3435 m	26 08.0N	018 54.6W
	1949-2223	Station 15419-CTD 13 cast out to 3635 m	26 23.1N	018 09.6W
08/05/04	0204-0436	Station 15420-CTD 12 cast out to 3640 m	26 35.8N	017 28.1W
	0815-1050	Station 15421-CTD 11 cast out to 3609 m	26 48.9N	016 47.1W
	1345-1442	Search for telemetry mooring EB3 – No success after a thorough Box search		
		Mean position throughout	26 59.9N	016 13.9W
	1528-1745	Station 15422-CTD 9 cast out to 3516 m	27 03.1N	016 07.5W
	2045-2255	Station 15423-CTD 8 cast out to 3130 m	27 14.0N	015 35.5W
09/05/04	0309-0500	Station 15424-CTD 7 cast out to 2594 m	27 26.0N	014 51.6W
	0825-1000	Station 15425-CTD 6 cast out to 2015 m	27 37.2N	014 13.7W
	1236-1445	Station 15426-CTD 5 cast out to 1545 m	27 49.7N	013 49.0W
	1514-1620	Station 15427-CTD 4 cast out to 1080 m	27 51.1N	013 33.0W
	1714-1755	Station 15428-CTD 3 cast out to 580 m	27 52.8N	013 25.2W
	1835-1905	Station 15429-CTD 1 cast out to 345 m	27 54.9N	013 22.5W
	1910	PES Fish inboard and secured		
	1917	Commenced bathymetric survey	27 55.0N	013 22.8W
	1930	Bathymetric survey completed - set course for Santa Cruz De Tenerife		
	Course 272 T	27 55.7N	013 21.6W	
END OF SCIENCE				
10/05/04	0900	ETA Santa Cruz		

## 8. CTD OPERATIONS – D279

Dave Teare, Pete Keen, Martin Bridger

### 8.1 CTD Main Instrumentation

Sea-Bird 9/11 plus CTD system; Chelsea Mk III Aqua tracker fluorometer; Chelsea MkII Aqua tracker transmissometer; Sea Tech light backscattering sensor; Benthos PSA-916T altimeter; 150kHz Broadband ADP s/n 1308; 2 x 300kHz L-ADP; 24 x 10L water sampling bottles on a 24 position rosette; Sea-Bird SBE35 deep ocean standards thermometer. CTD sensor serial numbers Tables 8.1, 8.2 and 8.3.

### 8.2 Sea-Bird CTD Configuration

Frequency 0 –SBE 3P temperature sensor (primary); Frequency 1 –SBE 4C conductivity sensor (primary); Frequency 2 –digiquartz temperature compensated pressure sensor; Frequency 3 – SBE 3P temperature sensor (secondary); Frequency 4 – SBE 4C conductivity sensor (secondary); SBE 5T submersible pump s/n 3607 or s/n 3195 (primary); SBE 5T submersible pump s/n 3609 (secondary); SBE 32 carousel 24 position pylon s/n 3231240-0243; SBE 11 *plus* deck unit s/n 11P24680-0598; Break-out Box s/n B019108

### 8.3 Voltage Channels<sup>1</sup>

V0: Oxygen, current s/n 13055; V1: Oxygen, temperature s/n 130551; V2: Fluorometer s/n 88-2360-108; V3: Altimeter s/n 1040; V4: Transmissometer s/n 161048; V5: LSS s/n 400

---

<sup>1</sup> Occasional changes were made to the original configuration. These are listed according to cast number in Table 8.4.

Table 8.1: D277 CTD sensor serial numbers. Primary sensors are those reported as the final data.

<b>Stat num</b>	<b>Primary Temp</b>	<b>Primary cond</b>	<b>Secondary temp</b>	<b>Secondary cond</b>	<b>Press</b>
001-012	2674	2231	4105	2571	78958

Table 8.2: D278 CTD sensor serial numbers.

<b>Stat num</b>	<b>Primary temp</b>	<b>Primary cond</b>	<b>Secondary temp</b>	<b>Secondary cond</b>	<b>Press</b>
001-009	2919	2407	4116	2840	78958
010-012	2758	2450	2880	2637	90573
013-016	2919	2407	4116	2840	78958

Table 8.3: D279 CTD sensor serial numbers. Primary sensors are those reported as the final data.

<b>Stat num</b>	<b>Primary temp</b>	<b>Primary cond</b>	<b>Secondary temp</b>	<b>Secondary cond</b>	<b>Press</b>
001-037	2919	2407	4116	2840	78958
038-093	2880	2637	2758	2450	78958
094-108	2758	2407	2880	2637	78958
109-125	2758	2407	2880	2840	78958

Table 8.4: List of changes to CTD configuration according to cast number.

Cast Number	Configuration Change
002	Oxygen sensor disconnected
007	Pump s/n 053607 swapped for s/n 053195
008	Oxygen sensor plugged back in
011	No 300kHz ADP
023	Fluorometer disconnected
025	Fluorometer, transmissometer and LSS disconnected
026	Transmissometer and LSS disconnected
027	Fluorometer changed to V2, altimeter to V4
035	Changed BB battery pack
038	Temp/conductivity sensors changed. 1° - T/C 2758/2450, 2° - T/C 2880/2637
042	BB battery pack changed
047	Fluorometer s/n 108 changed to s/n 163
057	Oxygen calibration file error discovered. Voltage offset changed from -0.4187 to -0.4817
061	Fluorometer changed to V3
070	BB battery pack changed
076	Small shrimp discovered lodged in 1° T/C intake, data reveals this occurred at 3000m on the downcast
088	300kHz slave (upward looking) ADP removed due to RSSI failure
094	1° conductivity sensor changed to s/n 2407

#### 8.4 CTD Temperature, Conductivity and Pressure Sensor Calibration Coefficients

Table 8.5: CTD temperature calibration coefficients. 2758 calibrated on 29<sup>th</sup> January 2004, 2880 calibrated on 29<sup>th</sup> January 2004, 2919 calibrated on 29<sup>th</sup> January 2004, 4116 calibrated on 29<sup>th</sup> January 2004 and 2674 calibrated on 15<sup>th</sup> December 2003

<b>Coeff</b>	<b>2674</b>	<b>4105</b>	<b>2758</b>	<b>2880</b>	<b>2919</b>	<b>4116</b>
G	4.35677202e-3	4.39439791e-3	4.35397384e-3	2.37981443e-3	4.31706705e-3	4.42588002e-3
H	6.42250609e-4	6.48223032e-4	6.37191919e-4	6.42919222e-4	6.44675270e-4	6.84231655e-4
I	2.34570815e-5	2.34748617e-5	2.19294527e-5	2.33575674e-5	2.29910908e-5	2.43414204e-5
J	2.29237427e-6	2.13130914e-6	2.05208215e-6	2.23078830e-6	2.17863836e-6	1.99246468e-6

Table 8.6: CTD conductivity calibration coefficients. 2450 calibrated on 29<sup>th</sup> January 2004, 2637 calibrated on 29<sup>th</sup> January 2004, 2407 calibrated on 29<sup>th</sup> January 2004, 2840 calibrated on 29<sup>th</sup> January 2004 and 2231 calibrated on 12<sup>th</sup> December 2003

<b>Coeff</b>	<b>2231</b>	<b>2571</b>	<b>2450</b>	<b>2637</b>	<b>2407</b>	<b>2840</b>
G	-1.02409209e+1	-1.02755424e+1	-1.05418122e+1	-1.02953467e+1	-1.02887317e+1	-1.00334576e+1
H	1.613274421	1.59430177	1.67829897	1.44378557	1.49174063	1.37702479
I	-3.29512721e-3	6.92468216e-6	-1.10832094e-3	9.41703627e-4	4.53878165e-4	5.80641988e-4
J	3.42685450e-4	1.17144243e-4	2.03695233e-4	3.10647797e-5	5.42327985e-5	3.83582725e-5

Table 8.7: Pressure calibration coefficients for digiquartz pressure sensors. S/n 78958 calibrated on 17<sup>th</sup> June 2003 and s/n 90573 calibrated on 9<sup>th</sup> June 2002.

<b>Coefficient</b>	<b>S/n 78958</b>	<b>S/n 90573</b>
C <sub>1</sub>	-4.276843e+04	-4.666978e+04
C <sub>2</sub>	-1.236301e+00	-2.615846e-001
C <sub>3</sub>	1.090850e-02	1.373870e-002
D <sub>1</sub>	3.910900e-02	3.884300e-002
D <sub>2</sub>	0.000000e+00	0.000000e+00
T <sub>1</sub>	3.011212e+01	3.015158e+001
T <sub>2</sub>	-5.894647e+01	-3.442071e-004
T <sub>3</sub>	3.484130e-06	4.048350e-006
T <sub>4</sub>	3.687850e-09	2.094500e-009
T <sub>5</sub>	0.000000e+00	0.000000e+00

## 8.5 Oxygen

Table 8.8: Oxygen calibration coefficients. SBE 43 s/n 0619 calibrated on 26<sup>th</sup> February 2004.

<b>Coefficient</b>	<b>Value</b>
Soc	0.31220
Boc	0.0000
Voffset	-0.4187
Tcor	0.0015
Pcor	1.350e-04
Tau	0

## 8.6 Fluorometer

Table 8.9: Fluorometer calibration coefficients from laboratory calibrations for s/n 88-2360-108 on 11<sup>th</sup> November 2002 and s/n 088163 on the 13<sup>th</sup> November 2002. 108 D279 stations 1 to 37, 163 stations 38 to 125.

Coefficient	88-2360-108	088163
V1 (1 µg chlorophyll per litre of acetone)	2.0767	1.9807
VB (Volt output – pure water)	0.3674	0.3983
Vace (Volt output – pure acetone)	0.2993	0.3078
Volts for mechanically blanked detector	0.2791	0.3150

## 8.7 Post Cruise CTD Sensor Calibrations

At the end of D279, all CTD sensors were returned to Sea-Bird for calibration and servicing. A number of conductivity sensors and the temperature sensor were broken or failed as noted in Tables 8.10 and 8.11. Most temperature sensors performed well and no post cruise adjustments to temperature were performed.



Table 8.10: Post cruise conductivity sensor calibrations.

<b>Cond</b>					
<b>Sensor s/n</b>	<b>Cruise</b>	<b>P/S</b>	<b>Statnum</b>	<b>Post Cruise Calibration</b>	<b>In Situ Calibration</b>
2231	277	P	001-012	Calibration satisfactory	
2571	277	S	001-012	Calibration satisfactory	
2407	278	P	001-009	End of conductivity cell broken, conductivity cell replaced	
2407	278	P	013-016		
2407	279	P	001-037		
2407	279	P	094-125		
2637	278	S	010-012	Conductivity cell failed, replaced	
2637	279	P	038-093		
2637	279	S	094-108		
2840	278	S	001-009	Calibration satisfactory	
2840	278	S	013-016		
2840	279	S	001-037		
2840	279	S	109-125		
2450	278	P	010-012	Sensor cleaned and replatinized	Did not produce calibratable data during cruise. Data had large pressure hysteresis that varied from station to station.
2450	279	S	038-093		

Table 8.11: Post cruise temperature sensor calibrations.

Temp Sensor s/n	Cruise	P/S	Statnum	Post Cruise Calibration (drift since last calibration)	Action for Post Cruise Data
2674	277	P	001-012	Drift +1.42m°C	None. This T sensor had a large positive drift - usually expect negative. FS current highly variable so T drift not critical here.
4105	277	S	001-012	Drift -0.48m°C	None
2919	278	P	001-009	Drift -0.27m°C, 10/11 residuals <0.06m°C, 1/11 0.13m°C at 15°C	None
2919	278	P	013-016		
2919	279	P	001-037		
2758	278	P	010-012	Drift -0.18m°C, residuals <0.08m°C	None
2758	279	S	038-093		
2758	279	P	094-125		
4116	278	S	001-009	Drift -0.08m°C, residuals <0.08m°C	None
4116	278	S	013-016		
4116	279	S	001-037		
2880	278	S	010-012	Drift -0.34m°C, residuals <0.08m°C	None
2880	279	P	038-093		
2880	279	S	094-125		

The SBE 43 dissolved oxygen sensor (s/n 430619) had a torn oxygen membrane so post calibration of the sensor was not possible. Given the problems calibrating the oxygen data during the cruise the whole data set must be considered as suspect.

## 8.8 CTD Sensor Calibration Equations

The following equations convert raw sensor frequencies to calibrated data:

### Temperature

$$T_{cal}(ITS-90)^{\circ}C = 1/\{g+h[\ln(f/f_o)]+i[\ln^2(f/f_o)]+j[\ln^3(f/f_o)]\}-273.15$$

$\ln$  = the natural log

$f$  = the output frequency (Hz)

$f_o$  = 1000, an arbitrary scaling for computational efficiency

### Conductivity

Conductivity sensors are calibrated over a 0 – 60 mS/cm range using natural seawater. The calibration equation is:

$$C(S/m) = (g+hf^2+if^3+jf^4)/10(1+dt + ep)$$

$f$  is the instrument frequency (kHz)

$t$  is the temperature ( $^{\circ}C$ )

$p$  is the pressure (db)

$d = -9.57 \times 10^{-8}$  and is the bulk compressibility

$e = 3.25 \times 10^{-6}$  and is the thermal coefficient of expansion for the borosilicate glass

### Pressure

Pressure is calibrated from:

$$P = C(1-T_o^2/T^2)(1-D(1-T_o^2/T^2))$$

where  $T$  is pressure period (ms).

$C$ ,  $D$ ,  $T_o$  are given by:

$$C = C_1 + C_2U + C_3U^2$$

$$D = D_1 + D_2U$$

$$T_o = T_1 + T_2U + T_3U^2 + T_4U^3 + T_5U^4$$

where U is the temperature (°C).

### Fluorometer

Chlorophyll is calculated from voltage output:

$$\text{Chl a} = (\log_{10}^{-1}(VS) - \log_{10}^{-1}(VB)) / (\log_{10}^{-1}(V1) - \log_{10}^{-1}(VA))$$

where VS is the output voltage, VB is the output voltage in laboratory pure water, V1 is the output voltage for a 1µg/l chlorophyll-a solution and VA is the output voltage for pure acetone.

## **8.9 CTD Deployment Procedure**

For each station the deployment procedure was identical and began with confirmation of being on station from the Bridge. On receiving this confirmation, the CTD deck unit was switched on and data logging initiated on the master and slave computers. Once data acquisition was confirmed, the winch operator was informed and the instrumentation package was deployed over the side and taken to 10 metres. The pack was held at 10 metres while sensors were thoroughly wetted and readings stabilized, typically for 2-3 minutes. At this point, the winch operator was asked to bring the package to just below the surface and then lower to a depth calculated to be approximately 50 metres above the bottom. Visual confirmation of height above the bottom was obtained using an acoustic pinger on the package in conjunction with the Simrad 500 echo sounder and in addition to altimeter readings. The package was then taken to approximately 10 metres above the bottom, marking the end of the downcast. At this point, bottle sample #1 was taken and a 10 second wait initiated if the SBE35 thermometer was present, in order for this instrument to acquire its full compliment of data. The upcast was then continued to the next predetermined stop determined by the amount of wire out rather than an absolute depth. In the early part of the cruise, casts were veered and hauled at 60 metres/minute, which is the normal speed of deployment. Later, on instructions from the Principal Scientist, veering and hauling was accomplished at 70 metres/minute and, for approximately the last third of the casts, hauling was done at 80 metres/minute while veering remained at 70.

Data acquisition was ceased once the instruments had been recovered and were on deck. SBE35 data was recovered using the SeaTerm package and all data files from the cast copied to a USB data key or otherwise transferred to a separate computer for data processing. CTD operators were not involved in data processing.

The early sections across the Florida Straight were beset by problems with some of the instruments, which were subsequently swapped or left out. One major issue appeared to arise from an excessive power drain by the fluorometer, which caused the altimeter to malfunction and give readings in the order of 6 metres once it made contact with the water. By separating these onto different channels, readings from the altimeter became more reliable. At another point, also early in the cruise, the slave computer malfunctioned and had to be swapped for an old spare. This gave rise to a slight increase in modulo error counts, probably as a result of the much slower processor speed of the replacement. In general it provided reliable service for the remainder of the trip.

### Data Logging

The incoming signal from the CTD, via the sea cable, entered the rear of the SBE 11*plus* deck unit. NMEA data from the ships Global Positioning System was also fed to the deck unit. These data were distributed to the main PC and a backup PC, via the SBE 11*plus* deck units RS232 port. Data were logged on both PCs.

## 9. CTD DATA PROCESSING AND CALIBRATION

Hannah Longworth and Stuart Cunningham

Raw CTD data files from the logging PC are transferred to another PC, on which modules from SEASOFT, the SeaBird CTD data processing package, are run manually since batch processing failed after the first station. Of the available SEASOFT routines, those employed are sequentially detailed below. Although the Filter option to smooth high frequency data is recommended by SeaBird, we omit this step. Output files are transferred onto the UNIX system by ftp and processing continued with PSTAR.

### 9.1 Data Conversion (DatCnv)

Converts raw CTD data to calibrated data, creating one file containing the down and upcast CTD data and a rosette summary file.

Input Files: D279nnn.dat, D279nnn.BL

The .dat file contains uncalibrated engineering data output from the CTD, processed by the deck unit and logged to PC. The .BL file contains one record for each bottle fire: bottle number, date, time, scan number start, scan number end. When a bottle fire confirmation is received from the rosette the bottle confirmation bit is set for 1.5s or 36 scans, and these are the scan numbers recorded in the .BL file.

Output Files: D279nnn.cnv, D279nnn.ros

The .cnv file contains 24hz calibrated CTD data, with output variables determined by parameters set in the DatCnv specification file DatCnv.psu. Calibration data are read from the configuration file, which can be either a master file for the cruise or usually from a configuration file created for each station: D279nnn.CON. For D279, the output variables are given in Table 9.1. The .ros file is created from an option set in the DatCnv.psu file (create both bottle and data file). For D279, we specify the scan range offset to be 0s and the scan range duration to be 0.001s. This specification means only the first scan marked with the bottle confirmation bit recorded in the .BL file is recorded in the .ros output file. This can be confirmed by inspecting the scan number start in the .BL file and comparing it to the scan number in the .ros file. NB the .ros file contains only a single scan of CTD data at the time at which the first bottle confirmation bit is set.

Table 9.1: Calibrated CTD data output by SeaBird data conversion module DatCnv.

Number	Parameter	Unit
1	Pressure, Digiquartz	db
2	Temperature	ITS-90, deg C
3	Conductivity	mS/cm
4	Temperature, 2	ITS-90, deg C
5	Conductivity, 2	mS/cm
6	Altimeter	M
7	Oxygen, SBE 43	μmol/Kg
8	Temperature Difference, 2 – 1	ITS-90, deg C
9	Conductivity Difference, 2 – 1	mS/cm
10	Pressure Temperature	deg C
11	Fluorescence, Chelsea Aqua 3 Chl Con	μg/l
12	Beam Attenuation, Chelsea/Seatech/Wetlab CStar	1/m
13	Beam Transmission, Chelsea/Seatech/Wetlab Cstar	%
14	Time Elapsed	seconds
15	Julian Days	
16	Latitude	deg
17	Longitude	deg
18	Flag	

## 9.2 Align CTD

Aligns parameter data in time relative to pressure to reduce spiking or hysteresis.

Input and Output File: D279nnn.cnv

Coefficients for temperature and conductivity sensors are set to zero (the time response of the former is 0.06s and the required advancement for the latter of 1.75 scans is performed by the deck unit). Oxygen is advanced by +5s relative to pressure, accounting for time delay of the sensor (5s at 0°C).

The following are added to the data file header by the program: Alignctd\_date – date and time the program was run; Alignctd\_in – input .cnv file; Alignctd\_adv – alignment times of relevant variables.

## 9.3 Wild Edit

Input and Output File: D279nnn.cnv

The mean and standard deviation of each parameter are separately calculated for blocks of 500 cycles. Points that lie outside two times the standard deviation are temporarily excluded for recalculation of the standard deviation. Points outside ten times of the new value are replaced by a bad flag.

## 9.4 Cell Thermal Mass

Input and Output File: D279nnn.cnv

Removes conductivity cell thermal mass effects with a recursive filter permitting salinity accuracy greater than 0.01 in regions of steep gradients. In such regions the correction may be of the order 0.005 but is otherwise negligible. The thermal anomaly amplitude ( $\alpha$ ) is 0.03 and the thermal anomaly time constant ( $1/\beta$ ) is 7.0.

Cell Thermal Mass adds the following to the header: Celltm\_date – date and time the program was run; Celltm\_in – input .cnv file; Celltm\_alpha – value of  $\alpha$ ; Celltm\_tau – value of  $1/\beta$ ; Celltm\_temp\_senso\_use\_for\_cond – the temperature sensors used for the primary and secondary conductivity filters.



## 9.5 Translate (Trans)

Input and Output File: D279nnn.cnv

Creates an ASCII version of the binary .cnv file.

## 9.6 CTD Processing

Processing of CTD profiles beyond the .cnv files and assimilation of bottle sample data are performed by PSTAR routines. Only those that differ to those of previous cruises (Bryden, 2003) are described fully here. PSTAR execs *ctd0*, *ctd1*, *ctd2*, *ctd3*, *fir0*, *sam0* and *position\_D279.exec* create files *ctd279{num}.24hz*, *ctd279{num}.1hz* and *ctd279{num}.10s*, *ctd279{num}.2db* and *ctd279{num}.ctu* files, preliminary plots, *fir279{num}*, *sam279{num}* and *{num}.position* files respectively (the ctu file is equal to the 1hz file between the start of the downcast and the end of the upcast). Positions are obtained from the GPS file *adnv2791*. *Instrument\_serial\_number.exec* extracts the temperature, conductivity and pressure sensor serial numbers from the .cnv file and writes these into the header of the 24hz file. *Adddepth.exec* and *Adddepth\_D279.exec* both write the water column depth at the times of the start, bottom and end of the CTD cast into the *{num}.position* file. The former uses the maximum depth from pressure and corresponding altimeter height from the 2db file. The latter extracts depths from the 5 minute averaged edited bathymetry file (*sim279k1.ed5min*) when altimeter data are not available or appear erroneous. This is the case for stations 1-24, 26, 61-63, 66, 67 96, 97 and 110 (the altimeter was not working or disconnected for the first 24 stations and for some deep stations the maximum depth was out of its range). Linear interpolation of depth on time is used if bad data have been edited out of the bathymetry file on station. Processing routines involved in calibration are described in the relevant sections below.

## 9.7 Calibration Introduction

All data processing for this cruise originates at the 24hz file (in contrast to the usual 1hz file). Conductivity and oxygen calibrations are applied to the 24hz version and worked through by *reprocess1.exec* that runs *ctd1* and *ctd2* then pastes the updated values into the firing and sample files. The final salinity offset, however, is applied to the 1hz and 10s files (see later). In retrospect, use of the 24hz files is not ideal, and creation of backup copies in calibration is slow and costly on disk space.

Bottle sample data are entered onto a Mac as text (tab delimited) files with names *{parameter}279{num}.txt*. The PSTAR exec *{parameter}.exec* transfers sample data onto the UNIX system and writes it into a PSTAR file *{parameter}279{num}.bot*. These values are pasted into the individual station sample files, *sam279{num}*, by *pas{parameter}*. Oxygen is an exception described

later. The *sam279{num}.calib* files are created by *botcond\_D279.exec*. Bottle conductivity (from bottle salinity) and (CTD – bottle) comparisons for conductivity, salinity and oxygen are calculated. The *sam279{num}.calib* are appended by *samappendcalib.exec* to *sam.append.calib* with statistics in *sam.append.calib.stat*.

## 9.8 CTD Conductivity Calibration

CTD conductivities are calibrated by comparing them to bottle conductivities derived from salinity samples obtained during the CTD upcast (see below for details). The CTD upcast is calibrated and applied to the downcast: the downcast and upcast must be free from hysteresis effects for this to be a valid procedure.

## 9.9 Method

The correction applied to CTD conductivity is a slope correction to account for sensor drift (usually to lower values with time). This is equal to the station mean ratio of bottle to CTD conductivity:

$$K = \langle C_{\text{bot}}/C_{\text{CTD}} \rangle$$

$C_{\text{bot}}$  is the bottle conductivity obtained from the salinity measured,  $C_{\text{CTD}}$  is the upcast CTD conductivity for the 10s around the bottle fire time (see below) and  $\langle \rangle$  denotes the station mean. The corrected CTD conductivity ( $C_{\text{corr}}$ ) is given by:

$$C_{\text{corr}} = K * C_{\text{CTD}}$$

Differences between  $C_{\text{bot}}$  and  $C_{\text{CTD}}$  are not solely due to calibration effects, particularly in the variable upper water column. To minimise the effect of the latter, differences between bottle and CTD conductivities are computed:

$$C_{\text{diff}} = C_{\text{bot}} - C_{\text{CTD}}$$

Bottles with  $C_{\text{diff}}$  outside the limits of Table 9.2 are rejected from the calibration dataset. For the remaining bottles, the mean ( $\mu$ ) and standard deviation ( $\sigma$ ) are re-computed and K values outside  $\mu \pm 2\sigma$  are rejected. The station mean K is that of the remaining points. For shallow stations with few bottles (2 and 3), bottle selection is by eye. Station groups are identified and the value of K applied is, when possible, the mean of a station group or determined from a linear fit of K to station number. K values applied are in Table 9.3.

Table 9.2:  $C_{\text{diff}}$  limits for pre-calibration bottle rejection.

First Station	Last Station	Upper limit of $C_{\text{diff}}$	Lower limit of $C_{\text{diff}}$
1	10	-0.015	0.015
12	37	-0.010	0.010
38	93	-0.015	0.010
94	125	-0.010	0.010

After the K value calibration, station groups 38-93 and 94-120 still showed pressure dependence in  $C_{\text{diff}}$  (note the sensor change at station 94). Correction by a pressure dependent offset added to conductivity of two forms was investigated: a linear temperature and pressure fit (dcond\_1) and a quadratic pressure fit (dcond\_2):

$$\text{dcond\_1} = -(a + b \cdot P + c \cdot T)$$

$$\text{dcond\_2} = d \cdot P^2 + e \cdot P + f$$

P and T are the upcast CTD pressure and temperature at the bottle stop. Coefficients are the mean fit to a subset of  $C_{\text{diff}}$  after first rejection of bottles with  $|C_{\text{diff}}| > 0.01$  and then rejection of those outside the recomputed  $\mu \pm 1.5\sigma$ . For stations 38-93, neither dcond\_1, dcond\_2 or a combination of both corrected the pressure dependence satisfactorily. The secondary temperature and conductivity sensors showed a reduced pressure effect and higher stability. The swap is made in the 24hz file and the primary (secondary) values renamed to secondary (primary). A pressure fit is still required, with best results achieved by dcond\_1 in the upper water column and dcond\_2 below, as is also the case for stations 94-120. The transition between corrections is at the pressure intersection between the two: pressure = Div in Table 9.4.

Table 9.3: CTD conductivity and salinity calibration coefficients applied. For coefficients of pressure fit A and B see Table 9.4.

Station	K	Pressure Fit	dsal	17	0.999860	None	0.0003	34	0.999889	None	-0.0003
1	1.000130	None	0.0004	18	0.999860	None	0.0001	35	0.999860	None	0.0000
2	1.000100	None	-0.0001	19	0.999860	None	0.0005	36	0.999831	None	0.0000
3	1.000070	None	-0.0001	20	0.999860	None	0.0008	37	0.999831	None	0.0001
4	1.000030	None	0.0002	21	0.999860	None	0.0001	38	0.999915	Fit A	0.0003
5	1.000030	None	0.0001	22	0.999860	None	-0.0004	39	0.999915		0.0002
6	1.000030	None	0.0005	23	0.999860	None	0.0007	40	0.999915		-0.0002
7	1.000030	None	0.0002	24	0.999860	None	0.0009	41	0.999915		0.0003
8	1.000030	None	0.0008	25	0.999860	None	-0.0001	42	0.999885		0.0000
9	1.000030	None	-0.0007	26	0.999860	None	-0.0003	43	0.999927		0.0003
10	1.000030	None	-0.0009	27	0.999860	None	-0.0002	44	0.999915		0.0000
11	NaN	NaN	NaN	28	NaN	NaN	NaN	45	0.999904		0.0001
12	1.000058	None	-0.0003	29	0.999860	None	0.0000	46	0.999893		0.0006
13	1.000046	None	-0.0002	30	0.999860	None	0.0001	47	0.999882		-0.0001
14	1.000033	None	0.0001	31	0.999700	None	0.0000	48	0.999871		0.0002
15	1.000021	None	-0.0002	32	0.999859	None	0.0001	49	0.999892		-0.0003
16	1.000008	None	0.0001	33	0.999873	None	-0.0004	50	0.999892		-0.0001

51	0.999892	Fit A	-0.0003	69	0.999900	Fit A	0.0004	87	0.999906	Fit A	0.0002	
52	0.999892	<div></div>	-0.0004	70	0.999905	<div></div>	-0.0002	88	0.999893	<div></div>	0.0000	
53	0.999892		0.0002	71	0.999911		0.0001	89	0.999913		-0.0001	
54	0.999892		-0.0001	72	0.999916		0.0000	90	0.999913		0.0001	
55	0.999892		-0.0001	73	0.999921		0.0002	91	0.999913		0.0001	
56	0.999892		-0.0001	74	0.999927		-0.0007	92	0.999913		0.0003	
57	0.999892		0.0000	75	0.999932		-0.0003	93	0.999915		0.0001	
58	0.999892		0.0003	76	0.999938		-0.0006	94	0.999977	Fit B	-0.0003	
59	0.999892		0.0000	77	0.999923		0.0002	95	0.999977	<div></div>	-0.0002	
60	0.999892		-0.0002	78	0.999923		0.0001	96	0.999977		0.0000	
61	0.999892		0.0000	79	0.999923		0.0003	97	0.999977		0.0008	
62	0.999892		0.0002	80	0.999923		0.0000	98	0.999943		0.0000	
63	0.999892		0.0006	81	0.999923		-0.0002	99	0.999964		0.0004	
64	0.999879		0.0001	82	0.999893		0.0002	100	0.999986		-0.0004	
65	0.999893		0.0002	83	0.999908		0.0002	101	0.999985		-0.0007	
66	0.999907		-0.0001	84	0.999908		0.0000	102	0.999985		-0.0001	
67	0.999889		0.0000	85	0.999932		-0.0001	103	0.999985	0.0004		
68	0.999894		0.0003	86	0.999919		0.0004	104	0.999985	-0.0002		
<div></div>				<div></div>				<div></div>				
<div></div>								<div></div>				

105	0.999985	Fit B	0.0001	123	0.999992	None	0.0000
106	0.999985		-0.0004	124	0.999992	None	0.0005
107	0.999985		0.0001	125	0.999992	None	-0.0002
108	0.999985		0.0001				
109	0.999985		-0.0004				
110	0.999985		-0.0002				
111	0.999985		0.0004				
112	0.999985		-0.0001				
113	1.000015		-0.0002				
114	0.999991		0.0000				
115	0.999991		0.0001				
116	0.999991		-0.0004				
117	1.000016		-0.0004				
118	1.000016		-0.0002				
119	1.000050		0.0000				
120	0.999950		-0.0005				
121	0.999992	None	0.0005				
122	0.999992	None	-0.0003				

Table 9.4: Coefficients of dcond\_1 and dcond\_2 applied.

	<b>a</b>	<b>b</b>	<b>c</b>	<b>Div (db)</b>	<b>d</b>	<b>e</b>	<b>f</b>
Fit A	-0.968	$1.51 \times 10^{-4}$	$1.1562 \times 10^{-1}$	2250	$1.213 \times 10^{-10}$	$-9.358 \times 10^{-7}$	$1.731 \times 10^{-3}$
Fit B	-0.482	$2.97 \times 10^{-4}$	$-4.661 \times 10^{-2}$	2050	$1.399 \times 10^{-10}$	$-1.284 \times 10^{-6}$	$2.107 \times 10^{-3}$

NB. Fit A is applied to stations 38-93, Fit B to 94-120 (see Table 9.3).

Finally a station by station salinity offset is added to CTD salinity:

$$dsal = \langle S_{bot} - S_{CTD} \rangle$$

Notation follows that used above with S denoting salinity. The station mean dsal is computed after rejection of bottles with  $|S_{bot} - S_{CTD}| > 0.002$  (0.003 for stations 12, 51 and 107 due to increased scatter), and subsequent rejection of those outside the recomputed  $\mu \pm 2\sigma$ . The statistics relating to this fit are in Table 9.5, with the final value applied in Table 9.3. The dsal correction is not applied to station 119 due to the large scatter in  $C_{diff}$  for this station, the source of which has not been determined. Final salinity residuals are plotted in Figures 9.1a and 9.1b. The station summary for cruise D279 is found in section 9.11.

Table 9.5: Bottle-CTD salinity residual mean ( $\mu$ ) and standard deviation ( $\sigma$ ).  $N_{tot}$  is the total number of bottle samples and N those used to compute the mean and % is the percent rejected.

$\mu$	$\sigma$	N	$N_{tot}$	%	Limits	Notes
0.0007	0.0003	2139	2626	18.5	$\pm 0.002, \pm 2\sigma$	Before application of dsal
0.0001	0.0011	2338	2626	11.0	$\pm 0.01, \pm 2\sigma$	Final data set
-0.00006	0.0005	1274	1305	2.4	$P > 1500db, \pm 0.002$	Final data set

## 9.10 Calibration Application

Three calibration execs are used: *ctdcondcal\_D279.exec*, *ctdcondcal\_D279.exec\_press* and *reprocess.exec\_final*. The first applies the K value correction to the primary conductivity in the 24hz file and writes the K value into the header. The second applies the pressure dependant fit detailed above, also to the 24hz file. The third applies dsal to salinity in the 10s and 1hz files, computes conductivity from the corrected salinity and works these through to the ctu, 2db, fir and sam files.

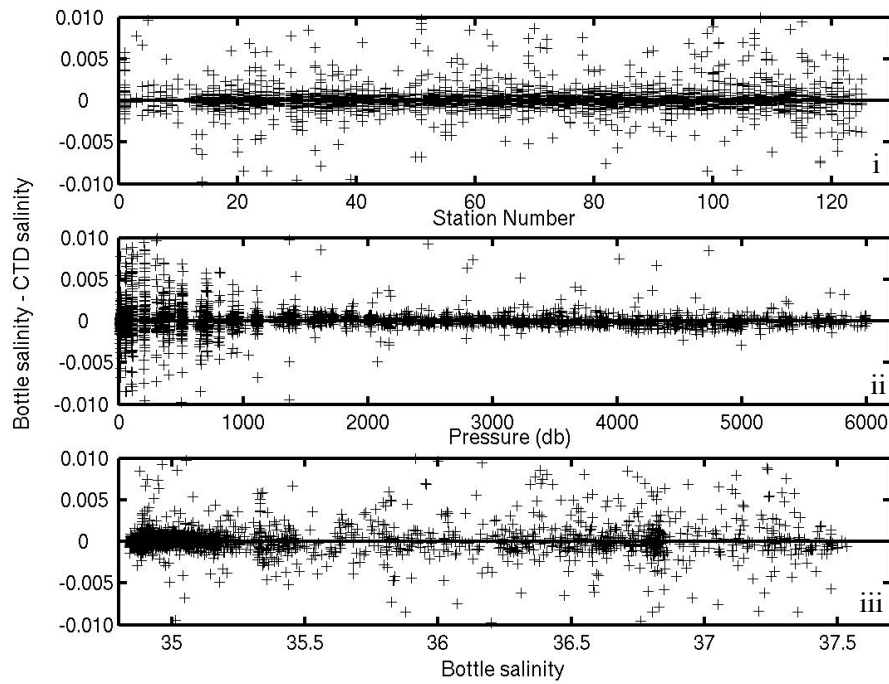


Figure 9.1a: Bottle – CTD salinity versus i. station number, ii. pressure and iii. bottle salinity. Selection limits are  $|S_{\text{bot}} - S_{\text{CTD}}| < 0.01$ .

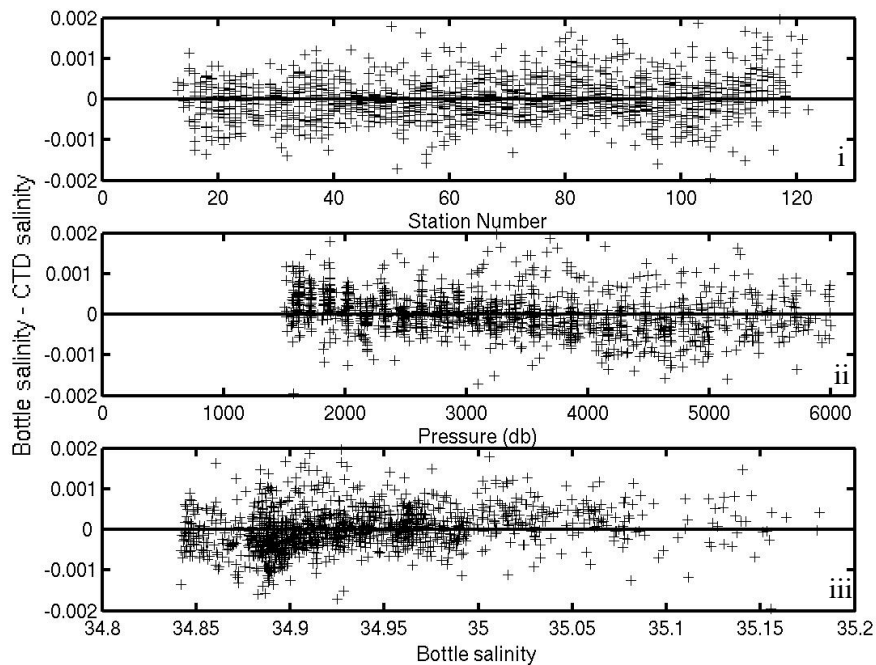


Figure 9.1b: Bottle – CTD salinity versus i. station number, ii. pressure and iii. bottle salinity for pressure  $> 1500\text{db}$ . Selection limits are  $|S_{\text{bot}} - S_{\text{CTD}}| < 0.002$  (refer to Table 9.5 for statistics of bottles rejected).



### 9.11 D277 and D278

CTD data were calibrated in the manner described above, but only applying corrections to the conductivity slope (Table 9.6). Residuals of bottle-CTD conductivities are given in Table 9.7. Station summaries are shown in Tables 9.8, 9.9 and 9.10.

Table 9.6: Conductivity slope and offset corrections.

Station Number	D277 Slope	D277 Offset	D278 Slope	D277 Offset
1	0.9999982	0.0	1.000012	0.0
2	0.9999982	0.0	1.000012	0.0
3	0.9999982	0.0	1.000012	0.0
4	0.9999982	0.0	1.000012	0.0
5	0.9999982	0.0	1.000012	0.0
6	0.9999982	-0.0023	1.000012	0.0
7	0.9999982	0.001	1.000012	0.0
8	0.9999982	0.001	1.000012	0.0
9	0.9999982	0.001	1.000012	0.0
10	0.9999982	0.001	0.999812	0.0
11	0.9999982	0.001	0.999812	0.0
12	0.9999982	0.001	0.999812	0.0
13			1.000012	0.0
14			1.000012	0.0
15			1.000012	0.0
16			1.000012	0.0

Table 9.7: Bottle-CTD conductivity residuals.

	<b>277</b>	<b>278</b>
<btc-uc>	-0.00002	-0.00002
sd	0.0010	0.0006
n bottles	40/43	84/93
<btc/uc>	0.999995	0.999996
Sd	0.000031	0.000023
n bottles	39/43	86/93

Table 9.8: D277 CTD Station Summary. Florida Current section stations 5 to 12 occupied east to west.

statnum	date				lat	lat	lon	lon	pmin	pmax	depth_pmax	cordepth	cordepth-depth_pmax
	yyyy	mm	dd	hhmmss	deg	min	deg	min	dbar	dbar	m	m	m
001	2004	3	8	151558	24	28.82	-55	55.56	1	6341	6209	6131.6	-77.3
002	2004	3	8	205158	24	26.64	-56	02.03	1	5119	5026	6451.7	1425.5
003	2004	3	9	012353	24	25.44	-56	01.38	1	6559	6419	6454.2	35
004	2004	3	12	155834	26	31.38	-72	38.26	1	5065	4973	5186.5	213.5
005	2004	3	14	203608	27	00.26	-79	12.23	1	477	473	485.7	12.5
006	2004	3	14	232834	27	00.16	-79	17.14	1	611	606	617.5	11.6
007	2004	3	15	010703	27	00.55	-79	23.30	1	689	683	681.9	-1.2
008	2004	3	15	031006	27	00.08	-79	29.55	1	759	752	764	11.6
009	2004	3	15	052013	27	00.84	-79	37.44	1	623	618	631.9	14.1
010	2004	3	15	074250	27	00.66	-79	41.19	1	525	521	535.1	14.4
011	2004	3	15	091803	27	00.57	-79	46.72	1	387	384	400	16
012	2004	3	15	105048	26	59.97	-79	51.89	1	263	261	275	14

Table 9.9: D278 CTD Station Summary: Coherent CTD section east to west can be made from stations: 1,2,3,4,15,14,13,12,11,10,9,8,7,6. Stations 4 and 16 are in the same position but station 4 makes a more synoptic section with the inshore boundary stations 1,2,3. Station 5 is only to mid-depth.

statnum	date				lat	lat	lon	lon	pmin	pmax	depth_pmax	cordepth	cordepth-depth_pmax
	yyyy	mm	dd	hhmmss	deg	min	deg	min	dbar	dbar	m	m	m
001	2004	3	22	111601	26	30.37	-71	58.12	1	5395	5293.1	5297.9	4.8
002	2004	3	22	213729	26	30.11	-73	21.07	1	5121	5027.4	5033.6	6.2
003	2004	3	23	073346	26	29.67	-74	42.24	1	4513	4436.6	4464.9	28.3
004	2004	3	24	042000	26	30.01	-76	03.72	1	4863	4776.9	4796	19.1
005	2004	3	25	194433	26	31.29	-76	39.34	9	1005	995.8	4496.2	3500.4
006	2004	3	27	042107	26	31.90	-76	53.67	3	39	38.7	38.8	0.1
007	2004	3	27	063515	26	31.47	-76	49.00	9	1377	1363.2	1409.5	46.3
008	2004	3	27	102718	26	30.88	-76	47.07	7	2631	2597.4	2679	81.6
009	2004	3	27	152620	26	30.99	-76	45.40	7	3693	3637.1	3654.2	17.1
010	2004	3	28	042408	26	30.24	-76	39.96	7	4555	4477.4	4487.6	10.2
011	2004	3	28	091344	26	30.65	-76	38.31	7	4687	4605.8	4576.6	-29.2

statnum	date				lat	lat	lon	lon	pmin	pmax	depth_pmax	cordepth	cordepth-depth_pmax
	yyyy	mm	dd	hhmmss	deg	min	deg	min	dbar	dbar	m	m	m
012	2004	3	28	134609	26	30.44	-76	32.06	7	4881	4794.3	4846.2	51.9
013	2004	3	28	210426	26	30.40	-76	26.16	7	4895	4807.9	4848.5	40.6
014	2004	3	29	033638	26	29.62	-76	18.64	7	4907	4819.6	4831.7	12.1
015	2004	3	29	092333	26	30.19	-76	13.04	7	4895	4808	4818.7	10.7
016	2004	3	29	145059	26	29.64	-76	05.45	7	4881	4794.4	-999	-999

Table 9.10: D279 CTD Station Summary

statnum	date				lat	lat	lon	lon	pmin	pmax	depth_pmax	cordepth	cordepth- depth_pmax	alt
num	year	mnth	day	hhmmss	deg	min	deg	min	dbar	dbar	m	m	m	m
002	2004	04	05	063352	027	0.86	-079	56.19	1.0	127.0	126.1	134.2	8.1	7.8
003	2004	04	05	084038	027	1.75	-079	51.75	1.0	255.0	253.1	269.7	16.6	8.3
004	2004	04	05	103021	027	1.04	-079	46.57	1.0	383.0	380.0	393.8	13.8	6.6
005	2004	04	05	130901	027	0.89	-079	40.95	3.0	525.0	520.7	532.2	11.5	6.6
006	2004	04	05	160717	027	0.94	-079	37.05	1.0	633.0	627.7	641.6	13.9	6.6
007	2004	04	05	185640	027	0.93	-079	30.21	1.0	763.0	756.4	755.1	-1.3	6.0
008	2004	04	05	213415	027	0.89	-079	23.28	1.0	677.0	671.2	665.6	-5.6	0.0
009	2004	04	05	234444	027	0.04	-079	16.84	1.0	605.0	600.0	606.6	6.6	0.0
010	2004	04	06	015718	026	59.92	-079	11.66	1.0	457.0	453.3	461.2	7.9	0.0
011	2004	04	06	175523	026	30.42	-076	55.64	1.0	343.0	340.4	305.5	-34.9	0.0
012	2004	04	07	210433	026	30.48	-076	55.64	1.0	263.0	261.0	248.7	-12.3	0.0
013	2004	04	07	232244	026	31.63	-076	48.38	1.0	1727.0	1708.4		1708.4	0.0

statnum	date				lat	lat	lon	lon	pmin	pmax	depth_pmax	cordepth	cordepth- depth_pmax	alt
num	year	mnth	day	hhmmss	deg	min	deg	min	dbar	dbar	m	m	m	m
014	2004	04	08	033038	026	30.76	-076	46.91	3.0	2359.0	2330.3		2330.3	0.0
015	2004	04	08	081613	026	30.91	-076	44.73	1.0	3875.0	3814.8	3813.0	-1.8	0.0
016	2004	04	08	141534	026	30.52	-076	41.29	3.0	4501.0	4424.9	4357.8	-67.1	0.0
017	2004	04	08	204428	026	30.45	-076	38.25	1.0	4687.0	4605.8	4594.5	-11.3	0.0
018	2004	04	09	081118	026	29.95	-076	31.67	1.0	4907.0	4819.6	4835.7	16.1	6.2
019	2004	04	09	150154	026	30.03	-076	25.75	3.0	4913.0	4825.4	4833.4	8.0	0.0
020	2004	04	09	211812	026	29.55	-076	18.11	1.0	4919.0	4831.3	4829.0	-2.3	0.0
021	2004	04	10	024826	026	29.23	-076	12.59	3.0	4883.0	4796.3	4807.4	11.1	0.0
022	2004	04	10	085617	026	29.93	-076	5.74	1.0	4881.0	4794.4	4797.9	3.5	0.0
023	2004	04	10	140639	026	30.15	-075	54.62	3.0	4819.0	4734.1	4737.0	2.9	0.0
024	2004	04	10	191130	026	29.50	-075	42.22	1.0	4763.0	4679.7	4682.9	3.2	0.0
025	2004	04	11	003243	026	28.92	-075	30.87	1.0	4757.0	4673.9	4685.1	11.2	5.9
026	2004	04	11	055337	026	29.49	-075	18.46	1.0	4713.0	4631.1	4630.4	-0.7	0.0

statnum	date				lat	lat	lon	lon	pmin	pmax	depth_pmax	cordepth	cordepth- depth_pmax	alt
num	year	mnth	day	hhmmss	deg	min	deg	min	dbar	dbar	m	m	m	m
027	2004	04	11	112156	026	30.93	-075	4.47	1.0	4675.0	4594.1	4603.8	9.7	6.4
028	2004	04	11	161900	026	30.63	-074	47.85	1.0	2829.0	2791.6	2846.6	55.0	14.6
029	2004	04	11	184935	026	30.57	-074	47.34	1.0	4601.0	4522.2	4532.5	10.3	10.3
030	2004	04	12	005450	026	31.20	-074	29.80	1.0	4551.0	4473.5	4487.3	13.8	7.7
031	2004	04	12	055538	026	30.58	-074	14.18	1.0	4593.0	4514.4	4528.7	14.3	8.8
032	2004	04	12	111717	026	30.07	-073	55.79	1.0	4737.0	4654.4	4665.6	11.2	7.2
033	2004	04	12	165524	026	30.63	-073	33.82	1.0	4953.0	4864.3	4872.4	8.1	6.0
034	2004	04	12	224252	026	29.97	-073	11.74	1.0	5131.0	5037.1	5048.1	11.0	6.3
035	2004	04	13	043711	026	30.13	-072	50.82	1.0	5223.0	5126.3	5136.2	9.9	6.0
036	2004	04	13	113152	026	29.98	-072	29.16	1.0	5291.0	5192.3	5204.2	11.9	5.9
037	2004	04	13	182505	026	29.29	-072	0.39	1.0	5381.0	5279.5	5287.2	7.7	6.5
038	2004	04	14	002334	026	28.98	-071	45.11	1.0	5465.0	5360.9	5373.3	12.4	10.5
039	2004	04	14	071010	026	30.48	-071	20.60	1.0	5579.0	5471.4	5482.9	11.5	6.3



statnum	date				lat	lat	lon	lon	pmin	pmax	depth_pmax	cordepth	cordepth- depth_pmax	alt
num	year	mnth	day	hhmmss	deg	min	deg	min	dbar	dbar	m	m	m	m
040	2004	04	14	131758	026	29.40	-070	59.20	1.0	5583.0	5475.2	5487.7	12.5	6.2
041	2004	04	14	200529	026	8.03	-070	36.07	1.0	5597.0	5488.9	5500.4	11.5	6.1
042	2004	04	15	024035	025	45.91	-070	14.29	1.0	5607.0	5498.8	5510.5	11.7	6.7
043	2004	04	15	092831	025	22.82	-069	52.64	1.0	5615.0	5506.7	5516.7	10.0	6.5
044	2004	04	15	163108	025	0.05	-069	30.37	1.0	5705.0	5593.9	5604.8	10.9	6.6
045	2004	04	16	001844	024	29.65	-069	8.80	1.0	5741.0	5629.0	5638.4	9.4	6.3
046	2004	04	16	082202	024	30.53	-068	24.80	1.0	5815.0	5700.6	5710.3	9.7	8.2
047	2004	04	16	162927	024	30.65	-067	40.24	1.0	5819.0	5704.5	5713.1	8.6	5.5
048	2004	04	17	000841	024	29.24	-066	55.39	1.0	5839.0	5723.8	5732.9	9.1	6.6
049	2004	04	17	073836	024	30.17	-066	11.54	1.0	5367.0	5266.7	5276.4	9.7	8.8
050	2004	04	17	151325	024	29.75	-065	27.81	1.0	5663.0	5553.5	5563.4	9.9	9.9
051	2004	04	17	230648	024	30.55	-064	39.57	1.0	5803.0	5689.0	5696.5	7.5	7.0
052	2004	04	18	064953	024	29.87	-064	0.08	1.0	5881.0	5764.4	5774.3	9.9	8.0

statnum	date				lat	lat	lon	lon	pmin	pmax	depth_pmax	cordepth	cordepth- depth_pmax	alt
num	year	mnth	day	hhmmss	deg	min	deg	min	dbar	dbar	m	m	m	m
053	2004	04	18	150313	024	30.30	-063	16.08	1.0	5901.0	5783.8	5791.8	8.0	6.4
054	2004	04	18	225903	024	30.24	-062	31.68	1.0	5995.0	5874.7	5890.3	15.6	7.1
055	2004	04	19	064743	024	30.45	-061	47.90	1.0	5793.0	5679.3	5692.2	12.9	6.8
056	2004	04	19	143709	024	30.07	-061	3.78	1.0	5963.0	5843.7	5850.1	6.4	6.2
057	2004	04	19	223811	024	30.71	-060	19.39	3.0	5955.0	5836.0	5859.9	23.9	8.1
058	2004	04	20	064117	024	30.92	-059	35.51	1.0	5903.0	5785.7	5796.7	11.0	7.4
059	2004	04	20	145036	024	29.89	-058	51.47	1.0	5997.0	5876.6	5914.9	38.3	6.5
060	2004	04	20	222259	024	29.97	-058	7.95	1.0	5927.0	5808.9	5822.4	13.5	8.2
061	2004	04	21	060806	024	30.13	-057	23.33	1.0	5989.0	5868.9	6274.7	405.8	6.0
062	2004	04	21	140223	024	29.71	-056	40.03	1.0	6003.0	5882.4	5985.2	102.8	12.6
063	2004	04	21	214934	024	31.02	-055	56.12	1.0	5959.0	5839.9	6462.4	622.5	6.6
064	2004	04	22	055315	024	30.27	-055	12.75	1.0	5993.0	5872.7	5884.5	11.8	11.8
065	2004	04	22	133440	024	29.98	-054	28.42	1.0	5297.0	5198.9	5209.4	10.5	6.1

statnum	date				lat	lat	lon	lon	pmin	pmax	depth_pmax	cordepth	cordepth- depth_pmax	alt
num	year	mnth	day	hhmmss	deg	min	deg	min	dbar	dbar	m	m	m	m
066	2004	04	22	212402	024	29.66	-053	44.17	1.0	5999.0	5878.5	5965.8	87.3	11.3
067	2004	04	23	042216	024	29.86	-053	10.68	1.0	5437.0	5334.6	5433.5	98.9	10.1
068	2004	04	23	111544	024	30.27	-052	38.24	1.0	5367.0	5266.7	5278.8	12.1	6.8
069	2004	04	23	172610	024	29.96	-052	9.68	1.0	5005.0	4915.5	4922.6	7.1	5.5
070	2004	04	24	003548	024	29.99	-051	32.27	1.0	5389.0	5288.1	5300.3	12.2	7.7
071	2004	04	24	072418	024	30.46	-050	59.82	1.0	5525.0	5419.8	5429.2	9.4	8.9
072	2004	04	24	141849	024	29.97	-050	26.50	1.0	4793.0	4709.5	4717.1	7.6	7.6
073	2004	04	24	203450	024	30.61	-049	52.51	1.0	4643.0	4563.7	4579.9	16.2	9.8
074	2004	04	25	031400	024	30.43	-049	20.04	1.0	5315.0	5216.3	5228.9	12.6	10.8
075	2004	04	25	095755	024	29.84	-048	46.48	1.0	4487.0	4411.9	4426.2	14.3	14.3
076	2004	04	25	171051	024	30.33	-047	57.76	1.0	4013.0	3950.0	3958.5	8.5	8.1
077	2004	04	26	002410	024	29.93	-047	7.50	1.0	3539.0	3487.2	3498.8	11.6	11.6
078	2004	04	26	060434	024	29.75	-046	34.48	1.0	3331.0	3283.8	3295.9	12.1	6.9

statnum	date				lat	lat	lon	lon	pmin	pmax	depth_pmax	cordepth	cordepth- depth_pmax	alt
num	year	mnth	day	hhmmss	deg	min	deg	min	dbar	dbar	m	m	m	m
079	2004	04	26	111506	024	29.73	-046	2.14	1.0	2795.0	2758.7	2764.1	5.4	5.4
080	2004	04	26	163918	024	30.29	-045	29.42	1.0	3467.0	3416.8	3426.6	9.8	5.8
081	2004	04	26	222743	024	29.15	-044	56.75	1.0	3653.0	3598.6	3605.2	6.6	6.6
082	2004	04	27	042956	024	30.12	-044	23.74	1.0	3933.0	3872.0	3884.0	12.0	6.8
083	2004	04	27	102807	024	30.01	-043	50.63	1.0	3831.0	3772.4	3781.8	9.4	9.4
084	2004	04	27	172542	024	30.58	-043	0.43	1.0	4171.0	4104.1	4111.8	7.7	7.7
085	2004	04	28	005257	024	29.94	-042	11.05	1.0	4031.0	3967.6	3980.2	12.6	7.6
086	2004	04	28	072045	024	30.52	-041	38.39	1.0	4687.0	4606.5	4618.8	12.3	10.0
087	2004	04	28	134951	024	30.19	-041	5.52	1.0	5215.0	5119.3	5129.1	9.8	9.8
088	2004	04	28	212726	024	30.71	-040	16.89	1.0	4931.0	4843.6	4853.9	10.3	8.8
089	2004	04	29	063628	024	29.87	-039	14.70	1.0	5257.0	5160.1	5172.3	12.2	12.2
090	2004	04	29	134617	024	29.94	-038	31.41	1.0	4699.0	4618.1	4626.8	8.7	8.7
091	2004	04	29	212907	024	29.95	-037	41.71	1.0	5621.0	5512.8	5531.9	19.1	6.9

statnum	date				lat	lat	lon	lon	pmin	pmax	depth_pmax	cordepth	cordepth- depth_pmax	alt
num	year	mnth	day	hhmmss	deg	min	deg	min	dbar	dbar	m	m	m	m
092	2004	04	30	053129	024	29.36	-036	52.80	1.0	5385.0	5284.2	5296.1	11.9	6.0
093	2004	04	30	130329	024	29.56	-036	2.75	1.0	5837.0	5721.9	5730.9	9.0	9.0
094	2004	04	30	204555	024	30.27	-035	13.72	1.0	5131.0	5037.8	5047.1	9.3	6.1
095	2004	05	01	042410	024	29.75	-034	23.35	1.0	5123.0	5030.0	5045.7	15.7	6.2
096	2004	05	01	115048	024	29.95	-033	34.39	1.0	5993.0	5872.7	6213.5	340.8	9.5
097	2004	05	01	200457	024	30.58	-032	39.43	1.0	5991.0	5870.8	6263.0	392.2	7.8
098	2004	05	02	043300	024	29.97	-031	43.85	1.0	5757.0	5644.5	5652.0	7.5	7.5
099	2004	05	02	125009	024	29.71	-030	48.76	1.0	5819.0	5704.5	5720.2	15.7	8.9
100	2004	05	02	210608	024	30.09	-029	53.41	1.0	5829.0	5714.1	5722.3	8.2	8.2
101	2004	05	03	052018	024	30.17	-028	59.25	1.0	5779.0	5665.8	5677.3	11.5	11.5
102	2004	05	03	133005	024	30.08	-028	4.11	1.0	5699.0	5588.3	5598.4	10.1	10.1
103	2004	05	03	213847	024	30.71	-027	8.91	1.0	5621.0	5512.8	5523.9	11.1	11.1
104	2004	05	04	054953	024	29.94	-026	13.87	1.0	5481.0	5377.2	5390.1	12.9	10.9

statnum	date				lat	lat	lon	lon	pmin	pmax	depth_pmax	cordepth	cordepth- depth_pmax	alt
num	year	mnth	day	hhmmss	deg	min	deg	min	dbar	dbar	m	m	m	m
105	2004	05	04	133241	024	30.07	-025	19.06	1.0	5379.0	5278.4	5285.3	6.9	6.9
106	2004	05	04	214116	024	29.72	-024	24.24	1.0	5235.0	5138.7	5150.9	12.2	8.2
107	2004	05	05	054902	024	30.81	-023	29.68	1.0	5095.0	5002.9	5015.3	12.4	12.4
108	2004	05	05	125135	024	44.29	-022	49.34	1.0	4977.0	4888.2	4895.1	6.9	7.0
109	2004	05	05	195445	024	59.10	-022	8.91	1.0	4843.0	4758.0	4768.0	10.0	6.1
110	2004	05	06	022701	025	13.30	-021	28.66	1.0	4601.0	4522.6	4576.7	54.1	7.5
111	2004	05	06	094020	025	27.01	-020	48.26	1.0	4497.0	4421.3	4434.0	12.7	7.4
112	2004	05	06	172535	025	38.99	-020	14.55	1.0	4259.0	4189.5	4199.4	9.9	6.4
113	2004	05	07	083840	025	55.22	-019	29.17	1.0	3833.0	3774.0	3786.8	12.8	5.9
114	2004	05	07	143050	026	8.01	-018	54.59	1.0	3489.0	3437.6	3445.8	8.2	5.9
115	2004	05	07	205726	026	23.13	-018	9.65	1.0	3665.0	3609.8	3621.7	11.9	6.1
116	2004	05	08	030508	026	35.79	-017	28.14	1.0	3693.0	3637.1	3648.4	11.3	11.3
117	2004	05	08	092313	026	48.87	-016	47.08	1.0	3667.0	3611.7	3621.7	10.0	6.3

statnum	date				lat	lat	lon	lon	pmin	pmax	depth_pmax	cordepth	cordepth- depth_pmax	alt
num	year	mnth	day	hhmmss	deg	min	deg	min	dbar	dbar	m	m	m	m
118	2004	05	08	162727	027	2.59	-016	7.32	1.0	3523.0	3470.9	3483.7	12.8	10.8
119	2004	05	08	214035	027	14.01	-015	35.53	1.0	3175.0	3130.4	3141.7	11.3	7.4
120	2004	05	09	035906	027	26.00	-014	51.62	1.0	2615.0	2581.5	2592.1	10.6	10.6
121	2004	05	09	090906	027	37.24	-014	13.72	1.0	2039.0	2015.4	2026.1	10.7	10.7
122	2004	05	09	130459	027	49.75	-013	49.05	1.0	1557.0	1540.6	1548.1	7.5	2.2
123	2004	05	09	154237	027	51.14	-013	33.06	1.0	1091.0	1080.7	1090.3	9.6	9.6
124	2004	05	09	173214	027	52.80	-013	25.19	105.0	603.0	597.9	604.7	6.8	6.8
125	2004	05	09	184757	027	54.94	-013	22.44	1.0	347.0	344.3	355.0	10.7	10.8

## 10. SBE35 DEEP OCEAN STANDARDS THERMOMETER

The SBE35 is a highly accurate and stable laboratory standard deep ocean thermometer that can be used in fixed point calibration cells and at ocean depths up to 6800m, and covers a temperature range from  $-5$  to  $+35^{\circ}\text{C}$ . It is unaffected by shocks and vibrations encountered in shipboard environments (Sea-Bird, 2004) (Table 10.1).

### 10.1 Measurement Method

An ultra stable, aged thermistor with a drift rate of less than  $0.001^{\circ}\text{C}/\text{year}$  and reference resistances are excited by an AC current, and the outputs from these converted to sensor output in raw counts (n).

$$\text{Sensor Output (raw counts, n)} = 1048576 \cdot (\text{NT} - \text{NZ}) / (\text{NR} - \text{NZ})$$

where NR is reference resistor output, NZ is zero ohms output, and NT is thermistor output. The measurement cycle takes  $1.1 \times 8 = 8.8\text{s}$ . In a thermally quiet environment, temperature noise standard deviation is  $0.000029 \times \sqrt{8/\text{ncycles}} = 0.29^{\circ}\text{mC}$ .

### 10.2 Linearisation and Calibration

Temperature is calculated from the sensor output raw counts by:

$$T90 = (1.0/a0 + a1 \ln(n) + a2 \ln^2(n) + a3 \ln^3(n) + a4 \ln^4(n)) - 273.15$$

Temperature residuals are better than  $\pm 50\mu\text{K}$ . Coefficients  $a0$  to  $a4$  are determined by Sea-Bird in a low-gradient temperature bath and against ITS-90 certified standard platinum resistance thermometers maintained at Sea-Bird's temperature metrology laboratory (Table 10.2).

Finally the sensor measurements are certified in a triple water point cell at  $0.0100^{\circ}\text{C}$  and a gallium cell at  $29.7646^{\circ}\text{C}$ , and slow time drifts corrected using slope and offset adjustments as required:

$$T90 = \text{slopet}90 + \text{offset} [\text{degC, ITS-90}]$$



### 10.3 Specification

Table 10.1: SBE 35 specification.

<b>Measurement Range</b>	-5 to +35°C
<b>Initial Accuracy</b>	0.001°C
<b>Typical Stability</b>	0.001°C/year
<b>Resolution</b>	0.000025°C
<b>Sensor Calibration</b>	-1.5 to +32.5°C
<b>Data Storage</b>	Up to 170 samples
<b>Real-Time Clock</b>	Watch-crystal type
<b>External Power</b>	9-16VDC
<b>Current</b>	
<b>On Power (~1 minute)</b>	140-160mA
<b>Operating</b>	60-70mA
<b>Housing Materials</b>	Aluminium, rated at 6800m
<b>Weight</b>	0.5kg in water, 0.9kg in air

### 10.4 Instrument Calibrations

Table 10.2: SBE35 Instrument calibration coefficients.

<b>Instrument s/n</b>	<b>0037</b>	<b>0048</b>
<b>Calibration Date</b>	<b>14/12/01</b>	<b>28/1/03</b>
<b>a0</b>	$3.39029780 \times 10^{-3}$	$4.21014933 \times 10^{-3}$
<b>a1</b>	$-8.90362832 \times 10^{-4}$	$-1.12827756 \times 10^{-3}$
<b>a2</b>	$1.48133804 \times 10^{-4}$	$1.74012910 \times 10^{-4}$
<b>a3</b>	$-8.46647755 \times 10^{-6}$	$-9.73030909 \times 10^{-6}$
<b>a4</b>	$1.85819563 \times 10^{-7}$	$2.09032576 \times 10^{-7}$

## 10.5 Temperature Measurement and Data Output Format for the SBE35

During D279, the SBE35 was set to average 8 (ncycles) temperature measurements at each bottle fire. Measurements occur when the SBE35 receives a valid bottle fire confirmation sequence. At the end of each CTD station, data are uploaded from the SBE35's EEPROM via a software interface and saved as an ascii file in the following format (Table 10.3):

Table 10.3: SBE35 data output format.

Column	Description
1	Sample number
2	Date (DD MMM YYYY –day, month year). The month is a 3-character alphabetic abbreviation; e.g., jan, feb, mar, etc).
3	Time (HH:MM:SS – hour, minute, second)
4	Bn=bottle position number
5	Diff=(maximum – minimum) raw thermistor reading during a measurement (provides a measure of the amount of variation during the measurement)
6	Val=average raw thermistor reading, corrected for <i>zero</i> and <i>full scale</i> reference readings
7	T90=average corrected raw thermistor reading, converted to engineering units (°C[ITS-90])

NB: SBE35 time is stored in the real-time clock with a back-up lithium battery. Time is kept when external power is removed. This time is not from the same source as time recorded within the CTD raw data files.

For comparison to the CTD 10s file, the following time line was adopted during D279:

Time (s) ->

1s *CTD stop* — — — — ➔ 10s *Bottle fire* — — — — ➔ 20s *CTD up*  
5s — — — — ➔ 15s *Average CTD data*  
10s — — *SBE35 record* — — ➔ 18.8s

Therefore, the CTD 10s average file and SBE35 records do not correspond in time but overlap only for the last 5s of the 10s average CTD data. It is important that the CTD is not hauled in sooner than 10s after the bottle fire.

## **10.6 Gallium Cell (A Thermometric Fixed Point)**

Temperature scales are defined by a series of fixed points along the scale. These fixed points are defined by the temperature at which pure materials have phase equilibrium between two or three states (solid, liquid, gas). The triple point of pure water has the assigned value of 0.01°C on the ITS (273.16K). Pure gallium has a solid-liquid equilibrium point temperature of 29.7646±0.00026°C (ITS-90), which is within the range of normal ocean temperatures and can be used as a reference standard for deep ocean thermometers. Isotech have produced a rugged, portable gallium cell that can be used aboard ship for periodic calibrations of the SBE35 deep ocean standards thermometer, and the cell is accompanied by a UK Accreditation Service certificate of traceability to the ITS-90 (Tavener, 2001).

For temperature measurements obtained from a CTD package, the standard deviation of temperatures from pairs of deep ocean platinum resistance thermometers is normally limited by the size of the oceanic vertical temperature gradient. Thus accurate comparisons are limited to ocean depths below the permanent thermocline (deeper than 2000m say), where 98% of the ocean has temperatures colder than 4°C. Hence, precise temperature comparisons of CTD temperature and deep ocean standard thermometers are at temperatures typically 26° to 30°C colder than the transfer standard of the gallium triple point cell.

The gallium in the cell initially begins in the liquid phase, is solidified and then the melting condition is established by holding the cell at a temperature just above the gallium melt temperature. The solid-liquid equilibrium temperature is unaffected by the temperature at which the cell is exposed but the duration of the constant temperature melt plateau is. Measurements of temperature are made by the SBE35 throughout: firstly, the temperature rises as the gallium approaches its melt temperature; secondly, the temperature remains constant until all the gallium has melted; and finally, the end of the melt plateau corresponds to a rise in temperature. The cycle time with the cell starting at 20°C is typically 32mins to reach the melt plateau, then 16 to 20 hours on the plateau and a final 4 hours to refreeze the gallium.

The gallium melt point cell (s/n Ga369) was certified as a temperature reference point (certificate number 04-02-14, issued on the 13<sup>th</sup> February 2004 by Isothermal Technology, Ltd.). The total uncertainty for Ga369 with respect to ITS-90 is ±0.26mK.

## 10.7 Comparison of SBE35 and CTD temperatures

In the upper water column, differences between SBE35 and CTD temperatures may be attributed not only to sensor effects but also to spatial variability in the temperature field:

- \* Noting this, the mean  $\mu \pm 2\sigma$  of the residuals after application of limit 1 is  $-0.001 \pm 0.006$  °C. With the exclusion of Group D ( $-0.003 \pm 0.012$  °C) this is reduced to  $-0.0007 \pm 0.005$  (Tables 10.4 and 10.5, Figure 10.1).

Both primary and secondary CTD temperature sensors appear to be biased towards warmer readings relative to the SBE35. In the deep water ( $> 2000$  dbar and limit 2) the mean bias is  $-0.0006$ °C, and is  $-0.0011$ °C over the full water column (limit 1).

In the deep water (pressures greater than 2000dbar) aspects of sensor performance may be deduced from the residuals:

- \* Figure 10.2 (ii) shows residuals up to  $-1.6 \times 10^{-3}$  °C at 6000dbar between both the primary and secondary CTD sensors and SBE35 for stations 39-89. This is not apparent in Figure 10.2 (iii) when the same CTD sensors are used but with SBE 0048, thus suggesting the large residuals of the former to be associated with a pressure effect in SBE35 0037.
- \* Agreement between CTD temperature sensors 2758 and 2880 and SBE35 00048 is good,  $\mu \pm 2\sigma$  of the residuals are  $0 \pm 0.0006$ °C (Groups C and F, Table 10.5).
- \* Higher variance in residuals of CTD temperature sensor 4116 (Group D), especially noticeable in the deep water with  $\sigma = 7.1 \times 10^{-4}$  °C (while that for other sensors ranges between  $3.0 \times 10^{-4}$  and  $3.9 \times 10^{-4}$  °C), but not in sensor 2919 (the corresponding primary) – this suggests a sensor problem in 4116.

Are primary CTD temperatures more accurate than those from the secondary sensor?

Looking at the performance of CTD temperature sensors relative to the SBE35, it is not conclusive that the CTD primary yields a more accurate and consistent temperature reading than the secondary sensor. Variance of the secondary sensor residuals are approximately double those of the primary over the full water column for Groups A&D and C&F, and in deep water are on average  $0.9 \times 10^{-4}$  °C lower for the primary compared to the secondary. Excluding sensor 4416 (for reasons noted above) decreases the difference to  $0.2 \times 10^{-4}$  °C, supporting the assumption of better performance of the CTD primary relative to the secondary due to sensor positions. The bias between CTD and SBE35 temperature, however, may be larger in the primary sensor (as seen for Groups A&D and

B&E in the deep water and B&E over full depth), contradicting the premise of improved accuracy of the CTD primary sensor relative to the secondary.

Table 10.4: Station groupings and sensor serial numbers for Table 10.5 and Figures 10.1 and 10.2. Primary and secondary refer to the position of the CTD temperature sensor. For stations 38-93, this is the reverse of Table 8.11 in the CTD operations section since in analysis of these stations the primary and secondary were swapped in name. This convention is not followed here since we prefer to compare sensors at the same position.

<b>Group</b>	<b>Stations</b>	<b>SBE35 serial No.</b>	<b>CTD temperature serial No.</b>	<b>Primary / Secondary</b>
A	12-37	0048	2919	Primary
B	39-89	0037	2758	Primary
C	38, 90-125	0048	2758	Primary
D	12-37	0048	4116	Secondary
E	39-89	0037	2880	Secondary
F	38, 90-125	0048	2880	Secondary

Table 10.5: SBE35 – CTD temperature residuals after application of limit 1 or 2. N is the number of residuals before selection in limit 1, and the number at pressures greater than 2000 dbar in limit 2.  $N_{\text{tot}}$  counts those remaining number after rejection of a percent (% reject).  $\mu$  and  $\sigma$  are the mean and standard deviations of the  $N_{\text{tot}}$  residuals. Note change of scale between  $\mu$  and  $\sigma$  columns for Limits 1 and 2.

Group	Limit 1: $\pm 0.05^{\circ}\text{C}$ , $\pm 2\sigma$ , $\pm 2\sigma$				Limit 2: $P > 2000$ dbar, $\pm 0.005^{\circ}\text{C}$ , $\pm 2\sigma$ , $\pm 2\sigma$			
	$N/N_{\text{tot}}$	% reject	$\mu$ ( $^{\circ}\text{C}$ $\times 10^{-3}$ )	$\sigma$ ( $^{\circ}\text{C}$ $\times 10^{-3}$ )	$N/N_{\text{tot}}$	% reject	$\mu$ ( $^{\circ}\text{C}$ $\times 10^{-4}$ )	$\sigma$ ( $^{\circ}\text{C}$ $\times 10^{-4}$ )
A	422/494	14.6	-0.4	2.1	194/208	6.7	-10.3	3.9
B	1026/1221	16.0	-1.4	2.3	549/589	6.8	-9.4	3.7
C	664/774	14.2	-0.2	2.5	302/331	8.8	-0.0	3.0
D	409/494	17.2	-3.0	5.8	191/208	8.2	-9.2	7.1
E	1055/1221	13.6	-0.3	2.1	552/589	6.3	-8.7	3.9
F	657/774	15.1	-1.1	4.4	306/331	7.6	-0.2	3.2

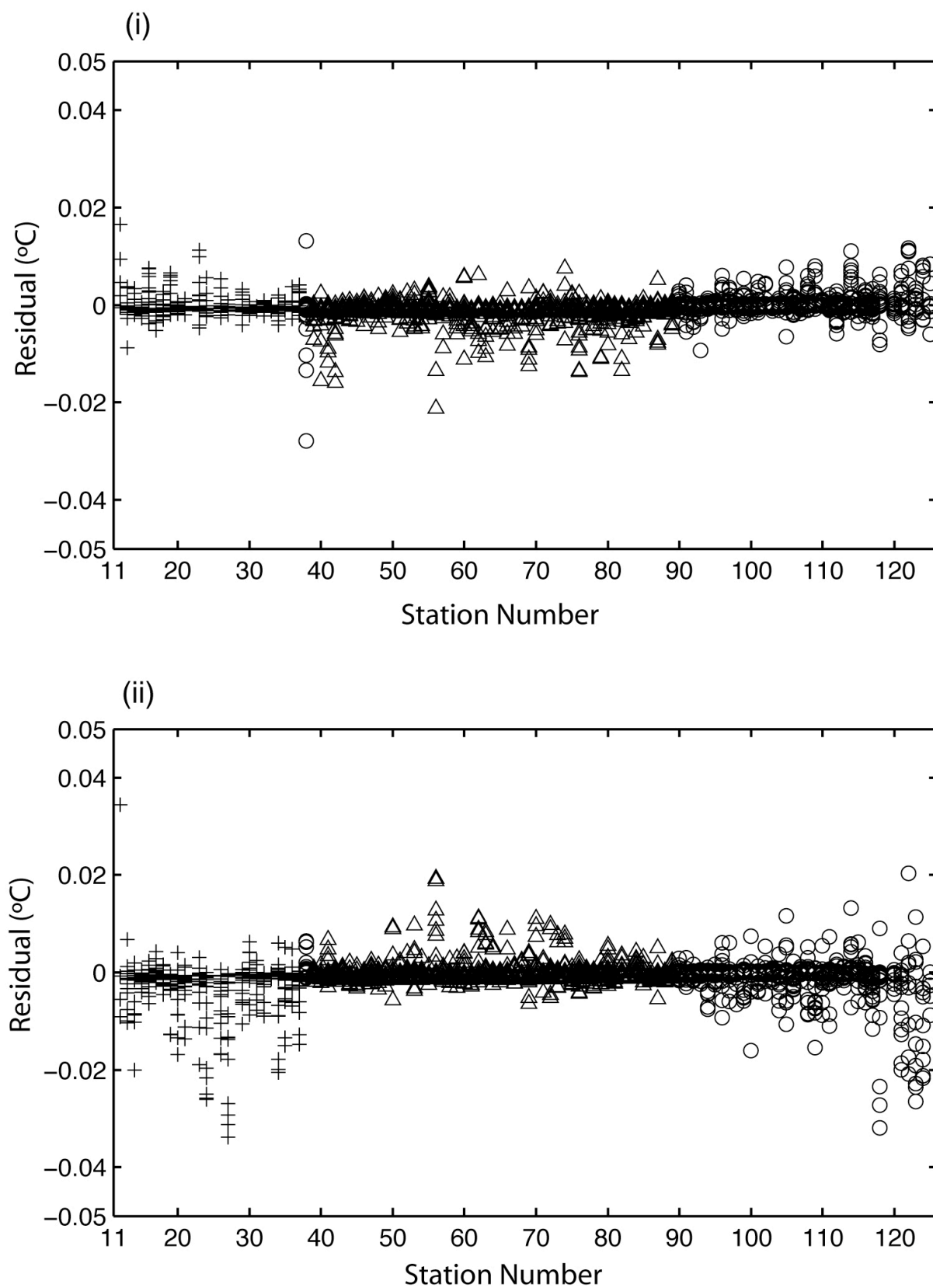


Figure 10.1: SBE35 – CTD temperature residual after application of limit  $1(\pm 0.05^{\circ}\text{C}, \pm 2\sigma, \pm 2\sigma)$ . (i) Primary CTD temperature sensors (Groups A – C). (ii) Secondary CTD temperature sensors (Groups D – F). Station groups are (+) A or D, ( $\Delta$ ) B or E and (o) C or F.

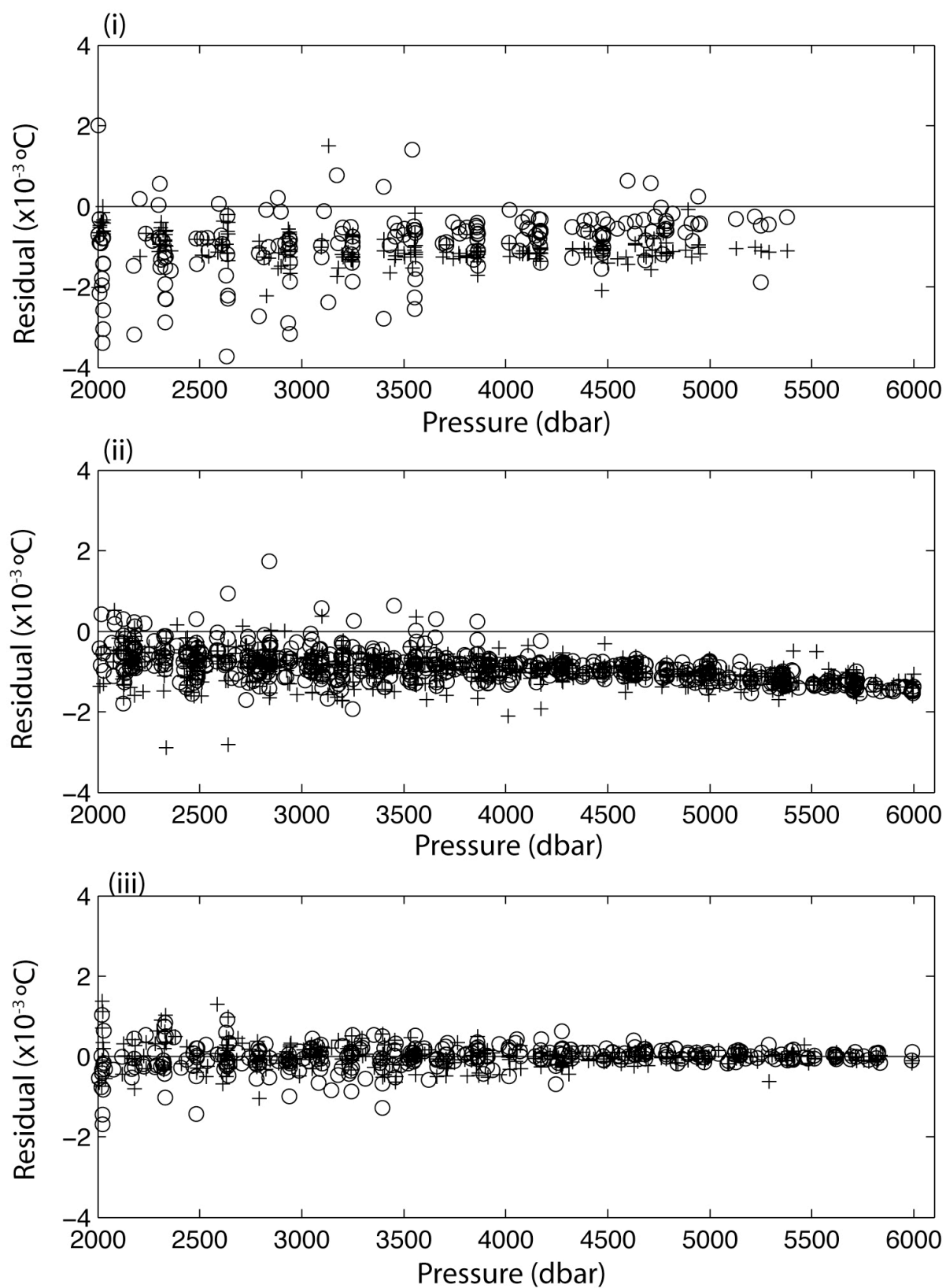


Figure 10.2: SBE35 – CTD temperature residual after application of limit 2 (pressure  $>2000$  dbar,  $\pm 0.005^\circ\text{C}$ ,  $\pm 2\sigma$ ,  $\pm 2\sigma$ ). (i) Groups A (+) and D (o), (ii) Groups B (+) and E (o), (iii) Groups C (+) and F (o).



## **11. WATER SAMPLE SALINITY ANALYSIS**

Hannah Longworth, Rachel Hadfield, Amanda Simpson, Rhiannon Mather

### **11.1 Equipment**

All salinity sample analysis was performed on the UKORS Guildline 8400B Salinometer in the Constant Temperature (CT) laboratory. The water bath temperature was set to 24°C and the laboratory temperature maintained between 21.5°C and 22.0°C. The laboratory thermostat was adjusted on day 100 following a drop to 20.0°C, analysis was suspended while the temperature stabilised. A leak in the salinometer between the external pump and the conductivity cell was repaired by replacement of a tubing section on day 101, with effect from Station 20 onwards. On day 121, the primary heater failed during analysis of Station 86, with no apparent effect on the results obtained. The heater was replaced before analysis of Station 87 and a delay of 19 hours resulted to allow stabilisation of the water bath temperature. On day 130, the peristaltic pump tube split and was replaced. 10% Decon solution and distilled water were rinsed through the salinometer before analysis of Station 116. During this station wires connecting the pump and switch had to be resoldered.

### **11.2 Sample Collection and Analysis**

On each CTD cast (except stations 11 and 28 when no bottles were fired), one water sample was drawn per Niskin bottle for salinity analysis. A duplicate sample was taken from the deepest bottle when less than 24 were fired. Samples were taken in 200ml glass sample bottles, rinsed three times and sealed with disposable plastic stoppers and screw on caps after drying the neck. Samples were stored in the CT laboratory for a minimum of 24 hours before analysis to allow equilibration to the laboratory temperature, except for the last 4 stations (shallower than 2000m) where the delay between sampling and analysis was reduced to 12 hours. Analysis followed the standard procedure. A sample of IAPSO Standard Seawater was run every 24 samples for salinometer calibration. Two Standard Seawater batches were used: P143 up to and including Station 7 and P144 subsequently. One bad standard in batch P144 was identified and rejected. The standardisation dial was set to 724 and not changed during the cruise. Rachel Hadfield, Hannah Longworth and Amanda Simpson carried out the majority of analysis with Rhiannon Mather helping in the last week. The 12 duplicate water samples taken had a mean salinity difference and standard deviation of 0.0003.

Stability of the salinometer during the cruise is indicated in Figure 11.1. Correction is the correction applied to the conductivity ratio measured by the salinometer (equal to the expected standard value minus the measured standard value). Correction has a range of -0.00019 to +0.00003, with a drift to increasingly negative corrections during the cruise.

### 11.3 Data Processing

Raw conductivities from the salinometer are converted to salinities using an Excel spreadsheet, accounting for salinometer calibration. Results are saved in a tab delimited text file with name *sal279{num}.txt*. After transfer to the UNIX system, the PSTAR routine *sal.exec* creates a PSTAR version of the text file, *sal279{num}.bot*, with the same parameters.

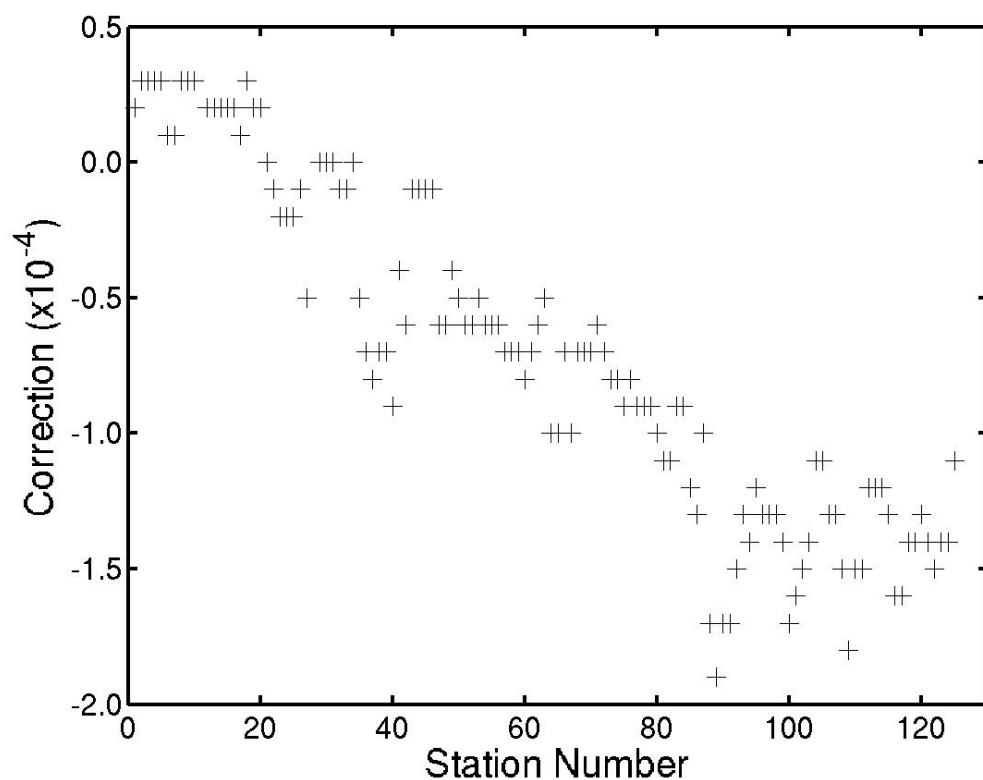


Figure 11.1: Correction applied to salinometer conductivity reading.

## 12. WINCHES

### 12.1 Standard CTD – Steel Armoured Electro-Optical Cable (Spare)

**Cable Specifications** (see also Table 12.1)

<b>MBL:</b>	82.3kN or 8.39Te
<b>Diameter:</b>	0.45" or ~11.43 mm
<b>Length:</b>	8000 metres
<b>Weight in Air:</b>	505kg.km <sup>-1</sup>
<b>Weight in Water:</b>	417kg.km <sup>-1</sup>
<b>Approved Manufacturer:</b>	The Rochester Corporation
<b>Type Number:</b>	A303418MW

### 12.2 Applications

Common applications for this cable include CTD and associated instrument deployments, water bottle rosette sampling and sound velocity profiling.

### 12.3 Handling

- A traction winch with level wind is required for the handling of this cable, as it is essential that the cable is stored under low tension.
- The storage drum shall be fitted with a Focal slip ring assembly. This slip ring shall contain one FORJ (Fibre Optic Rotating Joint) for a single mode fibre optimised at 1310/1550nm and two electrical passes each rated at 3kV, 10A or better.
- D:d ratio shall be 40:1 or better throughout.
- Pull capacity 5.0 Te.
- Line speed 2.0 ms<sup>-1</sup>
- Speed control continuously variable in increments of <0.03m/s between zero and maximum throughout length.

- An automatic render capability is required. This is to be capable of manual adjustment for any tension between 20% and 60% of MBL.
- Active heave compensation is required for this application.

Table 12.1: RSU CTD winch, 11.7mm electro-optical cable factors of safety, where MBL is maximum breaking load and yield is for the electrical conductor.

Load	Safety Ratio	Load (tonnes)	% of MBL	Notes
MBL	5:1	8.39	100	Test haul required
Lloyds standard	3:1	1.67	20	
Test haul	2.5:1	2.79	35	
Average	2:1	3.35	40	
Peak		4.19	50	
Yield		5.87	70	

Analysis of winch data from two deployments with different packages and deployment profiles is given below (Table 12.2).

Table 12.2: Stations used in analysis of standard CTD cable tensions.

File	Package Type	Weight (T) Air/Water	Haul/Veel Rate (m/min)	Max Wireout (m)	Maximum Tension (T)
win27701_winc htrial1_noCTD	Small frame with six pairs of mooring releases.	0.410/0.370	±50	3000	1.54
win279052	Full CTD package		±70	5755	3.09

#### 12.4 Analysis Method

Each cast is split into down cast and upcast profiles including only data deeper than 500 m where the veer rate is constant. For the CTD station, the upcast data are then further selected: 1) where the haul rate is 70 m/min and 2) where the haul rate is 0 m/min (i.e. package stopped to fire bottles). Each profile is fitted using a least squares fit of tension versus cableout (Table 12.3).

Table 12.3: Least squares fit of tension versus cableout for downcast veer, upcast haul and upcast stopped winch data for two stations with different packages. The coefficients are for the equation: Tension = C + M x cableout (km), where C is the weight of the package and M is the rate of increase in tension with cableout. Package and cable drag are estimated as the difference/2 of downcast veer and upcast haul package weight values C and the difference/2 of downcast veer and upcast haul rate of increase in tension with cableout M respectively.

Station	27701	279052
<b>C (down cast veer) T</b>	0.310	0.487
<b>M (down cast veer) T/km</b>	0.356	0.356
<b>C (up cast haul) T</b>	0.381	0.819
<b>M (up cast haul) T/km</b>	0.392	0.387
<b>C (up cast stopped) T</b>	0.345 (average of Cdown and Cup)	0.651
<b>M (up cast stopped) T/km</b>	0.373 (average of Mdown and Mup)	0.373
<b>Package drag T</b>	0.04	0.166
<b>Cable drag T/km</b>	0.018	0.016

On these two casts, the package weights in water were 0.345T and 0.651T, and haul/veer rates were 50 and 70 m/min. From these two analyses, the cable drag estimates are similar, approximately 0.017T/km, suggesting only weak dependence of cable drag on velocity. Estimates for the weight of cable in water are the same for both casts (0.373T/km) and are inconsistent with the manufacturers specification of 0.417T/km: a difference of 0.044T/km.

For the large CTD package, the model for estimating cable tensions as a function of cable out is:

$$\text{Tension(est)} = 0.651 + 0.373 \times \text{cableout(km)} \pm \text{up/down}(0.166 + 0.016 \times \text{cableout(km)})$$

From this equation, if the maximum average tension is 3.35T (safety factor 2.5:1 or 40% of maximum breaking load), the maximum wire out would be 6512 m. For the manufactures weight of wire this reduces to 6074 m.

A caveat to the above analysis is that no significant peak loads were observed due to the fine weather. Overall however, the performance of the new CTD cable is outstanding, easily achieving 6000 m depth.

## **13. ADCP AND BATTERY PACK**

Dave Teare

Three SADPs and two battery packs were fitted to the CTD frame. One Broadband (BB) 150kHz, in downward looking mode (serial no 1308), with its own battery pack, and two 300kHz Workhorse (WH) narrow band units, one upward looking (serial no 1881) and one downward looking (serial no 3726), with a shared battery pack. The 300kHz units were run in a master/slave mode and the 150kHz was free running.

### **13.1 BB 150kHz Unit**

This ran without problem. The battery pack was changed on occasions when the charge rate was unable to keep up with the usage.

### **13.2 Workhorse 300kHz Units**

Several problems occurred with these units. On cast 28, the battery pack flooded. This was replaced and the flooded unit rebuilt and held as a spare. The upward looking unit started to exhibit data download problems around cast 44 and at cast 63 failed to download. The problem was traced to a faulty cable on the CTD frame, which was replaced. Around cast 76, the upward looking unit started to lose meaningful data except at the surface and close to the bottom. Instrument receiver self tests were performed which indicated a loss of sensitivity in the receive circuits. The unit was removed from the frame, opened, and checked for loose/faulty connections. As there were no observable problems the unit was resealed. A second test revealed the same problem; the unit was left off for the rest of the cruise. The battery pack was changed on occasions when the charging could not keep up with the usage.

## 14. LOWERED ACOUSTIC DOPPLER CURRENT PROFILER

Louise Duncan

**Instruments Used:** BB 20 degree SOC 150Hz BB (unit S/N 1308); WH1 300kHz Workhorse LADP (unit S/N 1881); WH2 300kHz Workhorse LADP (unit S/N 3726)

### 14.1 Difficulties During Cruise

During the first part of the cruise, crossing the western boundary section, battery power was a big concern. We initially experienced problems with the Workhorse batteries, which failed during the upcast of cast 15. They failed again on station 17, which was delayed at the bottom due to winch problems. The Workhorse was not deployed for the next couple of stations and eventually was replaced on cast 22. On station 28, both the BB and WH batteries were changed but the WH battery air vent was left open, so the cast had to be aborted and the battery was returned flooded.

It was difficult during the cruise to determine the best charging rate to gain optimal performance. The BB has an intelligent charger, which regulates the amount of charge to that required. However, with the Workhorse charger it was hard to know the optimal charging rate. With the diode in place up to cast 62, it was more difficult to determine the voltage on the WH battery.

For stations 51 and 52, the master Workhorse was setup with an incorrect time stamp resulting in a one hour error in the output times. This was noticed prior to cast 53 and corrected. However, for stations 51 and 52 it was necessary to use the RDI tools to extract the time from the raw binary files and replace with the correct time. Once corrected, the binary files were ftp'd to UNIX and processed.

#### Communication with Slave WH

During the western boundary section, when stations were close together and deep, the download times for the Broadband were slow and starting to hold up the start of the next station. To resolve this, the download rate was changed from a baud rate of 38400 to 115200.

### 14.2 Processing

Two processing schemes were used during the cruise. The older Firing scheme was primarily used to process the Broadband LADP and sometimes the Workhorse LADP's. After station 24, the primary processing for the Workhorses was the Visbeck method, in which the Workhorses could be processed together. Outlines of the processing stages are provided below. For each instrument, the initial raw binary file for a cast is downloaded from the instrument to PC and then ftp'd to UNIX.

### **14.3 Firing Method**

The Firing processing scheme calculates absolute velocities by first calculating overlapping vertical shear profiles of horizontal velocity. These are averaged and combined to produce a full depth shear profile. This process removes any motion associated with the package. Integrating the shear profile obtains the baroclinic component of the water velocity. The barotropic part is then obtained from the unknown integration constant and is computed from the time-averaged, measured velocity and ship drift.

### **14.4 Visbeck Method**

The Visbeck method calculates velocities using an inverse problem to remove package motion solved using a least squares technique. The problem is over determined and can be solved using sensible constraints (Visbeck, 2002). This method of processing also allows the solution to be constrained by information from bottomtrack, CTD and SADP.

### **14.5 Processing Problems**

#### Firing

Processing using the Firing method went well. On stations 25 and 62, there were problems matching the LADP to CTD data. On station 25, the Broadband instrument was deployed as an upward looking ADP. It is unclear why the instrument changed from downlooking to upward looking for this one station. Command files sent to the instrument and station log files do not show any error by the user at the deployment stage.

During cast 62, there was a win explorer crash on the CTD PC during the upcast at wire out 3499m. It was unclear at the time whether any data loss had occurred for the CTD. However, a time gap was apparent on the first attempt to match the LADP to CTD data for this station. A new file was created specifically to use for matching CTD and LADP by filling in the time gap and linearly interpolating the salinity, temperature and pressure information. The new CTD file improved the match slightly, but it remains quite poor.

Generally, the Firing method matched the CTD and LADP quite well automatically. There were less than twelve occasions where interactive editing was required.



## Visbeck

Processing with the Visbeck method suffered a few more difficulties than the Firing scheme. The smaller number of steps involved in the Visbeck scheme made it more attractive to use, although it used more computer processor time than the Firing method.

Occasionally the CTD data was ignored by the Visbeck processing during run two. This occurred on four stations. Stations 25 and 62 have already been mentioned above and caused problems in the Firing method. On station 13, the CTD data was rejected because the first ascii file contained a number of spikes. The Visbeck scheme returned warnings at the end of the second run indicating a time difference between the bottom times of the ADP and CTD of 65 minutes! Once a new despiked CTD file was created, the CTD data was accepted and the processing ran without problems. (NB. Station 13 was rerun using the Firing method when the new CTD was available). Station 2 did not use the CTD data available, possibly due to the shallowness of the station (less than 200 metres).

For a number of casts, run two of the Visbeck processing reported a bottom time difference between the CTD and LADP (Table 14.1). Unlike the Firing scheme, the matching is performed within the processing automatically and does not allow external matching as an option. There was not enough time to investigate this error fully, however, some intervention maybe beneficial for the Visbeck scheme when using extra constraints. Time differences were usually about 1-2 minutes and occurred for both the Broadband and Workhorse LADP, but not necessarily on the same cast.

Table 14.1: Visbeck and Firing processing parameters (key at end of table)

Station	Visbeck Processing				Firing Processing			Comments
	Broadband		Workhorse		BB	Master	Slave	
	Run1	Run2	Run1	Run2				
1	A	B	C1	?	✓	✓	✓	
2	A	B X, td7	C1	D1 X, td6	✓	✓	✓	
3	A	B td8	C1	D1	✓	✓	✓	
4	A	B	C1	D1	✓	✓	✓	
5	A	B td2	C1	D1	✓	✓	✓	
6	A	B	C1	D1	✓	✓	✓	
7	A	B	C1	D1	✓	✓	✓	
8	A	B td1	C1	D1	✓	✓	✓	
9	A	B td1	C1	D1	✓	✓	✓	
10	A	B td2	C1	D1 td1	✓	✓	✓	
11	ND	ND	ND	ND	ND	ND	ND	Shallow station
12	ND	ND	ND	ND	ND	ND	ND	Shallow station

Station	Visbeck Processing				Firing Processing			Comments
	Broadband		Workhorse		BB	Master	Slave	
	Run1	Run2	Run1	Run2				
13	A	B	C1 nbot	D1 nbot	✓	✓	✓	Rerun - spikes in CTD data, caused CTD to be ignored first run
14	A	B	C1 nbot	D1 nbot	✓	✓	✓	
15	A	B	C1 ie	D1	✓	-	-	Downcast only for WH - lack of battery power
16	A	?	ND	ND	✓	ND	ND	
17	-	-	-	-	✓	-	-	Winch problems - delay 4hrs at bottom, WH battery returned dead
18	A	B	ND	ND	✓	ND	ND	
19	A	B td2	ND	ND	✓	ND	ND	WH battery flat on recovery
20	A	B td4	ND	ND	✓	ND	ND	
21	A	B	ND	ND	✓	ND	ND	
22	A	B	C1 ie	D1 td1	✓	✓	✓	
23	A	B td2	C1	D1 td1	✓	✓	✓	
24	A	B td1	C2	D2 td2	✓	✓	✓	Change WH cmd file to zero blank beyond transmit
25	A	B X,?	C2	D2	✓	✓	✓	Broadband deployed uplooking processed but bad match to CTD

Station	Visbeck Processing				Firing Processing			Comments
	Broadband		Workhorse		BB	Master	Slave	
	Run1	Run2	Run1	Run2				
26	A	B	C2	D2	✓	✓	✓	New WH and BB battery, WH battery flooded
27	A	B td1	C2 ie	D2 td1	✓	✓	✓	
28	ND	ND	ND	ND	ND	ND	ND	
29	A	B	ND	ND	✓	ND	ND	
30	A	B	C2 ie	D2	✓	✓	✓	New WH battery
31	A	B	C2 ie	D2	✓	✓	✓	
32	A	B	C2 ie	D2	✓	✓	✓	
33	A	B	C2 ie	D2	✓	✓	✓	
34	A	B	C2 ie	D2	✓	✓	✓	New BB battery
35	A	B td3	C2 ie	D2 td3	✓	✓	✓	
36	A	B td2	C2 ie	D2 td2	✓	✓	✓	
37	A	B td2	C2 ie	D2 td2	✓	✓	✓	
38	A	B	C2 ie	D2	✓	✓	✓	

Station	Visbeck Processing				Firing Processing			Comments
	Broadband		Workhorse		BB	Master	Slave	
	Run1	Run2	Run1	Run2				
39	A	B	C2 ie	D2	✓	✓	✓	
40	A	B	C2 ie	D2 td2	✓	✓	✓	
41	A	B	CM2 ie	DM2	✓	✓	✓	Slave not deployed - user error
42	A	B td2	C2 ie	D2	✓	✓	✓	New BB battery
43	A	B td1	C2 ie	D2 td2	✓	✓	✓	
44	A	B td1	C2 ie	D2 td1	✓	✓	✓	
45	A	B td1	C2 ie	D2	✓	✓	✓	
46	A	B td2	C2 ie	D2 td2	✓	✓	✓	
47	A	B td1	C2 ie	D2 td2	✓	✓	✓	
48	A	B td1	C2 ie	D2 td2	✓	✓	✓	
49	A	B td1	C2 ie	D2 td1	✓	✓	✓	
50	A	B td2	C2 ie	D2 td2	✓	✓	✓	
51	A	B	C2 ie	D2 td2	✓	✓	✓	Instrument time out by 1hour corrected prior to processing

Station	Visbeck Processing				Firing Processing			Comments
	Broadband		Workhorse		BB	Master	Slave	
	Run1	Run2	Run1	Run2				
52	A	B	C2 ie	D2	✓	✓	✓	Instrument time out by 1hour corrected prior to processing
53	A	B td3	C2 ie	D2 td3	✓	✓	✓	
54	A?	B td1, ??	C2 ie	D2 td2	✓	✓	✓	
55	A	B td2	C2 ie	D2	✓	✓	✓	
56	A	B td2	C2 ie	D2	✓	✓	✓	
57	A	B td1	C2 ie	D2	✓	✓	✓	
58	A	B	C2 ie	D2	✓	✓	✓	
59	A	B td1	C2 ie	D2 td1	✓	✓	✓	
60	A	B td2	C2 ie	D2 td1	✓	✓	✓	
61	A nbot	B nbot	C2 ie, nbot	D2 nbot	✓	✓	✓	
62	A	B X	CM2 ie, nbot	DM2 X, nbot	✓	✓	ND	Poor CTD match due to time jump in upcast CTD data
63	A	B	C2 ie, nbot	D2 nbot	✓	✓	✓	
64	A	B	C2 ie	D2	✓	✓	✓	

Station	Visbeck Processing				Firing Processing			Comments
	Broadband		Workhorse		BB	Master	Slave	
	Run1	Run2	Run1	Run2				
65	A	B	C2 ie	D2	✓	✓	✓	Broadband command file change to 20m bins
66	A	B	C2 ie	D2	✓	✓	✓	
67	A nbot	B nbot, td3	C2 ie,nbot	D2 nbot, td3	✓	✓	✓	
68	A	B	C2 ie	D2	✓	✓	✓	
69	A	B td1	C2 ie	D2 td1	✓	✓	✓	
70	Atrial	Btrial	C2 ie	D2	✓	✓	✓	
71	A	B	C2 ie	D2 td1	✓	✓	✓	
72	A	B td2	C2 ie	D2 td2	✓	✓	✓	
73	A	B	C2 ie	D2	✓	✓	✓	
74	A	B	C2 ie	D2 td2	✓	✓	✓	
75	A	B td1	C2 ie	D2	✓	✓	✓	
76	A	B td1	C2 ie	D2 td1	✓	✓	✓	

Station	Visbeck Processing				Firing Processing			Comments
	Broadband		Workhorse		BB	Master	Slave	
	Run1	Run2	Run1	Run2				
77	A	B	C2 ie	D2 td2	✓	✓	✓	
78	A	B td1	CM2 ie	DM2 nbot, td1	✓	✓	-	Slave returned with half cast good data
79	A	B td1	CM2 ie	DM2 td1	✓	✓	-	Slave stopped receiving data on up cast
80	A	B td1	CM2 ie	DM2	✓	✓	-	No good data returned from slave
81	A	B	CM2 ie	DM2	✓	✓	ND	
82	A	B td1	CM2 ie	DM2	✓	✓	ND	
83	A	B	CM2 ie	DM2	✓	✓	ND	
84	A	B	CM2 ie	DM2	✓	✓	ND	
85	A	B td1	CM2 ie	DM2 td1	✓	✓	ND	
86	A	B	CM2 ie	DM2 td1	✓	✓	ND	
87	A	B td1	CM2 ie	DM2 td2	✓	✓	ND	
88	A	B td1	CM2 ie	DM2 td2	✓	✓	ND	
89	A	B	CM2 ie	DM2	✓	✓	ND	



Station	Visbeck Processing				Firing Processing			Comments
	Broadband		Workhorse		BB	Master	Slave	
	Run1	Run2	Run1	Run2				
90	A	B	CM2 ie	DM2	✓	✓	ND	
91	A	B td1	CM2 ie	DM2	✓	✓	ND	
92	A	B	CM2 ie	DM2 td1	✓	✓	ND	
93	A	B td2	CM2 ie	DM2 td2	✓	✓	ND	
94	A	B	CM2 ie	DM2 td1	✓	✓	ND	
95	A	B td1	CM2 ie	DM2 td3	✓	✓	ND	
96	A nbot	B nbot	CM2 ie, nbot	CM2 nbot	✓	✓	ND	
97	A nbot	B nbot	CM2 ie, nbot	CM2 nbot	✓	✓	ND	
98	A	B	CM2 ie	DM2 td2	✓	✓	ND	
99	A	B td2	CM2 ie	DM2 td2	✓	✓	ND	
100	A	B	CM2 ie	DM2 td1	✓	✓	ND	
101	A	B td1	CM2 ie	DM2 td1	✓	✓	ND	
102	A	B td1	CM2 ie	DM2 td2	✓	✓	ND	

Station	Visbeck Processing				Firing Processing			Comments
	Broadband		Workhorse		BB	Master	Slave	
	Run1	Run2	Run1	Run2				
103	A	B td2	CM2 ie	DM2	✓	✓	ND	
104	A	B	CM2 ie	DM2 td1	✓	✓	ND	
105	A	B	CM2 ie	DM2	✓	✓	ND	
106	A	B	CM2 ie	DM2	✓	✓	ND	
107	A	B	CM2 ie	DM2	✓	✓	ND	
108	A	B	CM2 ie	DM2 td1	✓	✓	ND	
109	A	B td1	CM2 ie	DM2 td1	✓	✓	ND	
110	A	B	CM2 ie	DM2	✓	✓	ND	
111	A	B td1	CM2 ie	DM2 td3	✓	✓	ND	
112	A	B td1	CM2 ie	DM2	✓	✓	ND	
113	A	B td2	CM2 ie	DM2 td2	✓	✓	ND	
114	A	B	CM2 ie	DM2	✓	✓	ND	
115	A	B	CM2 ie	DM2 td1	✓	✓	ND	

Station	Visbeck Processing				Firing Processing			Comments
	Broadband		Workhorse		BB	Master	Slave	
	Run1	Run2	Run1	Run2				
116	A	B td1	CM2	DM2 td1	✓	✓	ND	
117	A	B td1	CM2 ie	DM2 td1	✓	✓	ND	
118	A	B	CM2 ie	DM2 td1	✓	✓	ND	
119	A	B td1	CM2	DM2	✓	✓	ND	
120	A	B td1	CM2 ie	DM2	✓	✓	ND	
121	A	B	CM2	DM2	✓	✓	ND	
122	A	B td1	CM2	DM2	✓	✓	ND	
123	A	B	CM2	DM2	✓	✓	ND	
124	ND	ND	ND	ND	ND	ND	ND	
125	ND	ND	ND	ND	ND	ND	ND	
126	ND	ND	ND	ND	ND	ND	ND	

Key: A = Broadband run 1 with ps.dz=16m and 0.5 weight on bin 1. NAV constraint

B = Broadband run 2 with ps.dz=16m, 0.5 weight to bin1. NAV, CTD constraints

Atrial = Broadband run 1 with ps.dz=20m and 0.5 weight on bin 1. NAV constraint

Btrial = Broadband run 2 with ps.dz=20m and 0.5 weight on bin 1. NAV, CTD constraints

C1 = Dual Workhorse run1 with ps.dz=10m, 0.5 weight to bin1. NAV constraint

C2 = Dual Workhorse run1 with ps.dz=10m, 0 weight to bin1. NAV constraint

CM2 = Dual Workhorse run1 with ps.dz=10m, 0 weight to bin1 and master only. NAV constraint

D1 = Dual Workhorse run2 with ps.dz=10m, 0.5 weight to bin1. NAV, CTD, BOT constraint

D2 = Dual Workhorse run2 with ps.dz=10m, 0 weight to bin1. NAV, CTD, BOT constraint

DM2 = Dual Workhorse run2 with ps.dz=10m, 0 weight to bin1 and master only. NAV, CTD, BOT constraint

nbot = No bottom track data available

ie = Increased error due to shear inverse difference

tdn = Bottom time difference between CTD and LADCP by n minutes

X = No CTD data

ND = Not Deployed

? = Plotraw.m does not run in visbeck processing

For a large number of stations, the first run of Visbeck processing for the Workhorse returned a message stating an increase error because of shear – inverse difference. This message is displayed from the Matlab script getshear2.m and is shown when  $uvds > \text{mean}(dr.uerr)$ , where  $dr.uerr$  is the velocity error derived by solving the linear inverse method and  $uvds$  is:

$$\sqrt{(\text{sd}(dr.u - \text{mean}(dr.u) - ds.ur)^2 + (\text{sd}(dr.v - \text{mean}(dr.v) - ds.vr))^2)}$$

Where  $dr.u$  and  $dr.v$  are velocities from the linear inverse problem and  $ds.ur$  and  $ds.vr$  are velocities derived by the older method of integrating average shear estimates from the bottom up.

## 14.6 Results

The Broadband LADP performed well during D279. For a large number of casts either side of and over the mid-Atlantic ridge, the lack of scatterers in the water below approximately 2500m resulted in a lack of samples with which to determine sensible water velocities. Figure 14.1 shows the velocities from station 67 and the impact of lack of scatterers on the result. As soon as we reach stations towards the end of the cruise, full sensible looking profiles were retrieved once the number of samples increased.

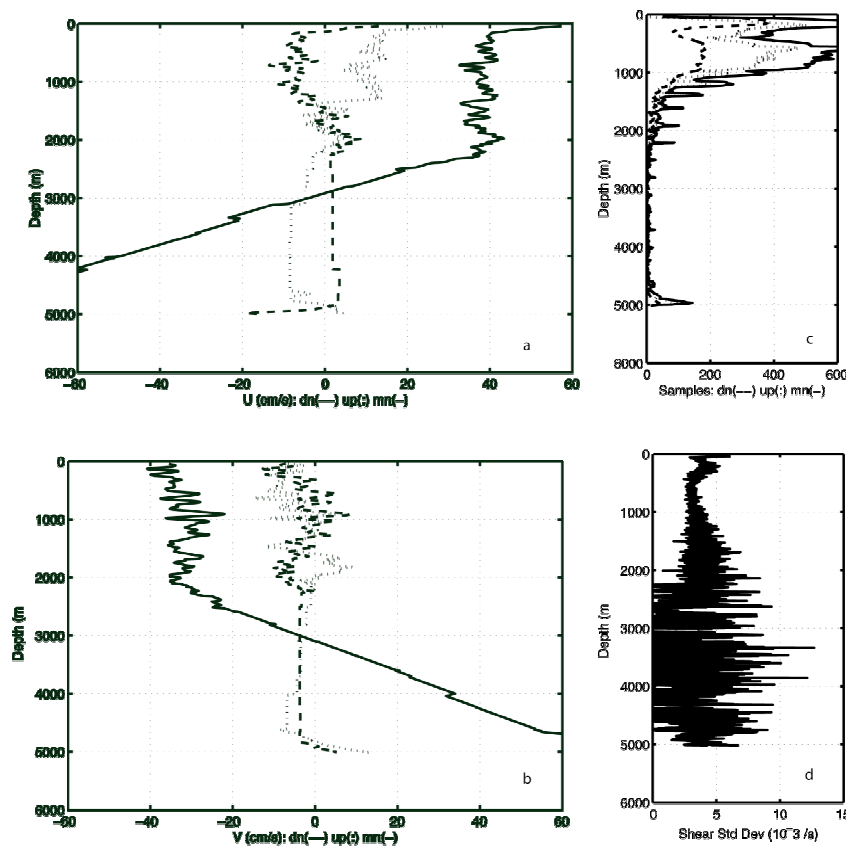


Figure 14.1: LADP data from station 67 showing U and V velocities (panels a and b) and the number of samples per bin (c) and the shear standard deviation (d).

The master Workhorse LADP performed well, but several problems were encountered during the cruise with the upward looking slave Workhorse. Initially we had problems downloading and talking to the slave Workhorse. This turned out to be a problem with the cable connection to the slave on the CTD frame itself. This cable was replaced prior to cast 64. No new problems with communication were experienced. On station 78, the slave Workhorse returned with only half a cast (downcast) of good data available (as suggested by scan.prl in the firing processing). On station 79, the slave again did not retrieve a full cast but collected its last good ensemble on the upcast at approximately 400 m depth. On station 80, the slave file gave a max depth of 0.3 and min/max depth of -517 using scan.prl. The three casts were examined on the deck laboratory PC using the RDI tools winADP. This allowed us to look at basic variables such as 'w' at a glance. The files all contained some velocity information. For station 80, the only velocity data available seemed to show the instrument tracking the surface, near the beginning of the cast and again near the end. RA tests were performed on the instrument. On cast 81, the instrument finally returned with no sensible data. In all stations after 78, the slave returned with a file with similar magnitude to the master Workhorse. However, the file was filled with absent data.

#### **14.7 Comparison of BB LADP and WH LADP With On-Station OS75 VM ADP**

A comparison of the velocities from the Broadband using both processing schemes, the Workhorse using the Visbeck scheme and the vessel mounted OS75 was performed during the cruise. Initially the velocities were compared visually using the script plot\_topbot\_uv.m. The comparison from station 23 is shown in Figure 14.2. In general, both the shear profiles compare well, although the Broadband processed using the Firing method would often show an offset from the Visbeck processed Broadband and OS75. For each cast, velocities from the Broadband and Workhorse were interpolated onto the same depth bins as the OS75 using the script profstats.m. Table 14.2 shows the mean and standard deviation of the Broadband from the OS75 using both the Visbeck and Firing processing.

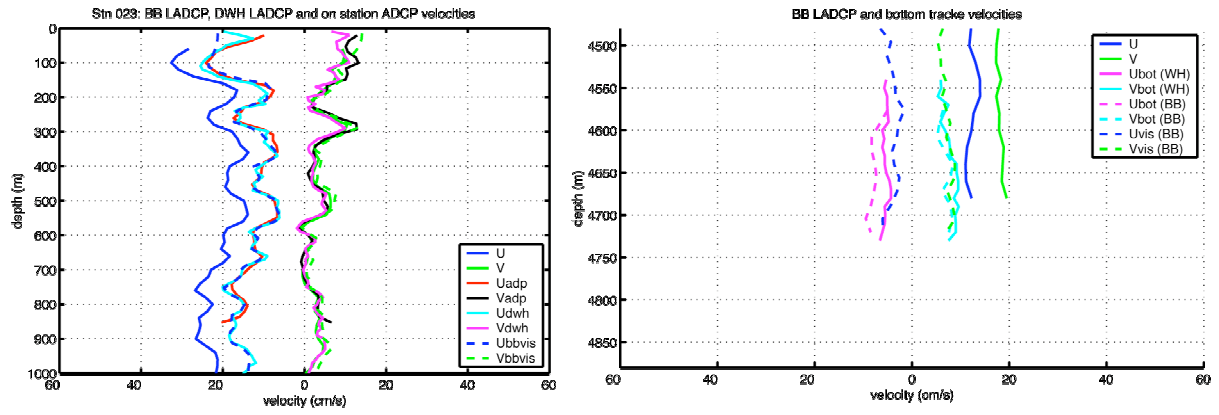


Figure 14.2: Station 23. Broadband LADP velocities processed using the Firing (U, V) and Visbeck (Ubbvis, Vbbvis) processing schemes, Workhorse LADP profiles processed using the Visbeck scheme (Udwh, Vdwh) and shipboard OS75 (Uadp, Vadp). Water track velocities are shown in the left panel and bottom track velocities on the right panel.

Table 14.2: Comparisons of BB LADP and WH LADP with on-station OS75 VM ADP

stat	Vessel Mounted OS75 - BB Firing				Vessel Mounted OS75 - BB Visbeck			
	mean u	sd u	mean v	sd v	mean u	sd u	mean v	sd v
	(cm/s)	(cm/s)	(cm/s)	(cm/s)	(cm/s)	(cm/s)	(cm/s)	(cm/s)
1								
2								
3	-10.99	5.95	-49.40	3.44	4.02	4.53	11.78	11.54
4	-1.80	4.59	-19.50	2.74	5.35	6.18	11.82	11.61
5	-1.61	2.20	-8.87	7.43	1.16	2.20	5.57	7.80
6	-2.91	2.49	-9.26	3.82	-1.35	4.58	8.40	4.60
7	-2.10	1.63	-6.31	5.45	-1.14	2.43	4.67	5.70
8	-3.64	1.87	1.14	2.18	-1.95	2.31	3.41	3.57
9	0.75	2.57	3.79	3.90	4.14	3.12	-1.57	6.52
10	0.11	3.25	-0.84	1.86	4.90	6.32	-10.59	11.15
11								
12								
13	-1.35	1.95	0.04	0.96	-0.93	3.22	6.00	2.77
14	-0.39	1.44	-1.62	1.15	-1.20	2.06	1.35	1.00
15	-3.83	1.61	-2.65	1.58	0.15	2.05	2.29	4.40
16								
17								
18	-8.38	1.14	10.37	0.89	-1.97	1.56	-0.02	1.10
19	-2.12	1.31	1.89	1.39	-1.85	2.06	0.40	1.70
20	-1.73	1.54	8.44	1.74	-0.21	1.27	0.19	1.64



stat	Vessel Mounted OS75 - BB Firing				Vessel Mounted OS75 - BB Visbeck			
	mean u	sd u	mean v	sd v	mean u	sd u	mean v	sd v
	(cm/s)	(cm/s)	(cm/s)	(cm/s)	(cm/s)	(cm/s)	(cm/s)	(cm/s)
21	0.59	1.08	10.78	1.32	-1.67	3.79	0.86	2.87
22	3.87	1.46	-8.83	1.63	0.35	2.11	-1.46	2.85
23	7.89	0.97	0.35	1.45	0.74	2.16	-0.81	1.42
24	-0.24	1.13	0.74	1.66	2.27	1.92	-1.10	5.34
25								
26	1.34	1.47	-0.86	1.16	1.29	2.57	-2.43	3.60
27	-2.25	1.26	0.24	0.92	-0.36	2.12	-2.50	0.96
28								
29	-1.82	1.44	0.70	0.94	1.73	9.23	-2.78	3.50
30	-1.52	1.02	-1.33	1.53	1.85	2.38	0.70	1.88
31	-5.91	1.52	5.47	1.47	3.55	2.37	-1.25	2.12
32	-1.98	1.27	5.15	1.48	1.19	3.21	-2.82	3.06
33	3.08	1.57	-3.87	1.12	1.22	3.07	0.78	5.63
34	-9.74	1.16	4.10	1.44	2.57	1.19	-1.32	1.13
35	-1.15	1.43	-2.51	1.63	-1.24	1.25	-0.88	2.05
36	11.71	1.21	-9.35	1.05	-0.64	1.38	-3.32	0.89
37	3.27	1.88	-4.25	1.54	-0.60	1.58	-1.90	3.72
38	7.23	1.39	-4.41	1.57	1.96	1.71	-0.93	3.20
39	-6.06	1.47	-1.30	1.42	-1.68	2.72	-0.91	1.44
40	-11.84	1.29	3.96	1.02	2.79	1.59	-2.76	1.45
41	-13.82	1.34	14.70	0.96	3.47	2.03	-2.37	1.99

stat	Vessel Mounted OS75 - BB Firing				Vessel Mounted OS75 - BB Visbeck			
	mean u	sd u	mean v	sd v	mean u	sd u	mean v	sd v
	(cm/s)	(cm/s)	(cm/s)	(cm/s)	(cm/s)	(cm/s)	(cm/s)	(cm/s)
42	-8.30	2.11	-3.39	2.28	-1.48	1.59	-0.51	1.43
43	7.19	1.63	-8.86	1.03	-2.54	1.46	-0.63	1.52
44	0.32	0.93	7.34	1.67	-2.59	2.48	-0.28	4.91
45	32.75	1.46	-12.60	1.15	-3.88	2.24	-1.26	1.59
46	1.02	1.00	-7.27	1.16	-3.70	2.01	-0.23	2.12
47	17.42	1.55	-19.06	1.10	1.12	1.65	-1.63	4.60
48	1.27	1.26	-4.55	1.25	1.19	1.65	-4.15	4.36
49	6.88	1.38	-6.25	1.32	2.87	3.95	-3.42	2.19
50	8.70	1.65	-12.87	2.20	-0.65	1.70	-2.66	2.52
51	-1.92	1.40	8.16	2.03	0.34	2.97	-2.62	4.69
52	6.00	1.46	-10.93	2.39	-0.16	1.50	-4.36	3.51
53	-15.88	1.00	8.41	1.30	0.30	1.04	-1.79	2.33
54	6.57	1.15	9.65	1.93	0.50	3.25	0.86	1.94
55	-10.00	1.41	11.04	1.32	0.63	1.60	-1.42	1.15
56	61.97	1.15	-49.22	1.57	0.06	1.89	-0.68	2.00
57	5.92	1.17	20.13	1.45	-1.03	2.47	-1.64	1.33
58	-5.26	0.87	-11.84	1.89	2.63	1.90	-3.54	1.60
59	-27.70	1.45	4.10	1.19	2.91	2.16	-0.10	1.83
60	2.42	1.71	2.93	1.17	-0.45	1.74	1.82	2.38
61	-12.59	1.45	4.53	1.79	2.97	2.60	-3.26	2.24
62								

stat	Vessel Mounted OS75 - BB Firing				Vessel Mounted OS75 - BB Visbeck			
	mean u	sd u	mean v	sd v	mean u	sd u	mean v	sd v
	(cm/s)	(cm/s)	(cm/s)	(cm/s)	(cm/s)	(cm/s)	(cm/s)	(cm/s)
63	6.35	1.16	3.68	1.41	-2.64	1.64	-2.52	1.27
64	15.07	1.33	-30.71	2.89	-1.04	1.79	-3.77	3.40
65	55.42	1.82	13.94	1.60	-1.40	2.44	-2.06	2.69
66	4.79	0.95	-9.19	0.99	0.60	1.46	-1.88	2.70
67	-41.71	1.28	30.31	1.61	0.48	3.75	-2.29	3.30
68	1.32	0.93	5.69	2.43	-0.83	1.13	-0.91	2.64
69	-4.90	1.43	-9.45	1.33	-1.38	2.15	-3.89	1.74
70	1.15	1.99	-1.31	2.63	-3.64	4.92	-0.82	3.59
71	17.75	1.70	-0.37	2.14	-0.97	2.83	-1.47	2.14
72	5.21	1.75	-11.18	1.52	-2.33	4.94	-3.00	6.09
73	1.76	1.13	-2.28	1.35	-0.06	2.14	-1.30	2.67
74	11.74	2.10	-7.63	1.57	-1.62	3.11	-0.18	2.27
75	-8.50	1.89	3.22	2.20	-1.18	2.26	-2.91	2.09
76	-6.00	1.31	-1.97	1.32	-1.70	2.04	-0.39	1.66
77	-9.73	1.00	-4.81	1.72	-0.55	0.76	0.16	1.95
78	2.32	1.56	9.52	1.31	0.77	1.82	-0.82	1.83
79	-3.86	1.58	-4.93	1.32	0.66	1.82	-0.03	2.86
80	6.76	1.31	-7.90	1.53	0.75	2.07	-0.52	1.50
81	-0.30	1.80	11.56	1.63	-0.79	1.75	-3.88	2.34
82	7.31	1.29	-8.56	2.78	-0.51	1.52	-3.31	2.43
83	-8.37	1.57	-1.47	1.60	-3.21	2.55	-1.96	3.10

stat	Vessel Mounted OS75 - BB Firing				Vessel Mounted OS75 - BB Visbeck			
	mean u	sd u	mean v	sd v	mean u	sd u	mean v	sd v
	(cm/s)	(cm/s)	(cm/s)	(cm/s)	(cm/s)	(cm/s)	(cm/s)	(cm/s)
84	-8.45	1.09	14.10	2.01	-2.30	1.09	2.63	2.39
85	15.04	1.88	8.13	1.21	0.49	1.53	-2.07	2.93
86	11.43	1.78	-7.58	1.62	-6.88	3.25	4.06	2.66
87	0.22	1.52	10.21	1.67	-3.47	1.33	0.69	1.69
88	-0.49	1.50	-15.61	2.26	-4.45	1.93	-0.73	3.44
89	-27.31	1.24	12.88	1.57	-0.07	1.69	-2.54	1.90
90	3.41	1.27	-7.18	2.28	-0.50	1.29	-2.73	2.59
91	-2.60	0.64	-16.81	1.50	1.99	1.84	-1.21	1.46
92	14.31	1.76	5.35	1.63	-0.94	1.91	-3.60	2.04
93	11.76	2.07	-10.82	1.81	-1.29	2.09	-2.05	3.54
94	10.03	1.85	-16.12	0.85	-0.90	3.01	-0.50	1.95
95	13.00	2.76	-8.39	1.49	3.26	2.90	-5.86	4.01
96	4.21	1.58	-3.59	1.88	2.12	1.75	-0.05	1.51
97	12.25	1.51	-6.06	1.31	-1.70	1.69	-1.64	1.25
98	-7.70	1.24	-10.73	2.08	-2.47	2.25	-3.00	2.93
99	12.18	1.42	1.86	1.03	-2.50	1.89	-2.43	1.51
100	-9.96	1.78	-7.68	1.61	-1.64	1.74	-1.31	1.32
101	12.64	0.97	-0.81	1.84	-3.40	2.66	-1.80	2.26
102	6.67	1.03	6.55	1.17	-0.12	1.64	-2.55	1.27
103	10.11	1.11	-8.90	2.00	0.87	1.74	3.10	2.67
104	-9.88	1.77	-12.68	1.96	-1.32	2.19	-0.78	1.28

stat	Vessel Mounted OS75 - BB Firing				Vessel Mounted OS75 - BB Visbeck			
	mean u	sd u	mean v	sd v	mean u	sd u	mean v	sd v
	(cm/s)	(cm/s)	(cm/s)	(cm/s)	(cm/s)	(cm/s)	(cm/s)	(cm/s)
105	16.19	2.08	6.46	0.96	2.15	2.05	-1.11	2.64
106	1.62	1.29	2.92	1.20	-0.67	1.42	-2.21	2.30
107	12.02	1.45	-8.25	1.70	-4.05	1.55	1.59	1.61
108	8.96	2.33	-8.46	1.39	0.92	2.71	0.83	1.48
109	1.17	1.32	-4.50	1.23	-0.43	1.76	0.35	1.90
110	-9.02	1.20	-7.55	1.50	1.16	1.61	-0.38	2.15
111	7.21	1.24	5.59	1.99	-1.10	1.88	-1.75	2.40
112	2.88	1.11	-8.89	1.09	2.54	1.50	-1.38	1.74
113	-5.43	1.55	5.02	1.05	3.30	9.84	-3.21	1.24
114	1.13	1.15	2.87	1.07	-1.26	1.29	1.21	2.44
115	0.43	1.06	-3.48	2.33	-0.30	2.60	-1.45	2.32
116	-0.83	1.09	1.12	1.66	-0.08	1.66	-1.88	3.12
117	5.16	1.06	2.01	1.26	0.28	1.50	0.49	6.53
118	-1.67	1.30	-2.83	1.19	-1.46	1.77	1.21	1.36
119	0.12	1.22	1.10	1.36	-1.05	1.27	-2.47	2.60
120	-4.64	1.60	-0.22	1.59	-4.35	1.86	-2.65	3.41
121	0.77	0.92	-1.88	0.85	-0.59	0.98	-1.31	0.82
122	0.06	1.21	-0.50	1.58	-0.94	1.10	-1.93	1.65
123	-0.12	1.25	0.08	1.28	0.27	1.81	-0.30	1.64

The velocity profiles were also compared visually to bottom track data from the master Workhorse and Broadband through the Visbeck processing (Figure 14.2).

## 14.8 Command Files

BB cmd

```
CR1          Retrieve Factory Parameters
PS0          Show System parameters (Xdcr)
CY
CT 0         Turnkey = off
EZ 0011101   Sensor source (C;D;H;P;R;S;T)
EC 1500      Speed of sound
EX 11101     Coord Transform (Xform:Type;Tilts;3Bm;Map)
WD 111100000 Data Out (V;C;A;Pg;St;Vsum;Vsum^2)
WL 0,4       Water ref layer?
WP 00001     Ping per Ensemble
WN 016       Number of depth cells
WS 1600      Depth cell size
WF 1600      Blank after transmit
WM 1         Profiling mode
WB 1         Bandwidth Control (1=med)
WV 350       Ambiguity Velocity
WE 0150      Error Velocity Threshold
WC 056       Low Correlation Threshold
CP 255       Xmt Power
CL 0         Leapfrog = on
BP 000       Pings per ensemble
TP 000000    Time per ping
TB 00000200  Time per burst
TC 2         Ensembles per burst
TE 00000080  Time per ensemble
CF11101     Flow Control (Enscyc;Pngcyc;Binry;Ser;Rec)
&?
CS          Go (start pinging)
```

BB trial

```
CR1
PS0
CY
CT 0
EZ 0011101
EC 1500
EX 11101
WD 111100000
WL 0,4
WP 00001
WN 013
WS 2000
WF 2000
WM 1
WB 1
WV 350
```

WE 0150  
 WC 056  
 CP 255  
 CL 0  
 BP 000  
 TP 000000  
 TB 00000200  
 TC 2  
 TE 00000080  
 CF11101  
 &?  
 CS

#### WHM

PS0	Show Sys Parameters
CR1	Retrieve Factory Parameters
CF11101	Flow Ctrl (EnsCyc;PngCyc;Binry;Ser;Rec)
EA00000	Heading Alignment
EB00000	Heading Bias
ED00000	Transducer Depth
ES35	Salinity ppt
EX11111	Coord Transform (Xform:Type;Tilts;3Bm;Map)
EZ0111111	Sensor Source (C;D;H;P;R;S;T)
TE00:00:01.00	Time per Ensemble (hrs:min:sec.sec/100)
TP00:01.00	Time per ping (min:sec.sec/100)
LD111100000	Data Out (V;C;A;Pg;St;Vsum;Vsum^2)
LF0000	Blank After Transmit
LN016	Number of depth cells
LP00001	Pings per ensemble
LS1000	Depth cell size
LV250	Ambiguity Velocity
LJ1	Receiver gain select
LW1	Mode 1 pings before
LZ30,220	
SM1	
SA001	
SW05000	
CK	Keep parameters as user defaults
CS	Go (start pinging)

#### WHS

PS0	Show sys parameters
CR1	Retrieve factory parameters
CF11101	Flow Ctrl
EA00000	Heading alignment
EB00000	Heading Bias
ED00000	Trasnducer Depth
ES35	Salinity ppt
EX11111	Coord Transform
EZ0111111	Sensor Source
TE00:00:01.00	Time per Ensemble
TP00:01.00	Time per ping
LD111100000	Data out
LF0000	Blank After transmit

LN016	Number of depth cells
LP00001	Pings per ensemble
LS1000	Depth cell size
LV250	Ambiguity Velocity
LJ1	Receiver gain select (1=high)
LW1	Mode 1 pings before
LZ30,220	
SM2	
SA001	
ST0	
CK	Keep parameters as user defaults
CS	Go (start pinging)



## **15. LOWERED ACOUSTIC DOPPLER CURRENT PROFILER DATA PROCESSING SOFTWARE TEST SUITE**

Steven Alderson and Amanda Simpson

There are two sets of software available for analysis of LADP profiles: the Firing software from the University of Hawaii (UH) and the Visbeck software from LDEO. However, there are characteristics of the outputs from both methods that are not well understood and do not seem to relate to the oceanography when compared to shipboard measurements. It would be desirable to evaluate the performance of both methods and the effect of introducing certain types of error and bias on the calculated velocities.

The Firing software is more established but the Visbeck uses a more sophisticated method to estimate the velocities. It is also written entirely in Matlab whereas the Firing method uses both Perl and Matlab scripts. For these reasons, the Visbeck method would be preferred. However, there are occasions when the Visbeck method produces different results to Firing, when Firing is found to agree with shipboard ADP observations.

The aim of this project is to develop a program capable of generating test LADP output files for which the ocean velocity is known. This could then be used to test the two methods under different conditions, the aim being to determine which produces the best answers and when. This project was undertaken during cruise D279, although it was not the intention to take it to completion during that time period.

A report documenting this software is available from Steven Alderson.

## 16. NAVIGATION AND SHIPBOARD ACOUSTIC DOPPLER CURRENT PROFILER

Steven Alderson and Amanda Simpson

RRS *Discovery* has two SADPs mounted in the hull: the tried and tested 150kHz and the new Ocean Surveyor 75kHz. The 150kHz ADP is mounted 1.75m to port of the keel, 33m aft of the bow and at a depth of ~5m. The 75kHz ADP is 4.15m forward and 2.5m to starboard of the 150kHz instrument. This was the known state of affairs before the recent refit. The positioning of the 75kHz ADP that much further forward means that it is more prone to bubble contamination when the ship is pitching, therefore depth coverage and quality deteriorates noticeably in rough seas. To avoid echoes between the two instruments, synchronisation is necessary. The intention was to set up the instruments so that the 75kHz was the master.

High quality navigation data is crucial for obtaining accurate measurements of ocean currents using both vessel mounted and lowered ADPs. The following sections describe the operation and data processing paths for both ADPs as well as the navigation data, crucial for obtaining accurate ADP current measurements.

### 16.1 Navigation

There are four GPS receivers on RRS *Discovery*: the Trimble 4000 (gps\_4000) which is a differential GPS; the Glonass (gps\_glos) which uses a combination of Russian and American satellite networks; the Ashtech (gps\_ash); and the GPS G12 (gps\_g12). Data from all instruments were logged to the RVS Level A system before being transferred to RVS Level C system.

### 16.2 GPS and Bestnav

A standard PSTAR best navigation file was updated regularly throughout each cruise from datastream bestnav, using the script navexec0. The preferred input for bestnav is the Trimble 4000, as it has been found on previous cruises to give higher positional accuracy. If there were gaps in the Trimble 4000 data, the bestnav process used other inputs as necessary in the order Glonass, Ashtech, G12.

From positions logged in port at the start of the cruise, the standard error in both lat and lon of the gps\_4000 was found to be 0.000003 degrees (between 0.3 and 0.4 m).

The gps\_4000 coverage was extremely good during D278, with only one time-gap:

time gap : 04 084 04:42:19 to 04 084 04:43:24 (65 s)

Surprisingly, gaps were found in the bestnav datastream. It is unknown why these gaps occurred. This should be investigated.

time gap : 04 078 20:00:10 to 04 078 20:01:00 (50 s); time gap : 04 078 20:01:00 to 04 078 20:02:00 (60 s); time gap : 04 078 22:01:10 to 04 078 22:02:10 (60 s); time gap : 04 079 08:46:30 to 04 079 08:47:50 (80 s); time gap : 04 080 07:25:40 to 04 080 07:26:50 (70 s); time gap : 04 080 15:46:20 to 04 080 15:48:00 (100 s); time gap : 04 081 10:42:50 to 04 081 10:44:40 (110 s); time gap : 04 081 19:00:50 to 04 081 19:02:40 (110 s); time gap : 04 083 02:27:50 to 04 083 02:29:20 (90 s); time gap : 04 084 10:03:10 to 04 084 10:04:30 (80 s); time gap : 04 085 02:43:40 to 04 085 02:44:20 (40 s); time gap : 04 085 04:59:30 to 04 085 05:00:40 (70 s); time gap : 04 086 04:15:20 to 04 086 04:17:10 (110 s); time gap : 04 087 07:40:10 to 04 087 07:41:40 (90 s); time gap : 04 087 18:16:40 to 04 087 18:17:40 (60 s); time gap : 04 087 18:17:40 to 04 087 18:18:20 (40 s); time gap : 04 087 20:07:30 to 04 087 20:08:10 (40 s); time gap : 04 089 07:51:00 to 04 089 07:52:50 (110 s); time gap : 04 089 16:08:20 to 04 089 16:09:10 (50 s)

These time gaps also occurred during D279, the longest being 110 seconds.

### **16.3 Ship's Gyrocompass**

The ship's gyrocompass provides a reliable (i.e. not dependent on transmissions external to the ship) estimate of the ship's heading. However, the instrument is subject to latitudinally dependent error, heading dependent error, and has an inherent oscillation following a change in heading.

Ship heading from the gyro was logged every second to the RVS level C. Processing consisted of regular acquisition of the gyro heading using PEXEC script gyroexec0. Data were edited for headings outside the 0-360 degree range, saved, and then appended to a separate master file for each cruise.

On cruise 279, a problem was noted with clock drift by the gyro Level A that affected all cruises to varying degrees. This is discussed further in the next section.

## 17. ASHTECH 3DF GPS ATTITUDE DETERMINATION

The Ashtech ADU2 (Attitude Detection Unit 2) GPS is a system comprising four satellite receiving antennae mounted on the bridge top. Every second, the Ashtech calculates ship attitude (heading, pitch and roll) by comparing phase differences between the four incoming signals. These data are used in post-processing to correct ADP current measurements for 'heading error'. This post-processing is necessary because in real-time the ADP uses the less accurate but more continuous ship's gyro heading to resolve east and north components of current. In processing, small drifts and biases in the gyro headings are corrected using the Ashtech heading measurements.

Processing the Ashtech data was broken down into a number of execs and manual steps as follows:

ashexec0	acquisition of raw data.	
ashexec1	merge Ashtech and gyro data. The difference between the Ashtech and gyro headings are calculated (a-ghdg) and set in the range between -180 and 180.	
ashexec2	quality control the data (ashexec2). This exec removes data outside the limits for the following variables:	

hdg	0	360
pitch	-5	5
roll	-7	7
attf	-0.5	0.5
a-ghdg	-7	7
mrms	0.00001	0.01
brms	0.00001	0.1

- Manually edit out any remaining outliers in a-ghdg using plxyed with ash.pdf.
- Interpolate a-ghdg and plot the resulting file.
- Append data to a master file for each cruise.

Data coverage for all three cruises was good, with only minor gaps.

i) 277

time gap: 04 060 06:55:04 to 04 060 06:56:37 ( $\approx 1.5$  min)

time gap: 04 060 06:57:02 to 04 060 06:58:50 ( $\approx 2$  min)

time gap: 04 065 12:04:36 to 04 065 12:05:39 ( $\approx 1$  min)

time gap: 04 069 21:29:17 to 04 069 21:33:49 ( $\approx 4$  min)

ii) 278

time gap : 04 080 21:17:05 to 04 080 21:18:46 (101 s)

time gap : 04 084 03:59:04 to 04 084 04:00:07 (63 s)

time gap : 04 085 23:51:38 to 04 085 23:52:42 (64 s)

iii) 279

time gap : 04 104 07:00:20 to 04 104 07:02:49

time gap : 04 120 07:36:13 to 04 120 07:37:19

time gap : 04 122 20:00:16 to 04 122 20:09:54

time gap : 04 123 22:00:27 to 04 123 22:02:00

time gap : 04 129 05:17:47 to 04 129 05:18:50

However, on 279, it was noted that the Ashtech-Gyro differences were increasingly noisy with time. At the start of day 120, the level A's for all navigation data streams were reset (because of a master clock jump). The differences for that day revealed almost no noise. On investigation, it was found that instead of keeping in step with the master clock, the gyro level A timebase had been slowly drifting. Up to the time of the level A resets, it had become 19 seconds adrift. As a consequence, all gyro, Ashtech, 150kHz and 75kHz ADP data were reprocessed from the beginning.

## **18. OCEAN SURVEYOR 75KHZ SHIPBOARD ACOUSTIC DOPPLER CURRENT PROFILER**

### **18.1 Configuration and Performance**

The 75kHz ADP is a narrow band phased array with a 30 degree beam angle. Data was logged on a PC, using RDI data acquisition software (version 1.3). The instrument was configured to sample over 120 second intervals, with 60 bins of 16m thickness, and a blank beyond transmit of 8 m. Data were then averaged into 2 minute averaged files (Short Term Averaging, file extension STA) and 10 minute averaged files (Long Term Averaging, file extension LTA). The former were used for all data processing. The software logs the PC clock time and its offset from GPS time. This offset was applied to the data during processing, before merging with navigation. Gyro heading and GPS Ashtech heading, location and time were fed as NMEA messages into the software, which was configured to use the gyro heading for coordinate transformation.

The method for calibration of this instrument (and of the 150kHz SADP) relies on the collection of bottom track data, where the velocity of the bottom relative to the ship can be measured in water depths less than 1000m. This reduces the amount of data collected in the rest of the water column and therefore increases the noise in the measurements. Consequently, the instrument is swapped into bottom track mode only when appropriate.

During D277 and D278, bottom tracking was switched on early in the cruise (until 081 1803hrs) and at the end (from 086 2222hrs).

A problem was encountered after a restart of the logging software on day 80 (0130 hrs), after which time the fully processed data appeared to be contaminated by the ship's motion. Since the processing routines still resulted in good data for earlier raw files, we came to the conclusion that it was a problem with the software or software/configuration file set up. The RDI logging software takes input firstly from the configuration file, in which certain parameters such as bindepth can be specified, and secondly from parameters set manually in the graphical user interface (GUI). In the GUI under 'options', 'transforms', the heading correction, phi, was set to 60 degrees as required. For some unknown reason, it was not logged as such. To correct for this, 60 degrees was subtracted from the phi value in surexec3, giving  $\phi = -60.3694$ . To attempt to correct the problem, we completely rebooted the system, including turning the ADP deck unit itself off. We also tried switching configuration files. None of these changes worked.

On day 85, four configuration tests were carried out, varying the number of bins and switching between bottom tracking and water tracking modes. Details can be found by comparing parameters in the raw output files from the instrument.

During D279, bottom tracking was employed at the beginning, covering some of the same ground as in D277. From day 97 to the end of the cruise, the instrument remained in water track mode. The configuration file for this is listed in Appendix 18.

## **18.2 Processing**

### i) D277, D278

Data were logged on the OS75 PC and transferred by ftp to a UNIX workstation for processing.

- surexec0: read data into PSTAR format from RDI binary file; write water track data into files of the form sur279nn.raw and equivalent, where nn is a two character code; write bottom track data where present into files of the form sbt279mm; scale velocities to cm/s and amplitude by 0.45 to dB; correct time variable by combining GPS and the PC times; set the depth of each bin.
- surexec1: edit data (status flag equal to 1 is bad data); edit on percent good variable; move ensemble time to the end of its interval.
- surexec2: merge data with Ashtech-gyro difference file (created by ashexec2) and correct heading.
- surexec3: calibrate velocities by scaling by factor A and rotating by angle phi.
- surexec4: calculate absolute velocities by merging with navigation data (bestnav) and removing the ship's velocity over the ground from the ADP data.

### ii) D279

On this cruise an additional script was introduced after surexec0.

- surexec0b: take a sequence of files created by surexec0, append them together and extract data spanning a complete day.

This was intended to create files for the 75kHz instrument with similar names and data ranges as the corresponding 150kHz data files and each of the navigation files. Output files from surexec0 were

given two character letter codes ('aa', 'ab', etc.) and those from surexec0b were assigned two digit numbers as usual.

### 18.3 Calibration

Calibration of the 75kHz ADP was undertaken using the following procedure:

- run through the normal processing steps as described above, with  $A=1$  and  $\phi=0$  in surexec3.
- convert bottomew/bottomns into speed and direction (botspd,botdirn using pcmcal)
- convert ve/vn into speed and direction (shipspd,shipdirn using pcmcal)
- calculate  $A$  ( $=\text{shipspd}/\text{botspd}$ ) and  $\phi$  ( $=\text{shipdirn}-\text{botdirn}$ )
- select a valid subset of data and calculate mean  $A$  and  $\phi$ .

#### i) D277

On this cruise, the only part of the track suitable for bottom tracking was at the end. This meant that no calibration could be performed. The processing used an amplitude factor  $A = 1.0$  and misalignment angle  $\phi = 0^\circ$ .

#### ii) D278

The bottom track data available when the ship was close to the Bahamas on cruise D277 was worked up on this cruise. The method involved the additional steps:

- data were first averaged into 20 minute bins (using pavrge) before calculation of speeds and directions
- after calculation of speeds and directions, the PSTAR file was saved in Matlab (using pmatlb)
- Matlab script ADP\_Aphi\_calib.m was run which undertook the following steps:
  - convert  $\phi$  such that it lies between -180 and 180 degrees
  - remove data from Florida Strait CTD section



- remove data where botspd < 200
- remove data where change in ship direction > 30 degrees between 20 minute averages
- remove outliers ( $A < 0.9$ ,  $A > 1.1$ ,  $\phi < -5$ ,  $\phi > 5$ )
- remove data that is over 2 standard deviations from the mean
- calculate A and phi from mean values of A and phi

The calibration values obtained were  $A = 1.0017$  (sd = 0.0103),  $\phi = -0.2743$  (sd = 0.6106). As noted earlier, for raw data files from 080 (0131 hrs), we had to use  $\phi = -60.2743$ .

### iii) D279

On this cruise, data were not averaged to 20 minutes and remained as 2 minute ensembles.

Calculation of the mean A and phi from spot values was undertaken by choosing good input data by visual inspection of the values. Two extra parameters were calculated: the minimum range (from each of the four transducers) to the bottom and the absolute difference of the minimum and maximum ranges. Records of data were included in the averaging if they occurred in a consecutive sequence of records, which involved stable heading, Ashtech correction and ship's speed, and if the range difference was less than 15m. All available bottom track data from D277 and D279 were used. This consisted of one section of data from D277 and two from D279. The selected data were then plotted, outliers removed and A and phi values averaged. The resulting calibration values were:  $A = 1.004$  and  $\phi = -60.12$  with standard deviations 0.007 and 0.44 respectively. Figure 18.1 shows the final distribution of data for these values.

With the luxury of more time on this cruise than on the previous cruises, a number of problems were corrected for the earlier data. Values of A and phi from the 150kHz instrument had been wrongly applied to the 75kHz during D278. These files were corrected with the above final calibration. Different files had been assigned different ranges of bin depths because of the wrong choice of a depth offset of the first bin. These were all adjusted to 21m for the first bin depth. As a consequence, all data from D277 were reprocessed from surexec0 and therefore followed the D279 processing path.

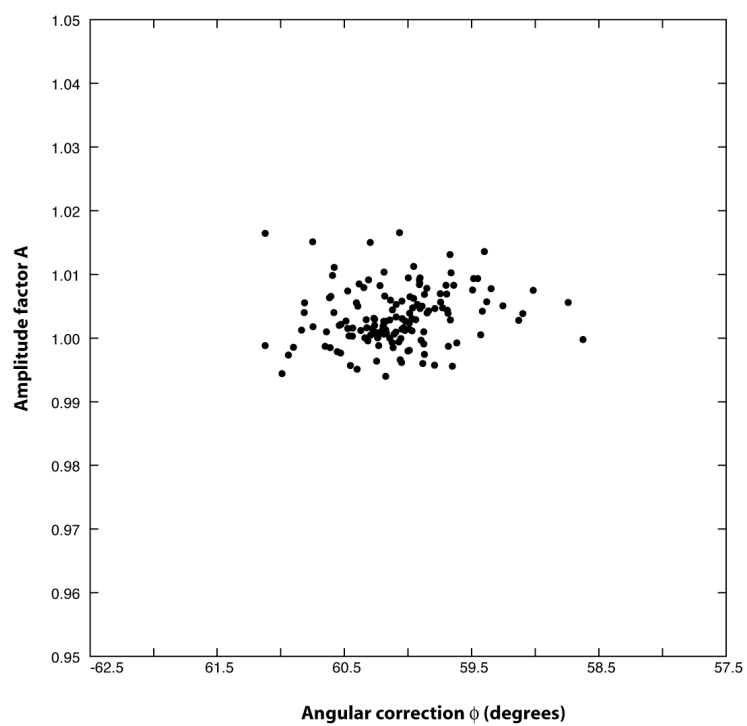


Figure 18.1: Scatter plot of amplitude correction  $A$  against angular correction  $\phi$  calculated from all suitable two minute averages from D277 and D279.

## Appendix 18

Configuration file used for the OS75 SADP for D279 water track mode.

```
;-----
-----\
; ADP Command File for use with VmDas software.
;
; ADP type: 75kHz Ocean Surveyor
; Setup name: default
; Setup type: Low resolution, long range profile(narrowband)
;
; NOTE: Any line beginning with a semicolon in the first
; column is treated as a comment and is ignored by
; the VmDas software.
;
; NOTE: This file is best viewed with a fixed-point font (eg.
courier).
;-----
-----/

; Restore factory default settings in the ADP
crl

; set the data collection baud rate to 115200 bps,
; no parity, one stop bit, 8 data bits
; NOTE: VmDas sends baud rate change command after all other
commands in
; this file, so that it is not made permanent by a CK command.
cb811

; Set for narrowband profile mode, single-ping ensembles,
; sixty 16m bins, 8m blanking distance, 390 mm/s ambiguity vel
NP001
NF800
NS1600
NN60

WP000

WF0800
WS1600
WN040

WV390

; Disable single-ping bottom track,
; Set maximum bottom search depth to 1200 meters
BP000
BX12000

; output velocity, correlation, echo intensity, percent good
WD111100000

; Two seconds between bottom and water pings
```

TP000200

```
; Two seconds between ensembles
; Since VmDas uses manual pinging, TE is ignored by the ADP.
; You must set the time between ensemble in the VmDas Communication
options
```

TE00000200

```
; Set to calculate speed-of-sound, no depth sensor,
; external synchro heading sensor, use internal
; transducer temperature sensor
```

EZ1020001

```
; Output beam data (rotations are done in software)
```

EX00000

```
; Set transducer depth to 5.3m
```

ED00053

```
; No synchro
```

CX0,0

```
; save this setup to non-volatile memory in the ADP
```

CK

## **19. 150KHZ SHIPBOARD ACOUSTIC DOPPLER CURRENT PROFILER**

### **19.1 Configuration and Performance**

The 150kHz ADP data was logged using the IBM DAS. It was configured to sample for 120 second intervals, with 64 bins of 8 m thickness, and a blank beyond transmit of 4 m. Where shallow water was encountered, the ADP was operated in bottom track (BT) mode, otherwise it was operated in water track (noBT) mode.

#### ii) D278

The ADP performed without malfunction for the entire cruise.

#### iii) D279

At the start of this cruise, considerable problems were encountered in starting the ADP. The PC software used to control the instrument repeatedly failed to connect to the deck unit. After many attempts with varying configurations, the ADP started. Unfortunately, the slave synchronization instruction was omitted in this permutation. Rather than risk it failing to start again, the instrument was left with this configuration for the duration of the cruise. Bottom tracking was permanently on. It should be emphasised that the 75kHz instrument is not a perfect replacement for the 150kHz since the 75kHz performs less well when the ship is underway, and has lower resolution in order to improve the statistics of measurements in each bin.

### **19.2 Clock Correction**

The ADP uses its own internal clock that drifts by a few seconds per day. To correct this to match the ship's master clock, careful track was kept of the deviations between the two clocks (see clockdrift.dat).

#### ii) D278

A Matlab program (clockdrift.m) was used to calculate the drift (assuming that it was linear) and correct the ADP times for it. As a result, the ADP time is synchronized to the ship's master clock.

#### iii) D279

On this cruise, data were processed in daily chunks and the clock corrections applied by linear interpolation from selected values spanning the day.

### 19.3 Processing

adpexec0:	read raw data into PSTAR format from the RVS level C; split into gridded depth dependent and non-gridded depth independent files; scale velocities to cm/s and amplitudes by 0.45 into dB; perform nominal edits and adjust bin depths to correct levels.
adpexec1:	correct data timebase.
adpexec2_clock:	merge data with Ashtech-gyro difference data and correct headings.
adpexec3:	apply calibration values to the velocities, scaling speed by A and rotating directions by phi.
adpexec4:	calculate absolute velocities by merging with bestnav navigation data and removing ship's speed over the ground.

### 19.4 Calibration

As for the 75kHz instrument, calibration of this ADP is necessary.

#### i) D276 and D277

During the transect between Glasgow and Santa Cruz de Tenerife (D276), the 150Khz was set up in bottom tracking mode. The calibration was done using the data coming off the British shelf, removing the outliers and averaging over 15 minutes. The following calibration values were obtained:  $A=1.0019\pm0.0022$  and  $\phi=-0.232\pm 0.1270$ . The misalignment angle differs markedly from previous cruises ( $\phi=3.82$  for D262 and  $\phi=3.814$  during D253), suggesting that the ADP's alignment was changed during the recent dry dock refit at Viano Do Castelo. These values were used throughout these two cruises.

#### ii) D278

On previous cruise (D277) it was noticed that the ADP calibration might not be correct, and therefore a new calibration was undertaken for both SADPs.

Data was taken from the period when the ADP was in bottom track mode and the ship was close to the Bahamas. The steps undertaken to calibrate the ADP are the same as for the 75kHz. The calibration procedure produced values of  $A=1.0129\pm0.0135$ ,  $\phi=-0.3694\pm0.5049$ .

### iii) D279

It was noted on this cruise that plots of absolute velocity vectors against time for the 150kHz ADP showed clear differences between on and off station data. This was not true of the 75kHz. This is an indication of a poor calibration. Examination of all bottom track data assembled together produced inconsistent estimates for  $A$  and  $\phi$ . Consequently, because of the quality of the calibration for the 75kHz, it was decided to use that instrument to calibrate the 150kHz.

Comparison of averaged relative velocities from the 150kHz and 75kHz ADP's led to correction terms:

$$dA=0.985 \text{ (0.0142,104) and } d\phi=0.0887 \text{ (0.17,94) and therefore an overall set of values of } A=0.9977 \text{ and } \phi=-0.2807.$$

Figure 19.1 shows a comparison of underway velocity profiles from both instruments after final calibration. Agreement between the two is remarkable.

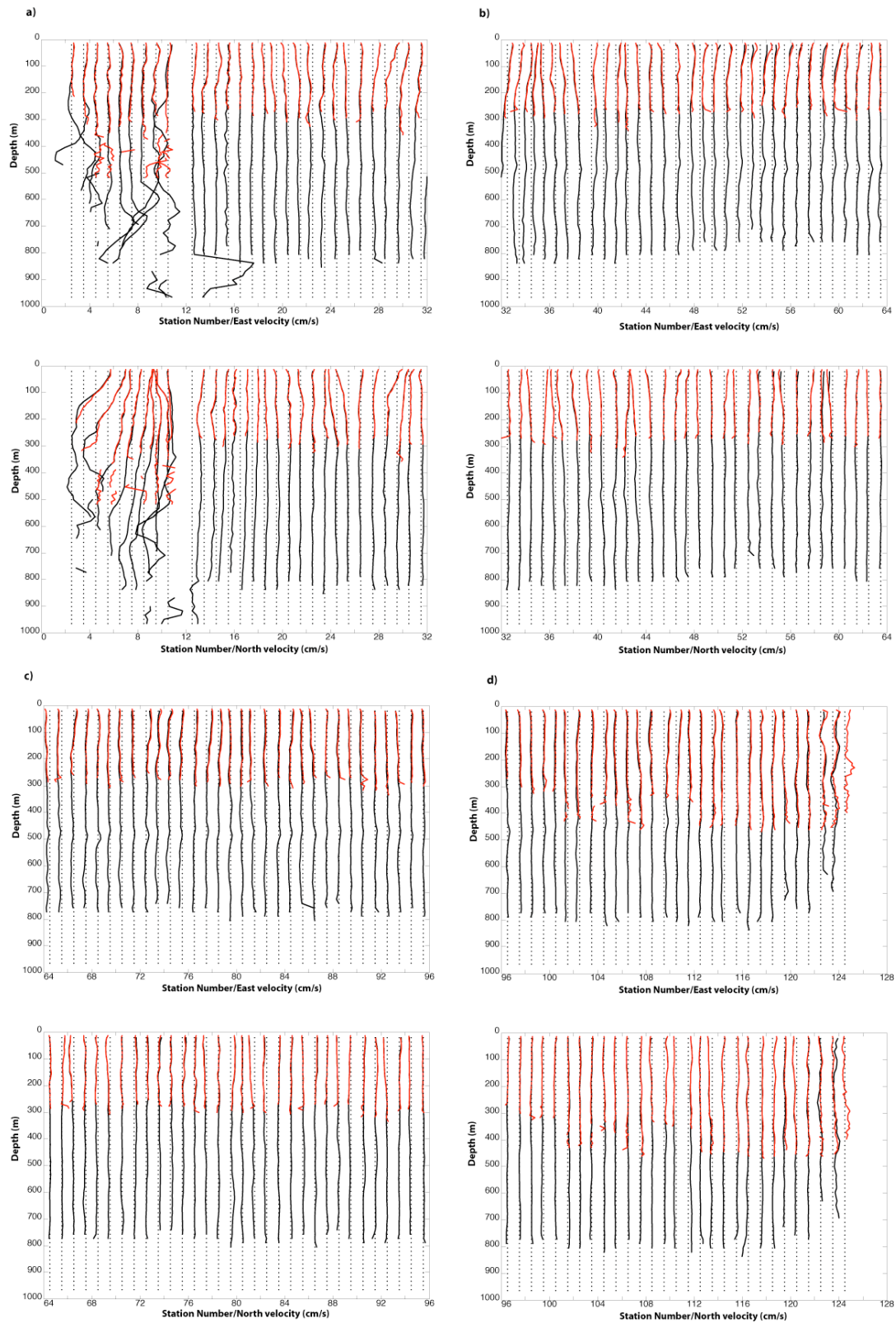


Figure 19.1: Velocity profiles from the 75kHz (black) and 150kHz (red) ADCP's averaged from underway data between each station pair. Each profile is plotted on an axis of station number at the halfway point at a scale of 50cm/s per station unit. A zero velocity line is shown as a black dotted line for each profile. a) Stations 2 - 32; b) Stations 32 - 64; c) Stations 64 - 96; d) Stations 96 - 125.



## Appendix 19

Water track configuration file for the 150kHz SADP used on all three cruises. Differences from the bottom track configuration are listed at the end.

```
AD,SI,HUNDREDTHS 120.00 Sampling interval
AD,NB,WHOLE 64 Number of Depth Bins
AD,BL,WHOLE 3 Bin Length
AD,PL,WHOLE 8 Pulse Length
AD,BK,TENTHS 4.0 Blank Beyond Transmit
AD,PE,WHOLE 1 Pings Per Ensemble
AD,PC,HUNDREDTHS 1.00 Pulse Cycle Time
AD,PG,WHOLE 25 Percent Pings Good Threshold
XX,OD2,WHOLE 5 [SYSTEM DEFAULT, OD2]
XX,TE,HUNDREDTHS 0.00 [SYSTEM DEFAULT, TE]
AD,US,BOOLE YES Use Direct Commands on StartUp
DP,TR,BOOLE NO Toggle roll compensation
DP,TP,BOOLE NO Toggle Pitch compensation
DP,TH,BOOLE YES Toggle Heading compensation
DP,VS,BOOLE YES Calculate Sound Velocity from TEMP/Salinity
DP,UR,BOOLE NO Use Reference Layer
DP,FR,WHOLE 6 First Bin for reference Layer
DP,LR,WHOLE 15 Last Bin for reference Layer
DP,BT,BOOLE NO Use Bottom Track
DP,B3,BOOLE NO Use 3 Beam Solutions
DP,EV,BOOLE YES Use Error Velocity as Percent Good Criterion
DP,ME,TENTHS 150.0 Max. Error Velocity for Valid Data (cm/sec)
DR,RD,BOOLE YES Recording on disk
DR,RX,BOOLE YES Record N/S (FORE/AFT) Vel.
DR,RY,BOOLE YES Record E/W (FORT/STBD) Vel.
DR,RZ,BOOLE YES Record vertical vel.
DR,RE,BOOLE YES Record error Good
DR,RB,BOOLE NO Bytes of user prog. buffer
DR,RP,BOOLE YES Record Percent good
DR,RA,BOOLE YES Record average AGC/Bin
DR,RN,BOOLE YES Record Ancillary data
DR,AP,BOOLE YES Auto-ping on start-up
XX,LDR,TRI 4 [SYSTEM DEFAULT, LDR]
XX,RB2,WHOLE 192 [SYSTEM DEFAULT, RB2]
DR,RC,BOOLE NO Record CTD data
XX,FB,WHOLE 1 [SYSTEM DEFAULT, FB]
XX,PU,BOOLE NO [SYSTEM DEFAULT, PU]
GC,TG,TRI 1 DISPLAY (NO/GRAPH/TAB)
GC,ZV,WHOLE 1 ZERO VELOCITY REFERENCE (S/B/M/L)
GC,VL,WHOLE -100 LOWEST VELOCITY ON GRAPH
GC,VH,WHOLE 100 HIGHEST VELOCITY ON GRAPH
GC,DL,WHOLE 0 LOWEST DEPTHS ON GRAPH
GC,DH,WHOLE 500 HIGHEST DEPTHS ON GRAPH
GC,SW,BOOLE NO SET DEPTHS WINDOW TO INCLUDE ALL BINS
GC,MP,WHOLE 25 MINIMUM PERCENT GOOD TO PLOT
SG,PNS,BOOLE YES PLOT NORTH/SOUTH VEL.
SG,PEW,BOOLE YES PLOT EAST/WEST VEL.
SG,PVT,BOOLE YES PLOT VERTICAL VEL.
SG,PEV,BOOLE YES PLOT ERROR VEL.
SG,PPE,BOOLE NO PLOT PERCENT ERROR
SG,PMD,BOOLE NO PLOT MAG AND DIR
```

SG,PSW,BOOLE NO PLOT AVERAGE SP. W.  
 SG,PAV,BOOLE YES PLOT AVERAGE AGC.  
 SG,PPG,BOOLE YES PLOT PERCENT GOOD  
 SG,PD1,BOOLE NO PLOT DOPPLER 1  
 SG,PD2,BOOLE NO PLOT DOPPLER 2  
 SG,PD3,BOOLE NO PLOT DOPPLER 3  
 SG,PD4,BOOLE NO PLOT DOPPLER 4  
 SG,PW1,BOOLE NO PLOT SP. W. 1  
 SG,PW2,BOOLE NO PLOT SP. W. 2  
 SG,PW3,BOOLE NO PLOT SP. W. 3  
 SG,PW4,BOOLE NO PLOT SP. W. 4  
 SG,PA1,BOOLE NO PLOT AGC 1  
 SG,PA2,BOOLE NO PLOT AGC 2  
 SG,PA3,BOOLE NO PLOT AGC 3  
 SG,PA4,BOOLE NO PLOT AGC 4  
 SG,PP3,BOOLE NO PLOT 3-BEAM SOLUTION  
 SS,OD,WHOLE 5 OffSet for Depth  
 SS,OH,TENTHS 45.0 OffSet for Heading  
 SS,OP,TENTHS 0.0 OffSet for Pitch  
 SS,ZR,TENTHS 0.0 OffSet for Roll  
 SS,OT,HUNDREDTHS 45.00 OffSet FOR temp  
 SS,ST,HUNDREDTHS 50.00 Scale for Temp  
 SS,SL,HUNDREDTHS 35.00 Salinity (PPT)  
 SS,UD,BOOLE YES Toggle UP/DOWN  
 SS,CV,BOOLE NO Toggle concave/Convex transducerhead  
 SS,MA,TENTHS 30.0 Mounting angle for transducers.  
 SS,SS,HUNDREDTHS 1500.00 Speed of Sound (m/sec)  
 XX,GP,BOOLE YES [SYSTEM DEFAULT, GP]  
 XX,DD,TENTHS 1.0 [SYSTEM DEFAULT, DD]  
 XX,PT,BOOLE NO [SYSTEM DEFAULT, PT]  
 XX,TU,TRI 2 [SYSTEM DEFAULT, TU]  
 TB,FP,WHOLE 1 FIRST BINS TO PRINT  
 TB,LP,WHOLE 64 LAST BIN TO PRINT  
 TB,SK,WHOLE 6 SKIP INTERVAL BETWEEN BINS  
 TB,DT,BOOLE YES DIAGNOSTIC TAB MODE  
 DU,TD,BOOLE NO TOGGLE USE OF DUMMY DATA  
 XX,PN,WHOLE 0 [SYSTEM DEFAULT, PN]  
 DR,SD,WHOLE 4 Second recording drive  
 DR,PD,WHOLE 4 First recording drive (1=A:,2=B: ... )  
 DP,PX,BOOLE NO Profiler does XYZE transform  
 SS,LC,TENTHS 5.0 Limit of Knots change  
 SS,NW,TENTHS 0.5 Weight of new knots of value  
 GC,GM,TRI 2 GRAPHICS CONTROL 0=LO RES, 1=HI RES, 2=ENHANCED  
 AD,PS,BOOLE YES YES=SERIAL/NO=PARALLEL Profiler Link  
 XX,LNN,BOOLE YES [SYSTEM DEFAULT, LNN]  
 XX,BM,BOOLE YES [SYSTEM DEFAULT, BM]  
 XX,RSD,BOOLE NO RECORD STANDARD DEVIATION OF VELOCITIES PER BIN  
 XX,DRV,WHOLE 4 [SYSTEM DEFAULT, DRV]  
 XX,PBD,WHOLE 3 [SYSTEM DEFAULT, PBD]  
 TB,RS,BOOLE NO SHOW RHPT STATISTIC  
 UX,EE,BOOLE NO ENABLE EXIT TO EXTERNAL PROGRAM  
 SS,VSC,TRI 0 Velocity scale adjustment  
 AD,DM,BOOLE YES USE DMA  
 TB,SC,BOOLE NO SHOW CTD DATA  
 AD,CW,BOOLE NO Collect spectral width  
 DR,RW,BOOLE NO Record average SP.W./Bin  
 DR,RRD,BOOLE NO Record last raw dopplers

```

DR,RRA,BOOLE NO Record last raw AGC
DR,RRW,BOOLE NO Record last SP.W.
DR,R3,BOOLE NO Record average 3-Beam solutions
DR,RBS,BOOLE YES Record beam statistic
XX,STD,BOOLE NO [SYSTEM DEFAULT, STD]
LR,HB,HUNDREDTHS 0.00 Heading Bias
SL,1,ARRAY5 1 1 8 NONE 19200 PROFILER
SL,2,ARRAY5 0 1 8 NONE 1200 LORAN RECEIVER
SL,3,ARRAY5 0 1 8 NONE 4800 REMOTE DISPLAY
SL,4,ARRAY5 2 1 8 NONE 9600 ENSEMBLE OUTPUT
SL,5,ARRAY5 0 1 8 NONE 1200 AUX 1
SL,6,ARRAY5 0 1 8 NONE 1200 AUX 2
DU,1,ARRAY6 100.00 100.00 60.00 0.00 0.00 YES D1
DU,2,ARRAY6 -100.00 -100.00 60.00 0.00 0.00 YES D2
DU,3,ARRAY6 200.00 200.00 60.00 0.00 0.00 YES D3
DU,4,ARRAY6 -200.00 -200.00 60.00 0.00 0.00 YES D4
DU,5,ARRAY6 200.00 19.00 60.00 0.00 0.00 YES AGC
DU,6,ARRAY6 0.00 0.00 60.00 0.00 0.00 NO SP. W.
DU,7,ARRAY6 0.00 0.00 60.00 0.00 0.00 NO ROLL
DU,8,ARRAY6 0.00 0.00 60.00 0.00 0.00 NO PITCH
DU,9,ARRAY6 0.00 0.00 60.00 0.00 0.00 NO HEADING
DU,10,ARRAY6 0.00 0.00 60.00 0.00 0.00 NO TEMPERATURE
DC,1,SPECIAL "FH00004" MACRO 1
DC,2,SPECIAL "DA24" MACRO 2
CI,1,SPECIAL "D277" CRUISE ID GOES HERE
LR,1,SPECIAL " " LORAN FILE NAME GOES HERE

```

The bottom track configuration file is the same except for the following exchanges:

DP,BT,BOOLE	NO Use Bottom Track	->	DP,BT,BOOLE	YES
Use Bottom Track				
SS,OD,WHOLE	5 OffSet for Depth	->	SS,OD,WHOLE	13
OffSet for Depth				
DC,1,SPECIAL	"FH00004" MACRO 1	->	DC,1,SPECIAL	
	"FH00001" MACRO 1			

## 20. MEASUREMENT OF DISSOLVED OXYGEN

Rhiannon Mather, Angela Landolfi, Richard Sanders

Dissolved oxygen samples were drawn from Niskin bottles on each CTD cast following the collection of samples for CFC analysis, and analysed using the Winkler whole bottle titration method. Between one and six duplicate samples were drawn on most casts from various Niskin bottles.

Samples were drawn through short pieces of silicone tubing into clear, pre-calibrated (approximately 100ml) wide-necked glass bottles. The temperature of each sample was taken using a handheld temperature probe immediately prior to fixing on deck with 1ml manganous chloride and 1ml sodium hydroxide. These chemicals were dispensed using Anachem dispensers, which were periodically rinsed throughout the cruise. The temperature at fixing of each of the samples was later used to calculate any temperature dependent changes in the volume of the sample bottles. After fixing, the lid of the sample bottles was inserted, taking care to ensure that no air bubbles were introduced, and the bottles shaken thoroughly. The samples were then taken to the CT (controlled temperature) laboratory, whereupon they were shaken once more, and then stored for later analysis. All reagents were prepared after Dickson (1994).

Analysis of the samples in the CT laboratory started a minimum of one hour after the collection of the samples. The SIS Winkler whole bottle titration method with spectrophotometric end-point was used for analysis. Immediately prior to titration, each sample was acidified with 1ml of sulphuric acid (using an Anachem dispenser) in order to dissolve the precipitate and release the iodate ions, and stirred with a magnetic stir bar set at a constant spin. Movement of the ship may have disturbed the magnetic stirrer bar, possibly resulting in less effective stirring, which would lead to a longer titration time, but it is unlikely that this would have affected the accuracy of the end-point determination.

The user variable parameters in the SIS supplied software (parameters screen in the options menu) were determined by trial and error at the start of the cruise and applied throughout. The following values were used: Stepsize 10, Wait time 10, Fast delay 3, Slow delay 3 and Fast factor 0.5. This parameter set resulted in titration times of less than four minutes.

Several batches of sodium thiosulphate solution ( $25\text{gL}^{-1}$ ) were made up during the cruise to titrate against the seawater samples. As the thiosulphate solution is unstable, it was standardised by titrating it against 5ml of certified standard 0.01N solution of potassium iodate every two to three days. The volume of thiosulphate required to titrate 5ml of this standard was then used in calculations of oxygen concentration in an MS Excel spreadsheet following the equations of Dickson (1994). Batch 3 of the thiosulphate solutions was very unstable (see Figure 20.1); the volume required to titrate 5mls of potassium iodate increased rapidly over a couple of days. Following this discovery, a new batch of

sodium thiosulphate solution was made up. To monitor the breakdown of the new solution more carefully and without using up the certified standards, a batch of potassium iodate solution was made up by dissolving 0.3567g of potassium iodate in 1L Milli-Q water. This new batch was relatively stable (see Figure 20.1), and results from the stations titrated using batch 3 were discarded. The reagent blank was evaluated at the start of the cruise and was found to be  $1.0 \times 10^{-3}$  ml for the single batches of reagents used during the cruise. This value was applied to all calculations undertaken.

The duplicate samples drawn at each station were compared and the percentage difference between them is shown in Figure 20.2, for a sample size of 77 pairs of duplicates. When obvious outliers are removed, the mean percentage difference between duplicate samples is 0.62% (standard deviation = 0.5487). Percentage differences greater than 3% accounted for 11.5 % of the samples.

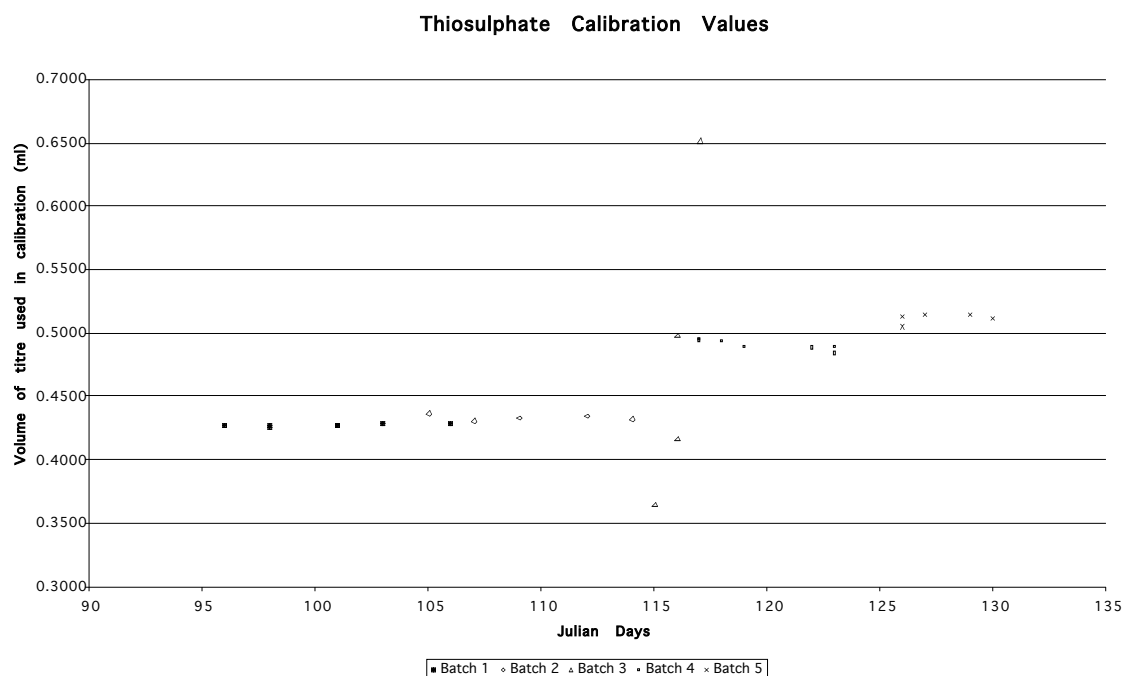


Figure 20.1: Volume of sodium thiosulphate used to titrate 5mls of certified standard of potassium iodate the duration of the cruise.

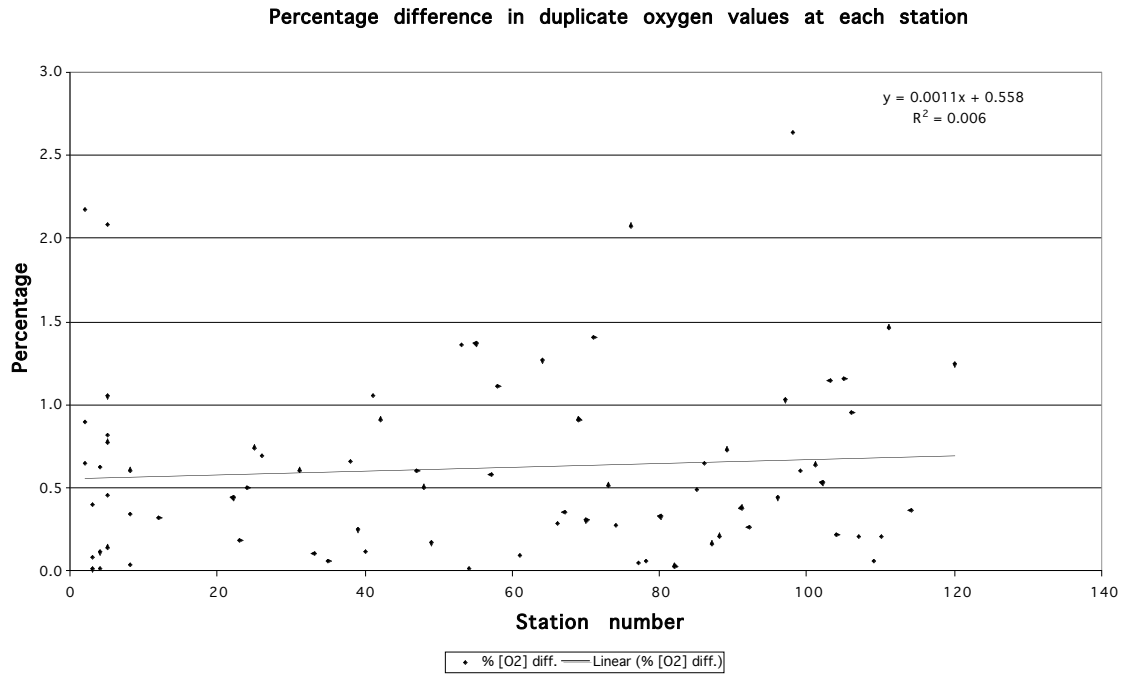


Figure 20.2: Percentage difference of oxygen concentration between duplicate samples.

## 20.1 Problems

In the time taken to sample the complete rosette of Niskin bottles, some of the later bottles may have warmed slightly in the sun. The handheld temperature probes are subject to a certain amount of variability and in several cases it was difficult to obtain reliable temperatures. Over the length of the cruise, several different thermometers were used. In total, 2699 samples were analysed using the SIS Winkler apparatus. During the cruise, there were 57 approximation failures (2.11% of samples). Other failures accounted for 0.74% of samples.

## 21. MEASUREMENT OF NUTRIENTS

Richard Sanders

Analysis for nitrate and nitrite (hereinafter nitrate), phosphate and silicate was undertaken on a Skalar sanplus autoanalyser following methods described by Kirkwood (1995), with the exception that the pump rates through the phosphate line were increased by a factor of 1.5, which improves reproducibility and peak shape. Samples were drawn from Niskin bottles into 25ml sterilin coulter counter vials and kept refrigerated at 4°C until analysis, which commenced within 24 hours. Stations were run in batches of 2-6 with most runs containing 3 or 4 stations. Overall, 34 runs were undertaken. An artificial seawater matrix (ASW) of 40 g/l sodium chloride was used as the intersample wash and standard matrix. The nutrient free status of this solution was checked by running Ocean Scientific International (OSI) nutrient free seawater on every run. In a departure from our previous methodology, a single set of mixed standards were made up at the start of the cruise and used throughout the cruise. These were made by diluting 5 mM solutions made from weighed dried salts in 1l of ASW into plastic 1l volumetric flasks that had been cleaned by soaking for 6 weeks in MQ water. This was in an effort to minimise the run to run variability in concentrations observed on previous cruises. OSI nutrient standard solutions were used sporadically during the cruise to monitor the degradation of these standards. Data were transferred to another computer initially using a zip disk, and then after station 66 by means of a memory stick. The zip disk transfer route was unreliable and resulted in a delay between sample analysis and data work up of 8-10 stations. After station 66, data were worked up immediately. This delay had the effect that the problems with the nitrate line described below could not be evaluated in close to real time. Data processing was undertaken using Skalar proprietary software. Generally this was straightforward, however a detailed examination of nitrate data from stations 20-60 was needed to achieve acceptable calibrations and bulk nutrient values. The wash time and sample time were 90 seconds, and the lines were washed daily with 0.25M NaOH (P) and 10% Decon (N, Si). Time series of baseline, bulk standard concentration, instrument sensitivity, calibration curve correlation coefficient, nitrate reduction efficiency and duplicate difference were compiled and updated on a daily basis.

### 21.1 Performance of the Analyser

1) In the early part of the cruise on runs 1-3 (stations 2-21), the phosphate baseline suffered frequent catastrophic baseline degradations. All the samples were rerun, but duplicates could not be run as the available duplicate time was used to reanalyse samples. This was alleviated mid run by removing the flow cell and shaking it vigorously, and eliminated over the longer term by refitting some elements of the line and reducing the pull through rate. Stations 49-52 were also affected by this problem and no P data is available for stations 51 and 52. Stations 71-74 were compromised by a

failure of the temperature water bath. These stations were reanalysed 24 hours later using samples from salinity bottles.

2) The nitrate line was very noisy between stations 22 and 60. Initially this was suspected to be due to a fault with the reagents, which were renewed several times. However, after this failed to rectify the situation, the cadmium column was repacked on two occasions. This also failed to rectify the situation and a new cadmium column was therefore fitted, which gave no problems during the rest of the cruise. Stations 22-60 were reprocessed to give bulk nutrient values in line with those from the remainder of the stations. The effect of this on data quality has yet to be systematically evaluated.

## 21.2 Analyser Performance

The performance of the autoanalyser is monitored via the following parameters: baseline value, calibration curve slope, regression coefficient of the calibration curve and nitrate reduction efficiency. Time series of these parameters are shown below in Figures 21.1 to 21.3.

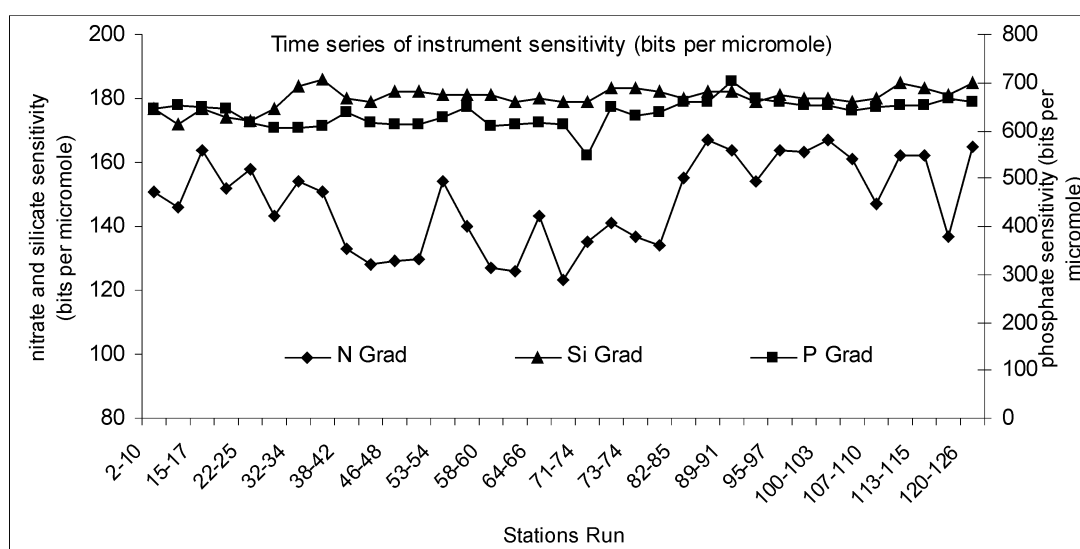


Figure 21.1: Autoanalyser sensitivity.

The instrument sensitivity for nitrate varied widely and unpredictably during the cruise by up to 40%. Phosphate and silicate sensitivity behaved much more reproducibly, with these parameters varying by about 10% over the 5 week period of observations.



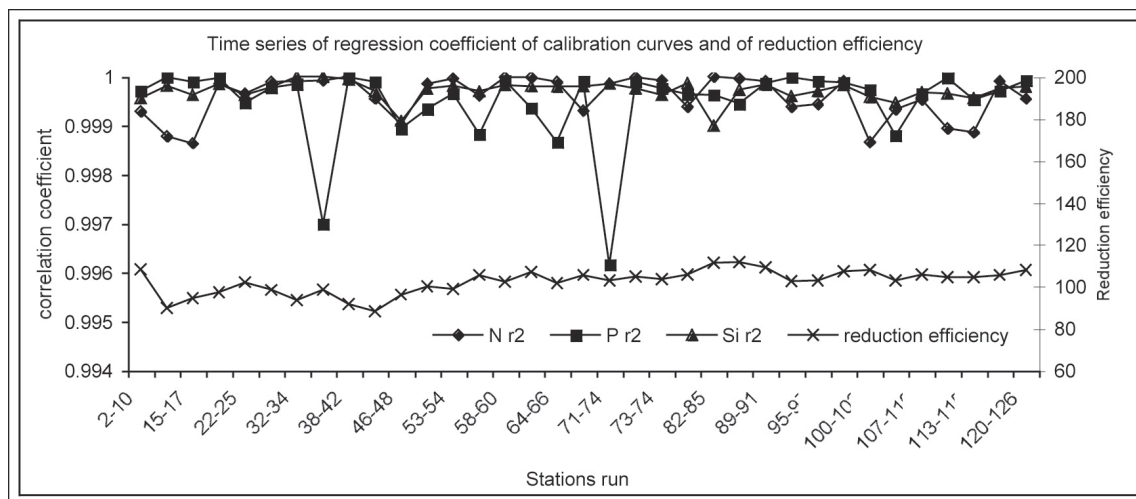


Figure 21.2: Calibration curve regression coefficients and reduction efficiency.

The quality of the calibration curves was generally good with 95% having regression coefficients better than 0.999. The reduction efficiency of the cadmium column was <100% during the early part of the cruise. The column was changed at station 66, after which the efficiency increased to approximately 100%.

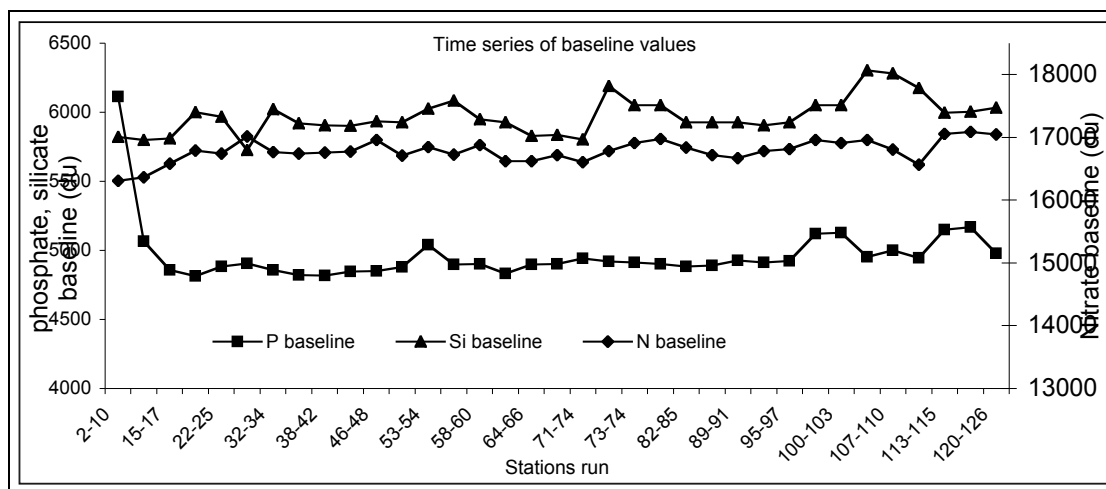


Figure 21.3: Baseline values.

The baseline value of the instrument barely changed through the cruise, with the exception of phosphate, which declined after the first run from 6300 to about 5900.

### 21.3 Data Quality

#### Precision of measurements

The short term precision of the measurements was evaluated by running one or two duplicate samples per station (thus 3-6 per run). Figure 21.4 shows time series of the percentage difference

between the duplicates for a) nitrate, b) silicate and c) phosphate together with five point running means through the data. The mean differences for Si, N and P were 0.67, 1.63 and 2.04%. However, this conceals substantial variability in both N and P precision during the cruise. A group of stations from approximately 25 – 60 had poor N precision but the precision of the phosphate analyses improved over the course of the cruise from about 5% to about 1%.

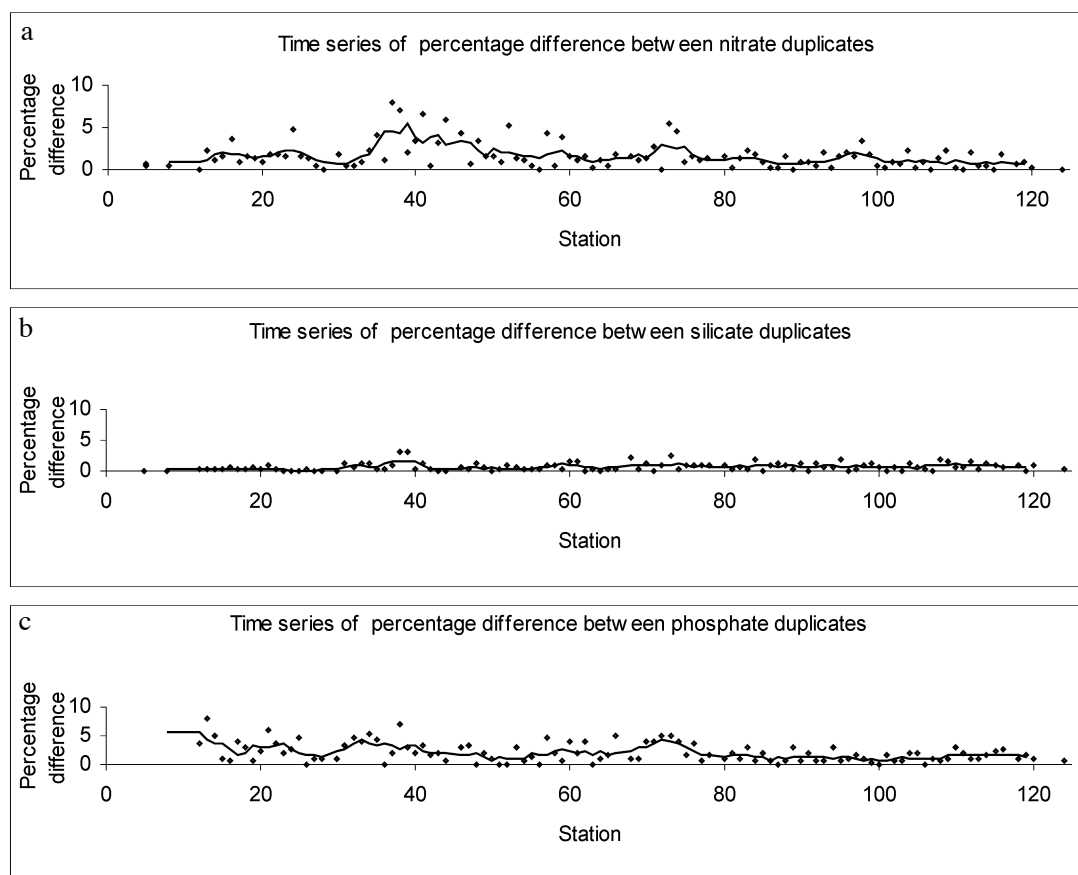


Figure 21.4: Percentage difference between duplicates for: a – nitrate, b – silicate, and c – phosphate.

#### Internal consistency of measurements

This was evaluated by using a deep water sample taken on station 1 and was run on every station. The concentrations of nitrate, phosphate and silicate in this sample over time are shown in Figure 21.5.

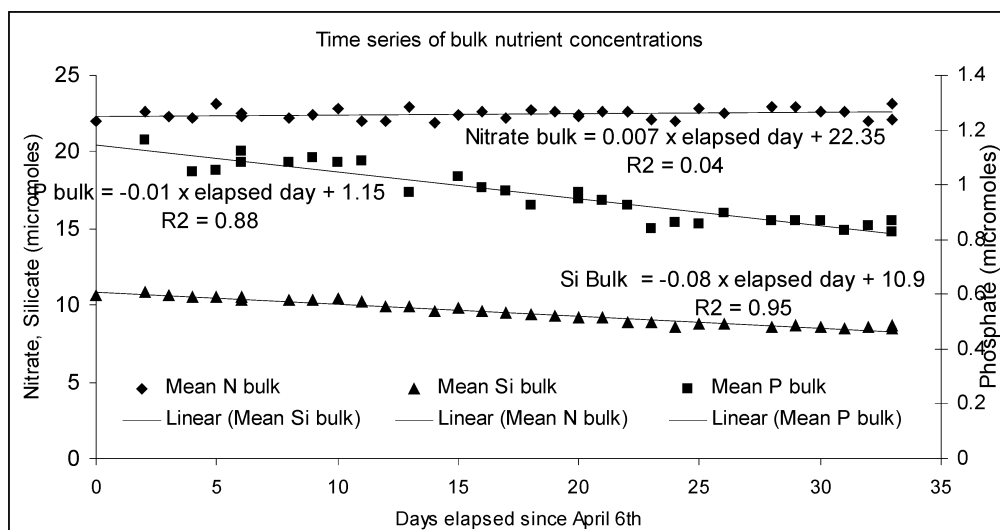


Figure 21.5: Concentrations of nitrate, phosphate and silicate with time.

Nitrate concentration appeared to be invariant whereas the P and Si concentrations declined markedly over the cruise. The variability of bulk nutrient concentration from the mean is indicative of the internal consistency of the dataset. For nitrate this is simple to evaluate (Figure 21.6), as the concentration appeared to be invariant. The residual concentration appears to be normally distributed and shows no significant trend over time. The absolute average residual value was 0.27 micromoles per litre or 1.2%.

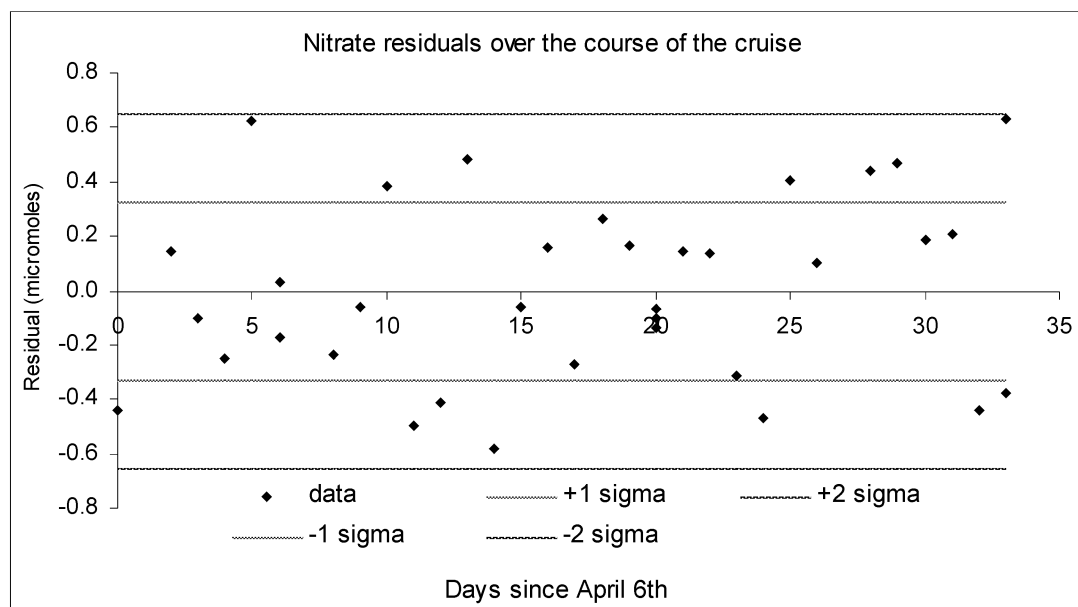


Figure 21.6: Nitrate residuals.

For phosphate and silicate, a linear function was fitted which predicted concentration as a function of elapsed day. This regression was used to generate values for P and Si for each day and the residual difference calculated (Figures 21.7 and 21.8)

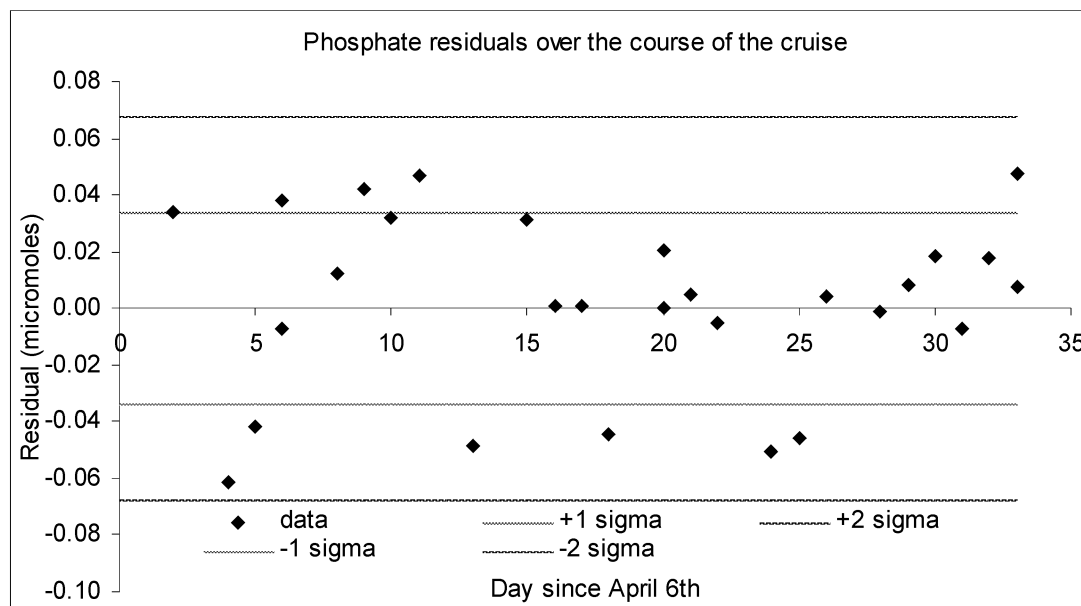


Figure 21.7: Phosphate residuals.

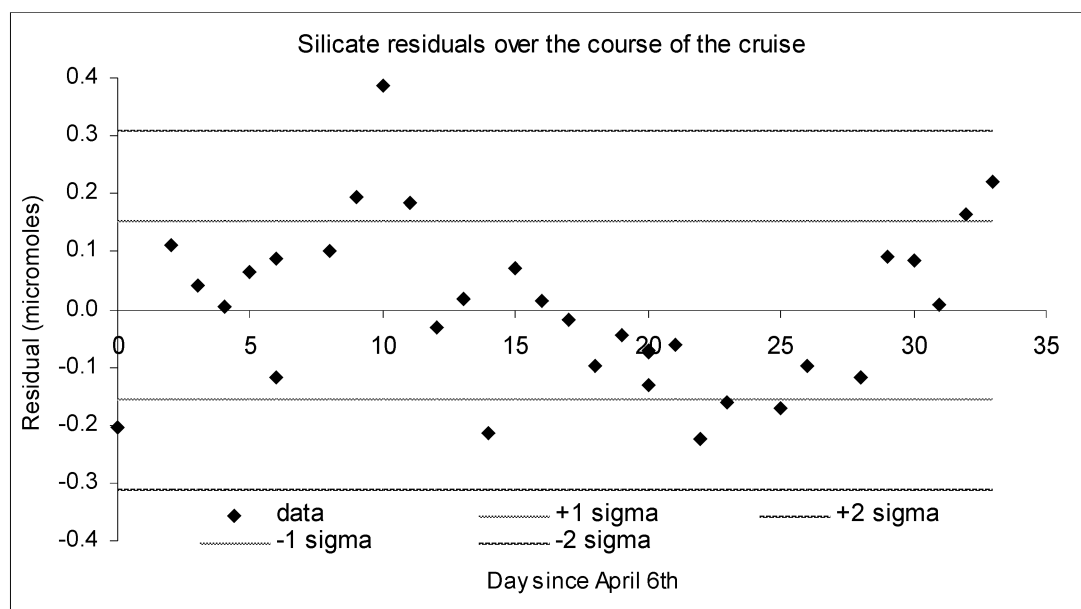


Figure 21.8: Silicate residuals.

Both P and Si residuals appear to have a normal distribution, with Si (and to a lesser extent P) residuals displaying a sinusoidal pattern with time for unknown reasons. The mean residual values are 0.12 micromoles per litre or 1.17% for Si and 0.03 micromoles per litre or 2.1% for P.

#### Accuracy of Measurements

The accuracy was monitored by the use of OSI nutrient standard solutions, which need to be diluted by the user. The analysis of these standards gave values of P 1.01 +/- 0.02 micromoles per litre for a nominally 1 micromolar solution, N 10.9 +/- 0.13 for a nominally 10 micromolar solution and Si 21.4 +/- 0.1 micromoles per litre for a nominally 20 micromolar solution. These imply that the N and Si results are too low by about 10 and 5% respectively. The standards used on this cruise have been retained for further investigation and a comparison with historical data will also be used to address this issue.

## 22. AUTOFLUX - THE AUTONOMOUS AIR-SEA INTERACTION SYSTEM

Margaret Yelland and Robin Pascal

AutoFlux is an autonomous, stand-alone system that obtains direct, near real-time (2hr) measurements of the air-sea turbulent fluxes of momentum and sensible and latent heat, in addition to various mean meteorological parameters. The two main aims of the present deployment were 1) testing of a new Licor sensor to determine its suitability for making direct measurements of the air-sea CO<sub>2</sub> flux, and 2) system development (detailed below). The AutoFlux system was mobilised in Govan, Glasgow in February 2004 prior to the start of cruise D276 and left to run autonomously until the beginning of D279. JRD and OED staff then joined the ship to install the new sensors and develop the system during D279. The system was then left to run autonomously during the return passage from Tenerife to Govan and was demobilised in Govan at the beginning of June.

Until this cruise, the system obtained flux measurements using the inertial dissipation (ID) method that relies on good sensor response at frequencies up to 10 Hz. The ID method has the advantage that the flux results a) are insensitive to the motion of the ship and b) can be corrected for the effects of the presence of the ship distorting the air flow to the sensors. Momentum and latent heat flux measurements have been successfully made using this method for a number of years. Sensible heat and CO<sub>2</sub> flux measurements are made more difficult by the lack of sensors with the required high frequency response. For these fluxes, the eddy correlation (EC) method provides an alternative. This method requires good sensor response up to only about 2 to 3 Hz, but is a) very sensitive to ship motion and b) the fluxes can not be directly corrected for the effect of air flow distortion. The development work on this cruise entailed testing and integration of a MotionPak sensor in order to measure the ship motion and thus make EC measurements of all the fluxes. Once EC fluxes are obtained, they can be corrected for flow distortion effects by comparison with the corrected ID fluxes where available. Since the scalar fluxes (sensible and latent heat and CO<sub>2</sub>) are all affected by flow distortion in the same fashion, only one ID scalar flux is required in order to quantify the effects of flow distortion on EC scalar fluxes. If the new CO<sub>2</sub> sensor performs adequately at low frequencies, direct measurements of the air-sea CO<sub>2</sub> flux will thus be obtained. In collaboration with the UEA carbon team, any successful CO<sub>2</sub> flux measurements will be used to improve the parameterisation of the CO<sub>2</sub> transfer velocity.

This report describes the AutoFlux instrumentation (Section 22.1). A brief discussion of the performance of the mean meteorological sensors is given in Section 22.2, where comparisons are made between the ship's instruments and those of AutoFlux where possible. As part of a separate project, visual observation of cloud cover were made and related to the downwelling long wave radiation measurements obtained from the AutoFlux system. These are also discussed in Section 22.2.

Initial flux results are described in Section 22.3. Appendix 22.A lists significant events such as periods when data logging was stopped, and Appendix 22.B contains figures showing time series of the mean meteorological data. All times refer to GMT.

More information on air-sea fluxes and the AutoFlux project in particular can be found at <http://www.soc.soton.ac.uk/JRD/MET/AUTOFLUX>.

## 22.1 Instrumentation

The SOC Meteorology Team instrumented the RRS *Discovery* with a variety of meteorological sensors. The mean meteorological sensors (Table 22.1) measured air temperature and humidity, wind speed and direction, and incoming longwave (4-50 micron) radiation. The Windsonic is a new 2-D anemometer on loan for trials from the manufacturers, Gill Instruments Ltd. The surface fluxes of momentum, heat, moisture and CO<sub>2</sub> were obtained using the fast-response instruments in Table 22.2. The HS and R3 sonic anemometers provided mean wind speed and direction data in addition to the momentum and sensible heat flux estimates. A new sensor based on a fast response thermistor was also trialled for the first time during D279. The data from the thermistor was logged via the analogue input of the R3.

To obtain EC fluxes, ship motion data from the MotionPak system has to be synchronised with those from the other fast response sensors. In order to achieve this, the MotionPak output was logged via the analogue input channel of the HS anemometer. In addition, a timer circuit was added in to the HS sonic interface unit. This circuit generated a square wave sync signal, which was input to the analogue channel of the Licor and to the PRT input to the HS. Once allowance was made for the 0.185-second delay in the H<sub>2</sub>O and CO<sub>2</sub> output from the Licor, this enabled synchronisation of all fast response data except those from the R3. The period of the sync signal was increased from 2.34 seconds (47 samples) to 8.6 seconds (172 samples) on day 111 at 2200, in order to remove any ambiguity when synchronising the data streams automatically.

Navigation data were logged in real time at 2-second intervals, using the ship's data stream rather than the separate AutoFlux GPS and compass. These data are used to convert the relative (measured) wind speed and direction to true wind speed and direction. The ship's mean meteorological data were also logged in real time at 2-second intervals. The details of the ship's meteorological instruments are given in Table 22.3.

All data were acquired continuously, using a 58 minute sampling period every hour (the remaining 2 minutes being used for initial data processing), and logged on "nimbus", a SunBlade 100 workstation. Processing of all data and calculation of the ID fluxes was performed automatically on "nimbus" during the following hour. Program monitoring software monitored all acquisition and

processing programs and automatically restarted those that crashed. A time sync program was used to keep the workstation time synchronised with the GPS time stamp contained in the navigation data. Both “nimbus” and all the AutoFlux sensors were powered via a UPS. The EC flux processing was developed during the cruise and performed on a second SunBlade 100 (“cirrus”) but was not integrated into the automatic processing.

All of the instruments were mounted on the ship’s foremast (Figure 22.1) in order to obtain the best exposure. The psychrometers and the fast response sensors were located on the foremast platform and the radiation sensors were mounted on a platform installed at the top of the foremast extension. The heights of the instruments above the foremast platform were: HS sonic anemometer 2.11 m; R3 sonic anemometer 2.81 m; psychrometers 1.85 m; thermistor sensor 1.80 m; Licor H<sub>2</sub>O / CO<sub>2</sub> sensor 1.21 m; and Windsonic anemometer 2.11 m.

## **22.2 Mean Meteorological Parameters**

### Air Temperature and Humidity

Two wet- and dry-bulb psychrometers were installed on the foremast and performed well until the end of day 117, when the starboard wet bulb stopped wicking. This did not cause any problems since the automatic processing chooses the lowest of the two wet bulb temperatures. The wicking problem was corrected on day 127. Excluding this period, 1 minute averaged data from the two psychrometers showed that the mean difference between the wet bulb temperatures was 0.05° (standard deviation of 0.07°), which is within the sensor specification. The difference between the dry bulb temperatures was only 0.005° (s.d. 0.15): the standard deviation was larger due to occasional drips from the wet bulbs falling on the dry bulbs. Again the problem was circumvented by the automatic processing, which selects the higher of the two temperatures. A comparison between the ship’s air temperature sensor and the best psychrometer data showed that the former was biased high by 0.18° (s.d. 0.12°). This could be due to the effects of solar heating, since the ship’s sensor is only ventilated rather than aspirated.

Relative humidity was calculated from the psychrometer data and compared to the ship’s humidity sensor. The ship’s sensor read high by 4.6 % (s.d 1%). Only 1% or less of this can be attributed to the automatic processing selecting the lowest wet bulb and the highest dry bulb, thus tending to bias the psychrometer humidities slightly low.

### Wind Speed and Direction

There were four anemometers mounted on the foremast platform (Figure 22.1). On the port side were the ship’s propeller anemometer and vane plus the 2-D Windsonic on trial from Gill Instruments



Ltd. On the starboard side were two fast response Solent sonic anemometers, an HS and an R3. Both measured all three components of wind speed and both were calibrated on a regular basis. The HS anemometer was the best exposed and will be used as the reference instrument in the following comparison. The measured wind speeds (uncorrected for ship speed) from each anemometer are compared to those from the HS in Figure 22.2, which shows the wind speed ratio (measured / HS measured) against relative wind direction for each anemometer. A wind blowing directly on to the bows is at a relative wind direction of 180 degrees. For a bow-on wind, the R3 sonic and the ship anemometer read high by about 5% and the Windsonic was high by nearly 15%. Some of the biases will be due to flow distortion. Accurate flow distortion corrections have yet to be determined for the precise anemometer locations, but previous work (Yelland et al., 2002) has shown that the bias at the Windsonic and HS anemometer sites should be between -1 and +2%. The 15 % bias in the Windsonic data is much greater than that expected due to flow distortion effects. Furthermore, the wind sonic and ship's anemometer were mounted close together, suggesting that the Windsonic is biased high by at least 10%. Figure 22.2 also clearly shows that the effects for flow distortion are, as expected, very sensitive to the relative wind direction. Since the HS and R3 sonics were located on the opposite side of the foremast extension to the other two anemometers, roughly 50% of the trend in wind speed error seen in the latter is actually due to the variation in flow distortion with wind direction at the HS anemometer site. The large dips in the speed ratios at 90 and 270 degrees are due to the HS/R3 and Windsonic/ship anemometers being in the wake of the foremast extension for winds from the port and starboard beams respectively. Figure 22.3 shows the difference in relative wind direction as measured by each anemometer compared to that from the HS. For bow-on winds, the HS, R3 and ship's anemometers agree to within 4 degrees but the Windsonic appears to be misaligned by 10 degrees.

### TIR and PAR Sensors

The ship carried two total irradiance sensors: one (Ptir) on the port side of the foremast platform and the other (Stir) on the starboard. These measure downwelling radiation in the wavelength ranges given in Table 22.3. Ptir functioned well throughout but Stir intermittently gave very noisy values for periods of up to a few days at a time. Figure 22.4 gives an example of this. It can be seen that from day 115 to day 118, the Stir values were very noisy even at night when zero  $W/m^2$  should have been measured. It was thought that the problem may lie in the cabling between the junction box on the foremast and the acquisition PC in the main laboratory. However, when the two sensors were plugged into each other's connector in the foremast junction box, the original Stir continued to be at fault, showing that the problem lies in the sensor itself or in the cable between sensor and junction box. The periods of noisy data seemed to occur during and after rain or times of high humidity, suggesting that moisture ingress may be the problem.

Mounted alongside each TIR sensor is a “PAR” (photosynthetically active radiation) sensor. Early examination of the data from these revealed a number of problems. The port sensor (Ppar) serial number was correct in the “surfmet” acquisition software and the correct calibration was applied in the data output from the surfmet PC to the AutoFlux system. However, the sensor is actually a solarimeter rather than a PAR sensor and measures radiation in a different wavelength range (Table 22.3). In contrast, the starboard (Spar) sensor was indeed a PAR sensor but its serial number was illegible. The surfmet sensor handbook contained calibrations for two possible sensors, and both of these were included in the “smtexec” processing scripts. However, in the scripts both calibrations were commented out. Matters were confused further when it was discovered that the calibration applied by the acquisition PC agreed with neither of those in the handbook. Determination of the correct calibration was not possible since there were no data from a second PAR sensor for comparison.

A complete overhaul of all TIR and “PAR” sensors is required.

### Long Wave Radiation

As part of the AutoFlux instrumentation, two Epply pyrgeometers were installed on top of the foremast extension. These sensors measure incoming long wave (LW) radiation. Following the procedure of Pascal and Josey (2000), three outputs from each sensor were recorded and a correction made for short-wave leakage. The P<sub>tir</sub> data were used for this purpose. From 1 minute averages of the resulting LW data, the mean difference between the two sensors was 5.6 (s.d. 2.3) W/m<sup>2</sup>, with sensor 31170 reading relatively high. Although this is within the expected accuracy of the sensors, the difference between the two was seen to depend on shortwave radiation. Figure 22.5 shows the difference vs. P<sub>tir</sub>. It can be seen that the difference is 5 W/m<sup>2</sup> or less for low levels of shortwave radiation, but increases with shortwave to a maximum of over 8 W/m<sup>2</sup>. This suggests that the short-wave leakage term for sensor 31170 is too small.

### Visual Cloud Observations

During D279, visual cloud observations were made every hour by the scientific watch according to the classifications given in the Met. Office guide “Cloud types for observers”. Since visual observations are rather subjective it is usual to obtain a second independent set of observations wherever possible.

The observations of the scientific staff will be used to parameterise the downwelling longwave radiation in terms of cloud cover and type (Josey et al., 2002). The parameterisation will allow calculation of the LW radiation to be made from the visual observations routinely obtained by the

7000-strong Voluntary Observing Ship fleet, thus ultimately improving the accuracy of weather forecast models.

### Sea Surface Temperature

Sea surface temperature (SST) data from the thermosalinograph (TSG) was logged on the AutoFlux acquisition workstation as part of the “surfmet” data stream. A comparison of the TSG SST data with those obtained from the CTD at 10 m depth showed that the TSG was biased high by about 0.08 degrees (s.d. 0.15). Some of this bias may be due to the TSG intake being at a depth of about 5 m rather than 10 m.

### Ship Borne Wave Recorder (SBWR)

The SBWR was switched on prior to the ship leaving Govan. On arrival at the ship for the start of D279, it was seen that the starboard accelerometer was permanently registering full scale. The logging PC and deck unit, both located in the main lab, were checked and found to be working correctly. The fault seems to lie with the starboard accelerometer itself, or with the cabling from the sensor (located in the winch room) to the deck unit. Repairs to the SBWR are required.

## **22.3 Initial Flux Results**

### Inertial Dissipation (ID) Flux Measurements

The ID momentum flux obtained from the HS sonic anemometer is shown in Figure 22.6, where the drag (transfer) coefficient is shown against the true wind speed corrected to a height of 10 m and neutral atmospheric stability. The drag coefficient is defined as ( $10^3 * \text{momentum flux} / \text{wind speed}^2$ )

The mean drag to wind speed relationship from previous cruises (Yelland et al., 1998) is also shown. The drag coefficient is about 10% lower than that found during previous cruises. About half of this difference is due to the ship’s draught being 1 m less than shown on the general arrangement plans, since the ID flux calculation depends on the height of the anemometer above the water. Although flow distortion corrections have not yet been determined for the exact HS anemometer position, it has been shown that the vertical displacement of the flow varies little with anemometer position or relative wind direction (Yelland et al. 2002). In contrast, the mean bias in the measured wind speed is sensitive to both these factors. The remaining 5% bias in the drag coefficient would be explained by a bias in the measured wind speed of only 1 to 2%, possibly due to a combination of calibration error and/or the effect of flow distortion on the mean wind speed. All the anemometers will be re-calibrated after the cruise, and accurate flow distortion corrections applied.

Figure 22.7 shows the ID latent heat flux obtained from the Licor H<sub>2</sub>O data. The agreement with results from previous experiments is good.

Figure 22.8 shows the ID sensible heat flux obtained from the sonic anemometer temperature data. In this case the measured fluxes are biased high. This is due to high frequency noise contaminating the temperature spectra at all frequencies above about 2 Hz. The temperature spectra obtained from the thermistor were likewise not suitable for the calculation of the heat flux via the ID method due to poor high frequency response.

### Eddy Correlation (EC) Flux Measurements

This section shows “quick look” EC results for the small proportion of data processed by the end of the cruise: a proper analysis of the results will take place after the cruise.

Figure 22.9 shows the EC momentum flux obtained from the HS sonic against the 10 m wind speed. The ID fluxes are also shown for comparison. For EC fluxes, a sampling period of 30 minutes or more is usually required, but the data shown in Figure 22.9 were obtained from periods of only 12.8 minutes for processing and initial quality-control reasons. The data were obtained for relative wind direction within 10 degrees of the bow, and grouped according to whether the ship was on station (deploying the CTD) or on passage between stations. It can be seen that a) the EC momentum flux is somewhat larger than the ID flux and b) the scatter in the EC flux may be less when the ship is on passage. The increase in scatter when the ship is on station could be due to the small changes in ship speed and heading required for deployment of the CTD. When the ship is on passage its speed and direction are much more likely to be constant. Figure 22.10 shows the EC fluxes binned against ID fluxes for various relative wind directions. The ID fluxes have been corrected for the vertical displacement of the flow at each direction (maximum correction of 3%), whereas those from the EC method cannot be corrected. The 5% low bias in the ID flux due to the change in the ship’s draught has not been removed from these data. From this it can be seen that the EC fluxes are biased high by about 10-20% for winds blowing on to the bow (relative wind direction of 180 degrees). For wind directions up to 30 degrees to starboard of the bow this bias may reduce somewhat, but for directions up to 30 degrees to port of the bow the bias is increased to about 40-50%. This asymmetry is a result of the HS sonic being located at the starboard edge of the foremast platform.

Figure 22.8 shows the EC and ID sensible heat flux results from the HS anemometer, obtained when the wind was within 10 degrees of the bow. The ID results are clearly very poor and consistently overestimate the flux compared to a bulk formula. However, the EC sensible heat flux is in good agreement with the bulk estimate, and does not seem to show the bias seen in the EC

momentum flux data. The EC sensible heat flux data were too scattered to identify any dependence of the EC flux on relative wind direction.

Figure 22.7 shows the EC and ID latent heat fluxes from the Licor H<sub>2</sub>O data when the wind was within 10 degrees of the bow. The measured fluxes are displayed against a bulk formula estimate of the flux. Again, it can be seen that the EC data are more scattered than the ID except when the ship is on passage. As for the EC sensible heat flux data, the EC latent heat flux does not seem to be significantly biased compared to the ID results. There were not enough data available to examine the dependence of the EC latent heat flux on relative wind direction, since the data processed to date were selected to coincide with periods where the Licor was shrouded.

In summary, the initial results from the EC flux calculations are very encouraging. The excellent ID and EC latent heat flux results mean that the effects of flow distortion on all the scalar fluxes (sensible heat, latent heat and CO<sub>2</sub>) is quantifiable for the first time.

#### CO<sub>2</sub> Flux Measurements.

The major difficulty with measuring the CO<sub>2</sub> flux is that it is usually very small, about two orders of magnitude smaller than the latent heat flux. There are additional practical difficulties such as:

- 1) The “dilution effect”, whereby the measured CO<sub>2</sub> flux is affected by both sensible and latent heat fluxes. The magnitude of this effect is similar to that of the CO<sub>2</sub> flux itself.
- 2) The Licor sensor head is not completely rigid. During pre-cruise trials of the sensor it was found that changing the angle of the head to the vertical resulted in a significant shift in the CO<sub>2</sub> signal. During the cruise, the Licor head was periodically shrouded using an empty water bottle. Data from these periods were examined in conjunction with data from the MotionPak in an attempt to quantify and remove the effect of the distortion to the sensor head.

The analysis performed during the cruise was encouraging in that the small sample of calculated CO<sub>2</sub> fluxes were of a reasonable magnitude and were steady over periods of a few hours or more. A full analysis requires more detailed examination of the periods when the instrument was shrouded in order to determine the best correction for the angle of the head from the vertical. Since the magnitude of the CO<sub>2</sub> flux depends on both the wind speed and the air-sea CO<sub>2</sub> concentration difference, it will only be possible to judge the quality of the results once  $\Delta p$  CO<sub>2</sub> data from the UEA carbon team are available.

## 22.4 Summary

Significant progress was made in the development of the AutoFlux system:

- a) The new Licor and MotionPak sensors were fully integrated into the automatic data acquisition system.
- b) The H<sub>2</sub>O data from the Licor were processed in near real time to produce inertial dissipation estimates of the latent heat flux.
- c) Software was written to produce eddy correlation calculations of all the fluxes. The main reason for not integrating this into the automatic processing was lack of disk space for the large hourly files produced.

The relatively small sample of EC flux results produced during the cruise were very encouraging. As expected, the EC momentum fluxes were shown to be more sensitive to flow distortion than those from the ID method. The EC scalar fluxes of latent and sensible heat agreed well with bulk and/or ID data, but determination of their sensitivity to flow distortion will not be possible until the entire data set is processed. The Licor sensor produced excellent latent heat fluxes via both methods: this will allow the effects of flow distortion on any of the scalar fluxes to be quantified for the first time. Finally, preliminary examination of the performance of the Licor in obtaining CO<sub>2</sub> fluxes is encouraging.

## Acknowledgements

The AutoFlux system was developed under MAST project MAS3-CT97-0108 (AutoFlux Group, 1996)). The developments described in this report were funded under a SOC TIF project (Yelland and Pascal, 2003). Thanks are due to Rachel Hadfield and Amanda Simpson for helping with the visual cloud observations.

Table 22.1: The mean meteorological sensors. Front left to right the columns show; sensor type, channel number, rhopoint address, serial number of instrument, calibration applied, position on ship and the parameter measured.

Sensor	Channel, variable name	Address	Serial No.	Calibration $Y = C0 + C1*X + C2*X^2 + C3*X^3$	Sensor position	Parameter (accuracy)
Psychrometer 1	1 pdp1	\$ARD	IO2002 DRY	C0 -10.744746 C1 4.0231547E-2 C2 -7.5710697E-7 C3 1.2482544E-9	Port side of foremast platform	Wet and dry bulb air temperatures and humidity (0.05°C)
Psychrometer 1	2 pwp1	\$BRD	IO2002 WET	C0 -10.432580 C1 4.0010589E-2 C2 -2.3751235E-7 C3 9.3405703E-10		
Psychrometer 2	3 pds2	\$CRD	IO2001 DRY	C0 -10.439874 C1 3.9174703E-2 C2 7.6768407E-7 C3 5.7930693E-10	Port side of foremast platform	Wet and dry bulb air temperatures and humidity (0.05°C)
Psychrometer 2	4 pws2	\$DRD	IO2001 WET	C0 -1.443511 C1 4.0045908E-2 C2 -3.6063794E-7 C3 1.0917947E-9		
Epply LW dome temp	6 Tdl	\$3RD	31170	C1 1	Top of foremast platform,	Incoming longwave radiation (10
Body temp	7 Tsl	\$KRD	31170	C1 1	port position	W/m2)
Thermopile	8 El	\$LRD	31170	C1 1		

<b>Sensor</b>	<b>Channel, variable name</b>	<b>Address</b>	<b>Serial No.</b>	<b>Calibration Y = C0 + C1*X + C2*X<sup>2</sup> + C3*X<sup>3</sup></b>	<b>Sensor position</b>	<b>Parameter (accuracy)</b>
Epply LW dome temp	9 Td2	\$MRD	31172	C1 1	Top of foremast platform, stbd position	Incoming longwave radiation (10 W/m2)
Body temp	10 Ts2	\$NRD	31172	C1 1		
Thermopile	11 E2	\$ORD	31172	C1 1		
Wind Sonic U component	WSU	?Q	025127	C1 1	Port side of platform	Windspeed
Wind Sonic V component	WSV	?Q	025127	C1 1	Port side of platform	Windspeed

Table 22.2. The fast response sensors.

<b>Sensor</b>	<b>Program</b>	<b>Location</b>	<b>Data Rate (Hz)</b>	<b>Derived flux/ parameter</b>
Gill HS Research Ultrasonic Anemometer serial no. 000027	gillhsd	stbd side of foremast platform	20 Hz	momentum and sensible heat
Licor-7500 CO <sub>2</sub> /H <sub>2</sub> O sensor serial no. 75H0614	licor3	90 cm directly beneath HS	20 Hz	latent heat and CO <sub>2</sub>
Gill R3 Research Ultrasonic Anemometer serial no. 000227	gillr3d	94 cm to port of HS	20 / 100 Hz	momentum and sensible heat
MotionPak ship motion sensor serial no. 0682	via gillhsd	114 cm directly aft of HS	20 Hz	EC motion correction
Thermistor sensor	via gillr3d	100 cm below R3	20 Hz	heat



Table 22.3. The ship's meteorological sensors. All logged by Vaisala QLI50 (R381005).

Name	Sensor	Type	Serial No.	Sensitivity	Cal
STIR	Kipp & Zonen CM6B (335 – 2200 nm)	Pyranometer	973135	11.88 $\mu$ V/W/m <sup>2</sup>	8.688097E4
PTIR	Kipp & Zonen CM6B (335 – 2200 nm)	Pyranometer	99433	10.27 $\mu$ V/W/m <sup>2</sup>	9.737098E4
PPAR	ELE DRS-5 (0.35 to 1.10 $\mu$ m)	Solarimeter	1843B- 1-35901	10.05 $\mu$ V/W/m <sup>2</sup>	9.9502488E4
SPAR	ELE DRP-5 (0.35 to 0.70 $\mu$ m)	PAR?	30470	7.18 $\mu$ V/W/m <sup>2</sup>	1.39275766E5
			30471	8.20 $\mu$ V/W/m <sup>2</sup>	1.21951219E5
			unknown	6.48 $\mu$ V/W/m <sup>2</sup>	1.5432099E5
Pressure	Vaisala PTB100A	Barometric	S361 0008	800-1060 mbar	
Wind speed	Vaisala WAA151	Anemometer	P50421	0.4-75 m/s	
Wind Dir	Vaisala WAV151	Wind Vane	S21208	-360 deg	
Air temp	Vaisala HMP44L	Temp	U 185 0012	-20-60 deg C	
Humidity	Vaisala HMP44L	Humidity	U 185 0012	0-100%	
TSG	See section 24				

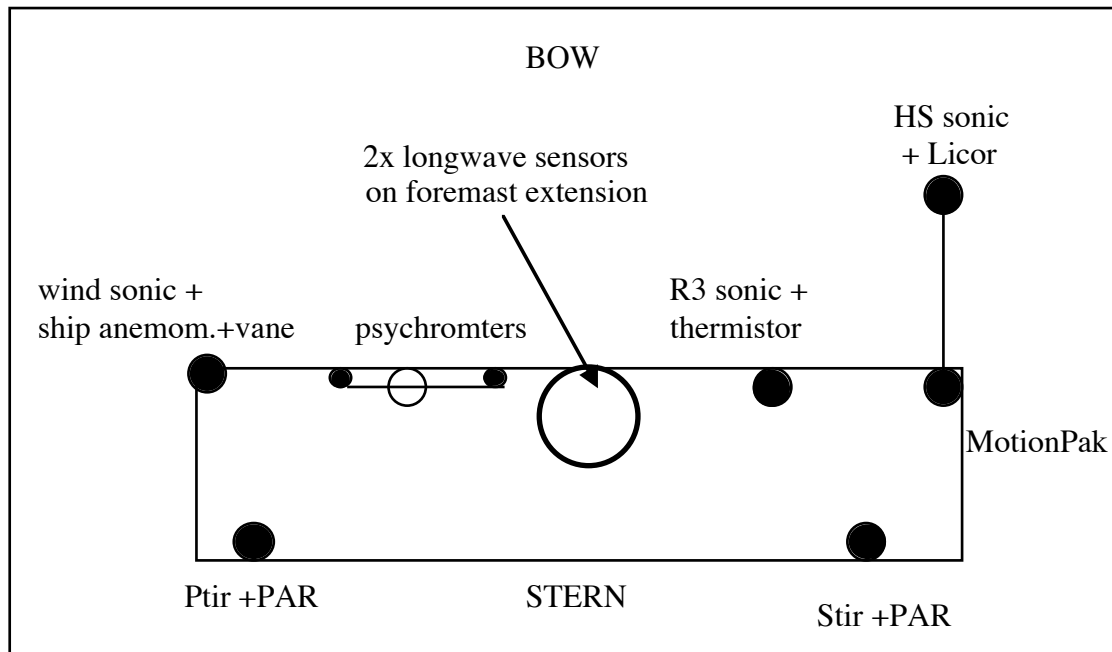


Figure 22.1: Schematic plan view of the foremast platform, showing the positions of the sensors.

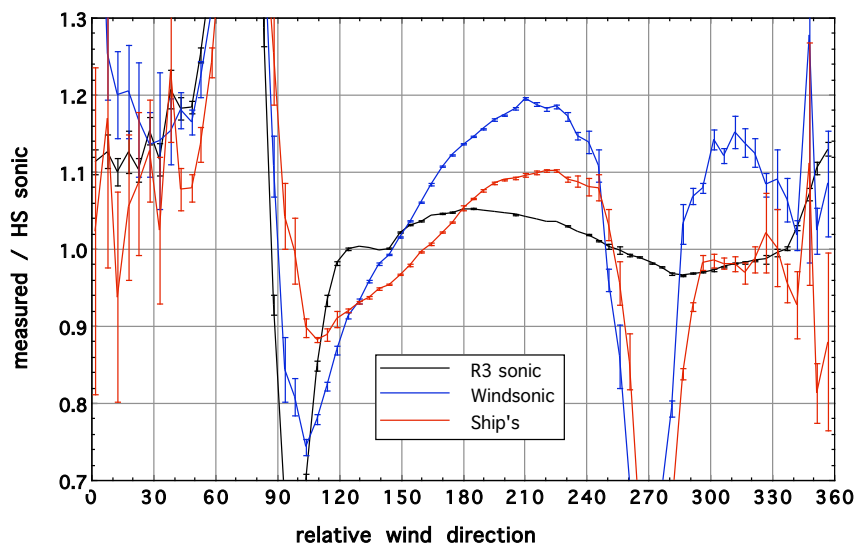


Figure 22.2: Measured wind speed/wind speed from the HS sonic for the R3 sonic, the Windsonic and the ship's anemometer each binned against relative wind direction. Error bars indicate the standard deviation of the mean. A relative wind direction of 180 degrees indicates a flow directly on to the bow of the ship. R3 sonic – black, windsonic – blue, ship's anemometer - red.

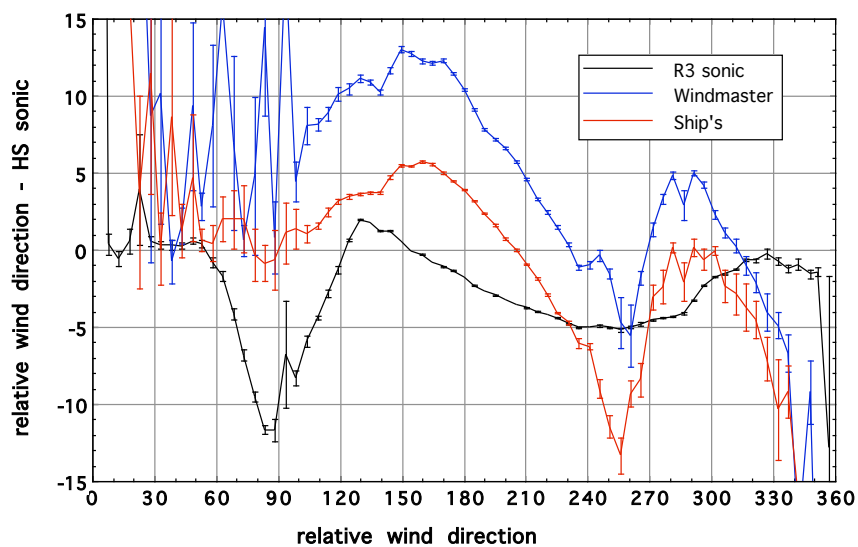


Figure 22.3: As Figure 22.2 but showing the difference (measured - HS) in the relative wind direction from the three anemometers. R3 sonic – black, windsonic – blue, ship's anemometer - red.

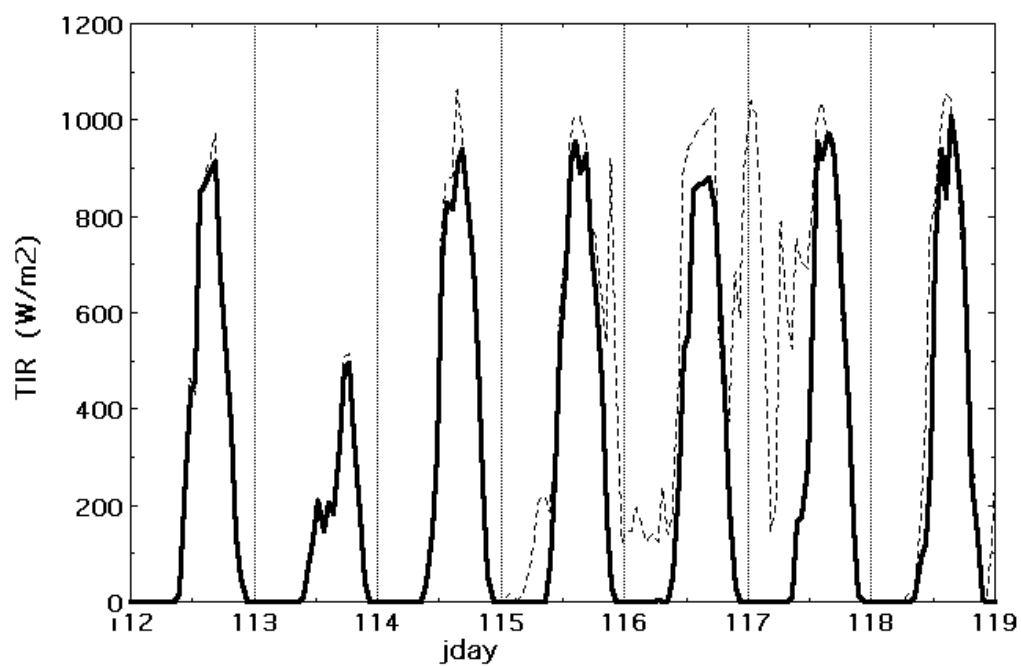


Figure 22.4: Time series of downwelling short wave radiation from the Ptir (solid line) and the Stir (dashed). The data have been averaged over periods of one hour.

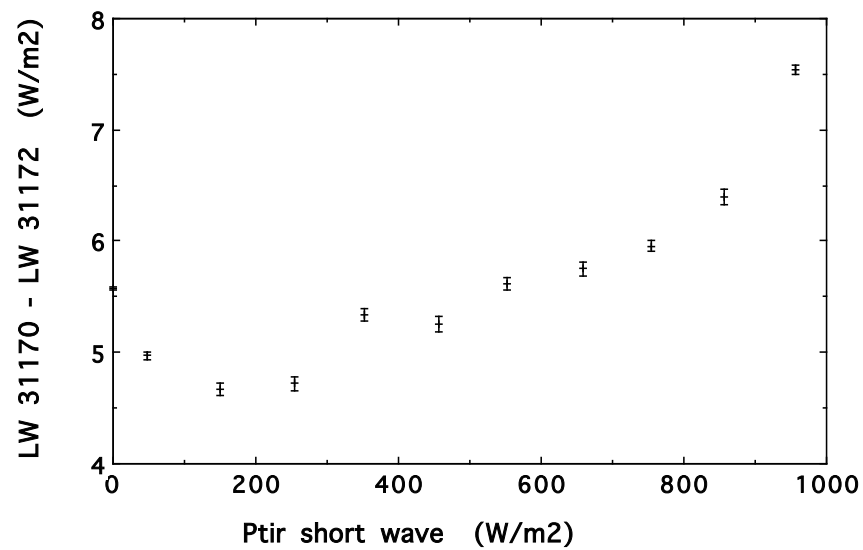


Figure 22.5: Difference between the two longwave sensor data binned against short wave radiation from the Ptir sensor. Error bars show the standard deviation of the mean.

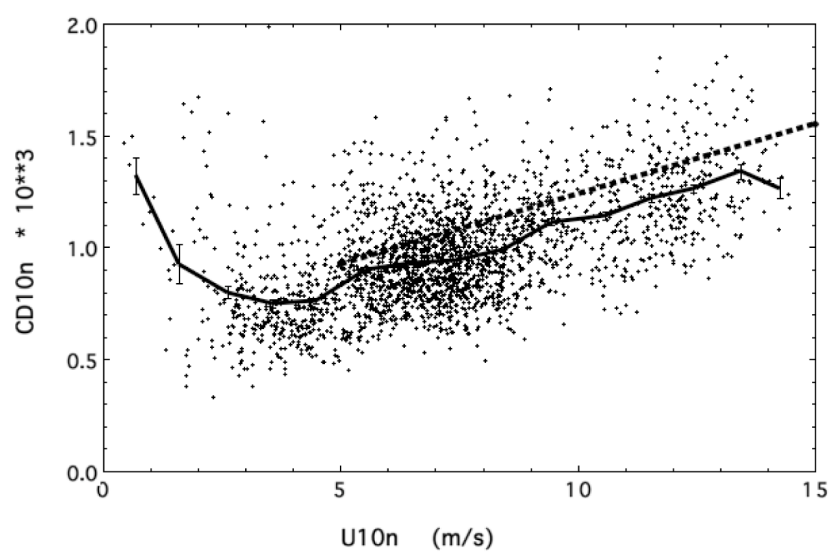


Figure 22.6: Fifteen minute averaged values of the measured ID drag coefficient (dots), plus the mean results (solid line) binned against the 10 m neutral wind speed. The Yelland et al. (1998) relationship is shown by the dashed line.

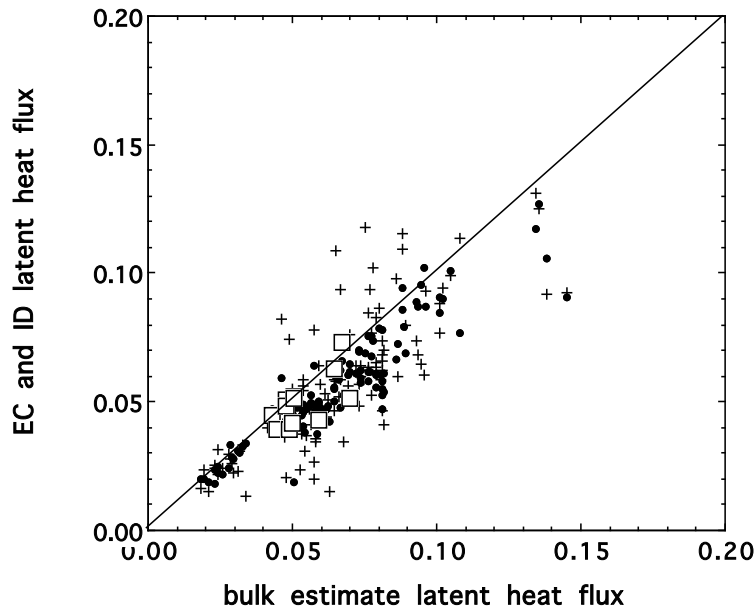


Figure 22.7: Direct measurements of the kinematic latent heat flux from the ID method (solid circles) and the EC method when wind was within 10 degrees of the bow, shown against a flux estimated from a bulk formula (Smith, 1988). The EC data are separated according to whether the ship was on station (crosses) or on passage (open squares).

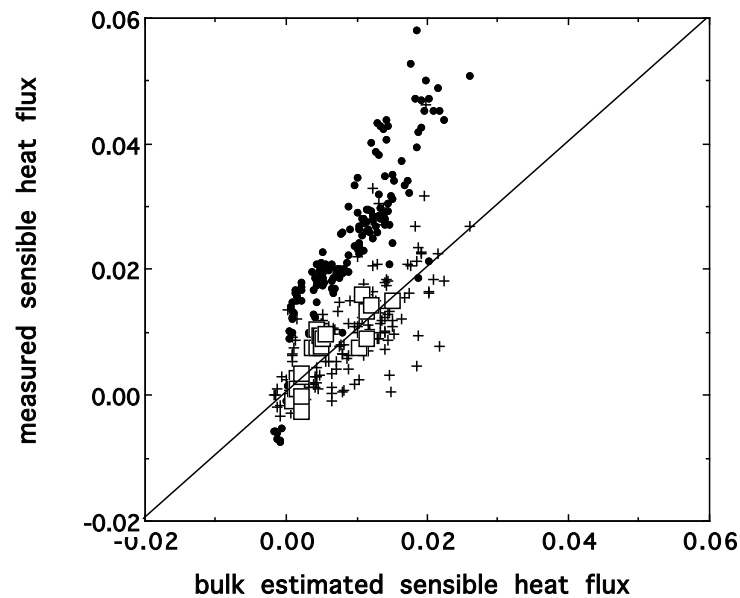


Figure 22.8: Direct measurements of the kinematic sensible heat flux from the ID method (solid circles) and the EC method when wind was within 10 degrees of the bow, shown against a flux estimated from a bulk formula (Smith, 1988). The EC data are separated according to whether the ship was on station (crosses) or on passage (open squares).

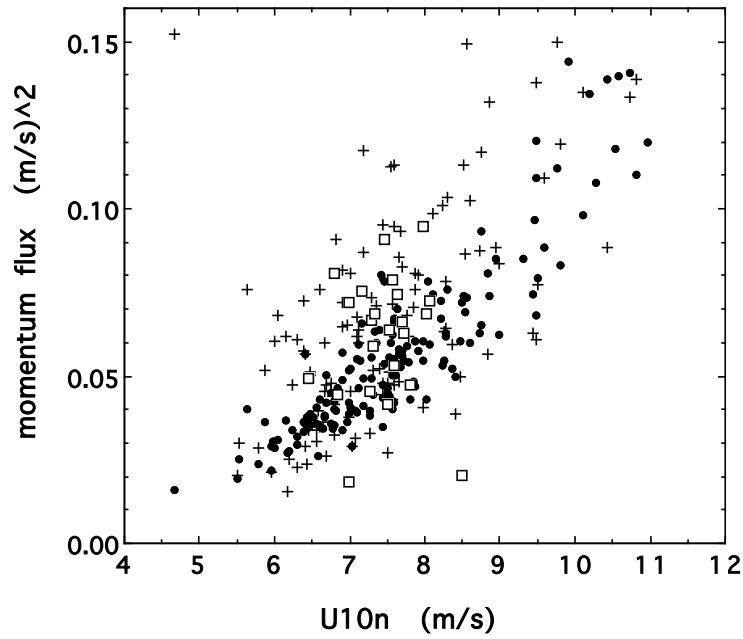


Figure 22.9: Momentum flux measurements from the ID method (solid circles) and the EC method against the 10 m wind speed. The EC results are shown for periods when the ship is on station (crosses) and on passage (open squares).

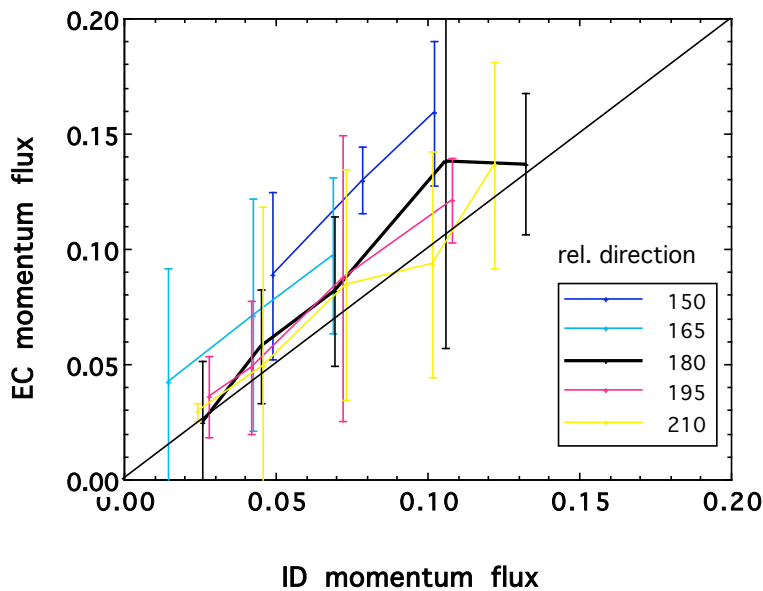


Figure 22.10: EC momentum flux binned against ID momentum flux data. The data have been grouped according to the relative wind direction as shown by the key in the figure. A bow-on wind is at a direction of 180 degrees, winds to port of the bow are shown by the blue lines and to starboard by the red and yellow lines.

## Appendix 22.A - List of significant events

**Day 044** One day after sailing from Govan, a LW rhopoint blew and took out the power supply for the mean meteorological data stream. LW sensors unplugged at the end of D278. Data from Govan to the end of D277 were reprocessed using the surfmet data instead of AutoFlux mean met data; **Day 062** HS and R3 data stopped logging at 14:00 and did not restart until the workstation was rebooted on day 074 at 03:00. Logging probably stopped while staff on the ship tried to diagnose the problem with the mean met data stream; **Day 094** Prior to start of D279, RC filter on MotionPak output changed from a cutoff frequency of 4.79 Hz to 30 Hz; **Day 111** Period of time sync signal changed from 47 samples (2.3 seconds) to 172 (8.6 seconds). This allows unambiguous automatic syncing of data streams; **Day 115** Stopped logging R3 sonic anemometer to Nimbus. Started logging R3 to Cirrus at 100 Hz; **Day 116** Swapped Ptir and Stir at foremast junction box at 18:30; **Day 117** Ptir and Stir swapped back again at 17:30. Reprocessed data in AutoFlux 1 minute master files so that Ptir and Stir in correct channels; **Day 117** Starboard psychrometer wet bulb stopped wicking. Corrected on day 127; **Day 122** Nimbus stopped for backups at 0100. Restarted ready for 0500; **Day 122** Nimbus system administration error caused data loss from 1400 to end of 1700.

Table 22.A.1: Periods during which the **Licor was shrouded** using an empty water bottle. NOTE: on day 128, used the Licor calibration tube as well as the water bottle and covered the outside of the latter with foil. Removed the foil (only) just before 128 22:00, then removed the rest on day 129 at 16:58.

Shroud	<b>099</b> 17:20	<b>109</b> 16:30	<b>114</b> 16:55	<b>120</b> 14:58	<b>124</b> 14:50	<b>128</b> 13:45
Removed	<b>100</b> 01:15	<b>110</b> 00:50	<b>114</b> 23:57	<b>120</b> 20:55	<b>124</b> 20:58	<b>129</b> 16:58

Table 22.A.2: Day and time when sensors were cleaned.

Licor cleaned	TIR sensors cleaned	LW sensors cleaned
095 12:00	095 12:00	095 12:00
100 10:15	-	-
105 18:40	105 18:40	105 18:40
108 21:58	108 21:40	108 21:40
110 00:50	-	-
-	-	114 16:35
124 13:30	124 13:30	-
127 17:00	127 17:00	127 17:00

## Appendix 22.B - Time series of mean meteorological and air-sea flux data

Figures 22.B.1 to 22.B.5 show time series of 1 minute averages of the mean meteorological data. Only basic quality control criteria have been applied to these data. Each page contains four plots showing different variables over a seven day period.

<b>Top panel</b>	the best wet (pwUSE) and dry (pdUSE) bulb temperatures from the two psychrometers plus sea surface temperature (SST) from the TSG.
<b>Upper middle panel</b>	downwelling radiation from the two shortwave TIR sensors and the two longwave sensors, all in $\text{W/m}^2$ .
<b>Lower middle panel</b>	relative wind direction (relld = 180 degrees for a wind on the bow) and true wind direction (TRUdd) from the HS anemometer. The ship's true heading is also shown.
<b>Bottom panel</b>	relative (spdENV) and true wind (TRUspd) speeds in m/s from the HS anemometer. The ship's speed over the ground is also shown in m/s. When the relative wind direction was to port of the bow, the significant flow distortion is apparent as steps in the true wind speed.



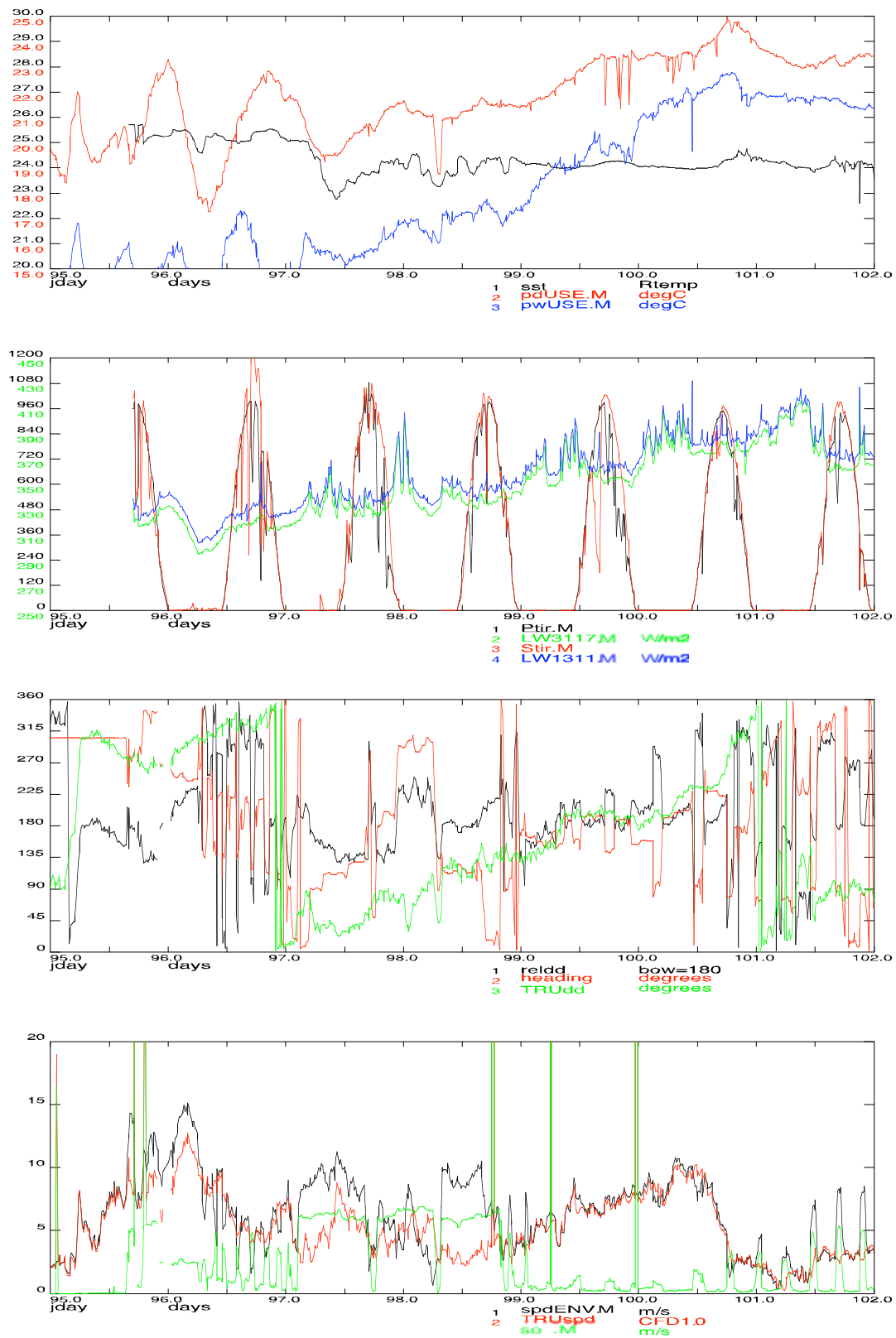


Figure 22.B.1: Mean meteorological data for days 095 to 102.

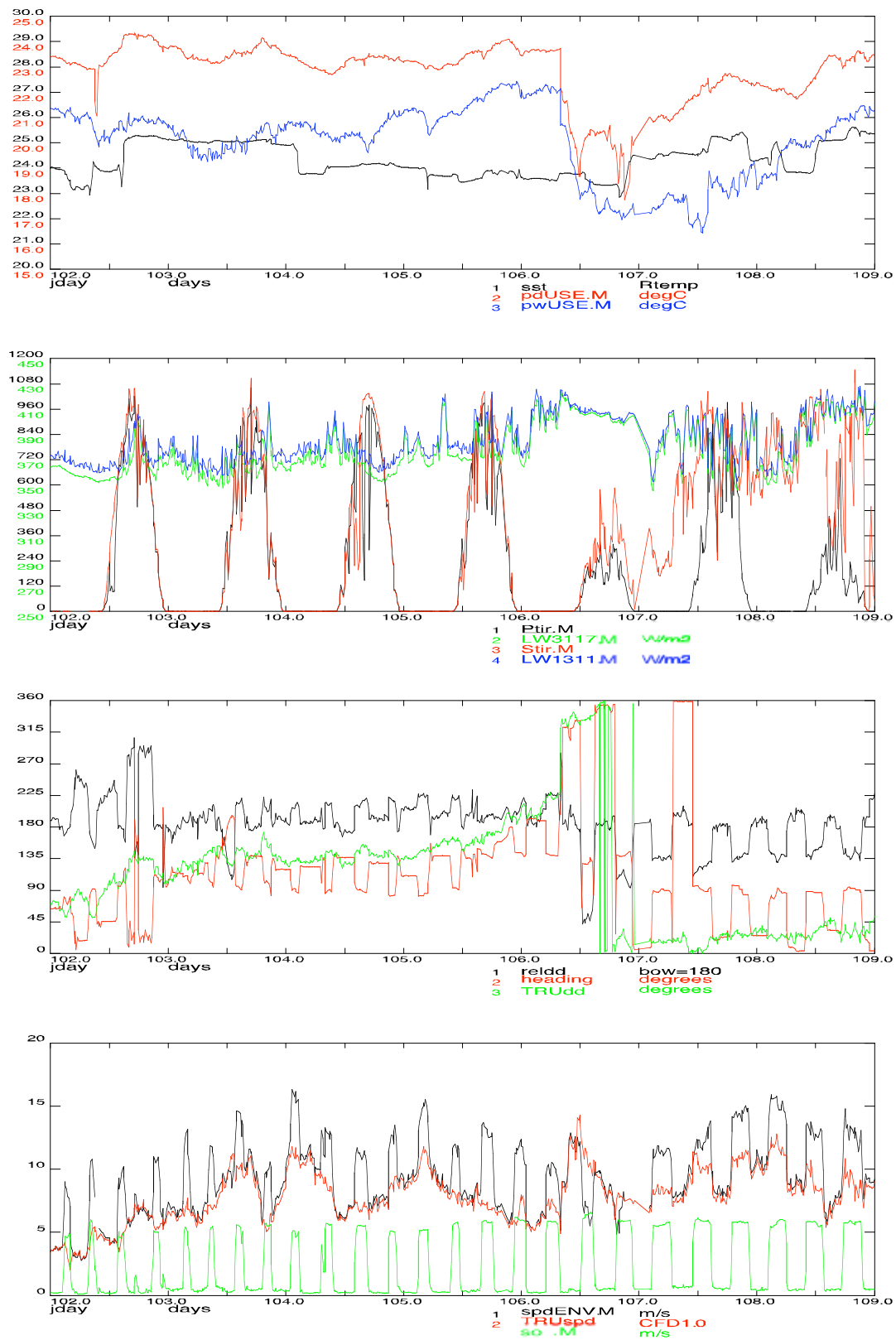


Figure 22.B.2: Mean meteorological data for days 102 to 109.

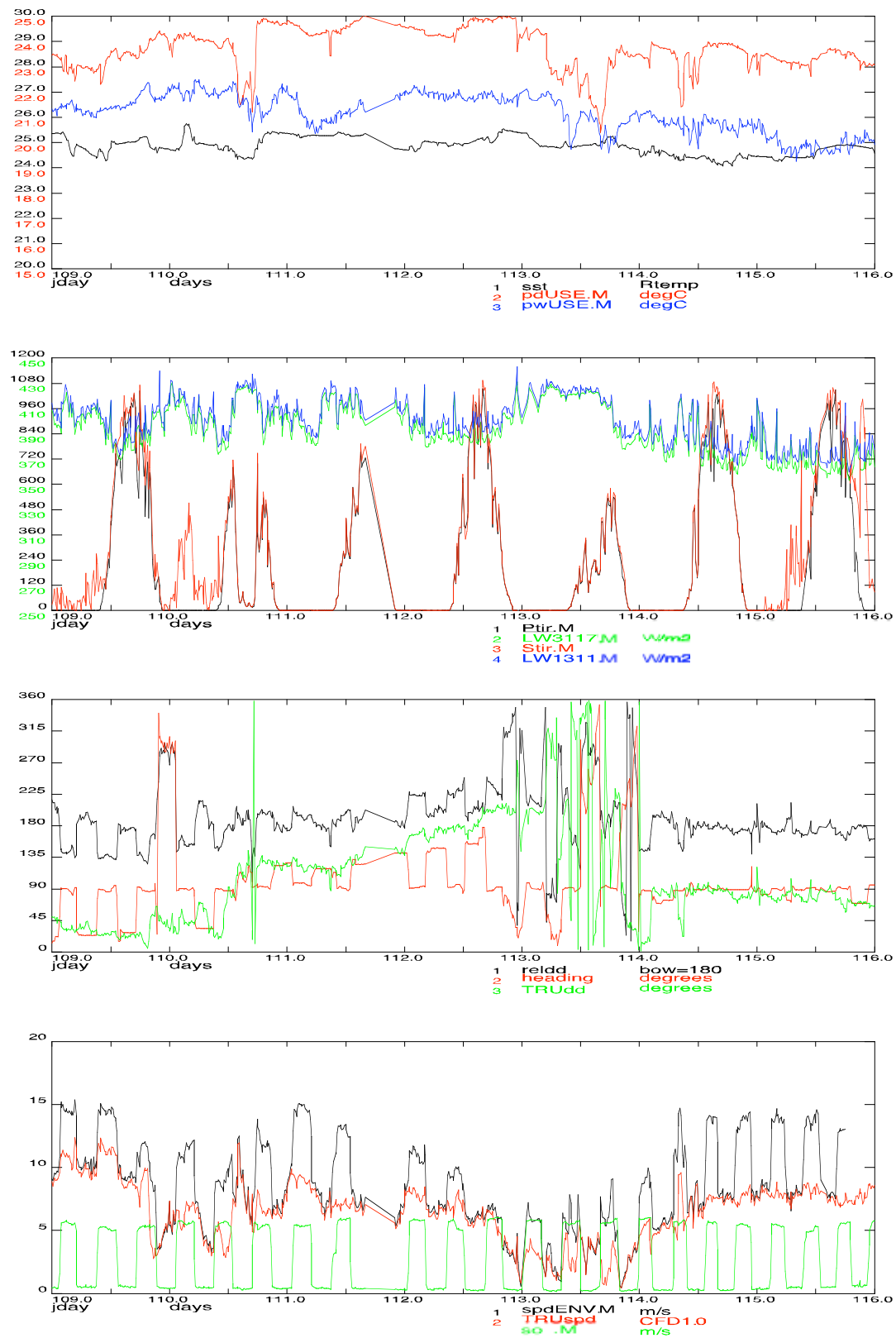


Figure 22.B.3: Mean meteorological data for days 109 to 116.

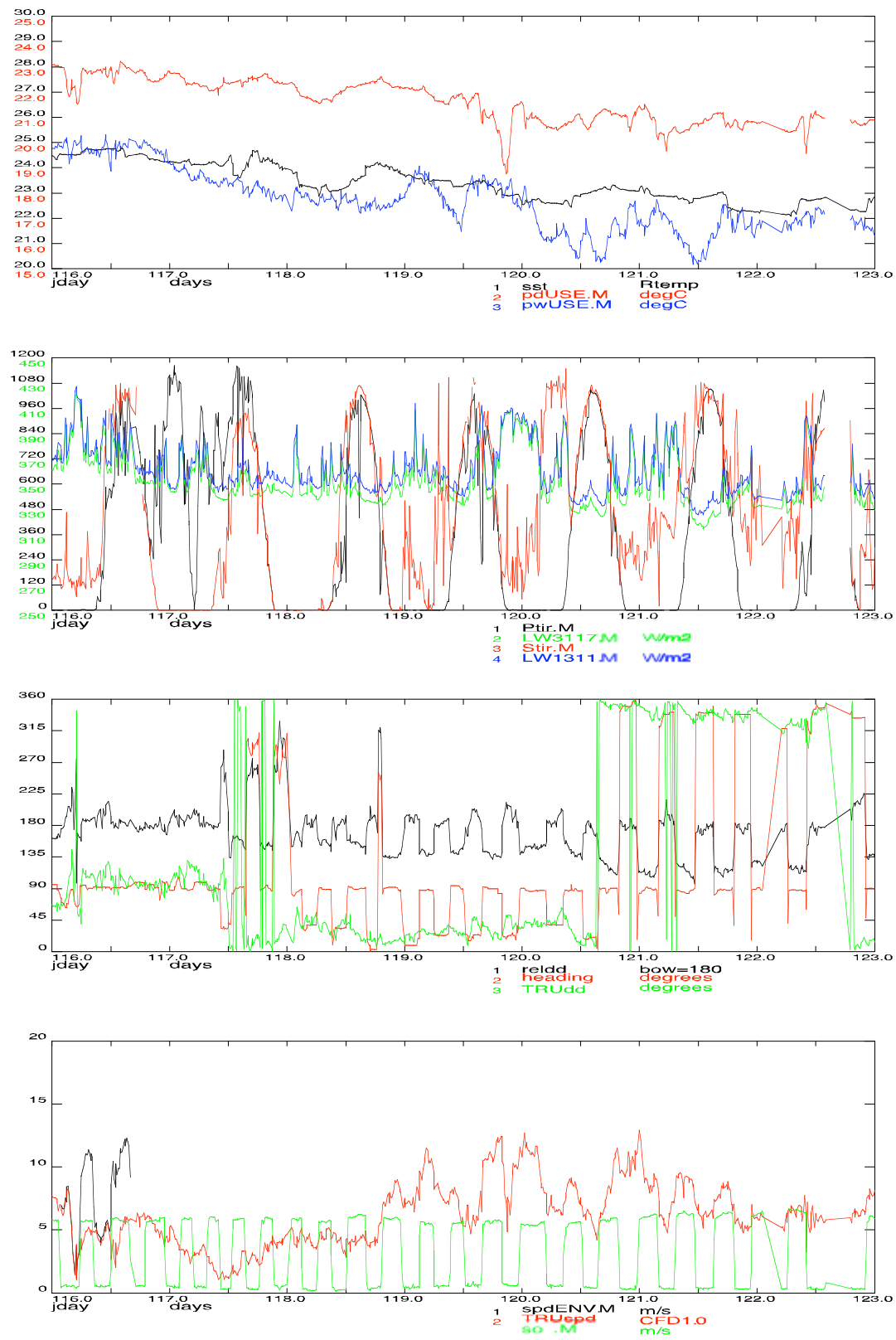


Figure 22.B.4: Mean meteorological data for days 116 to 123.

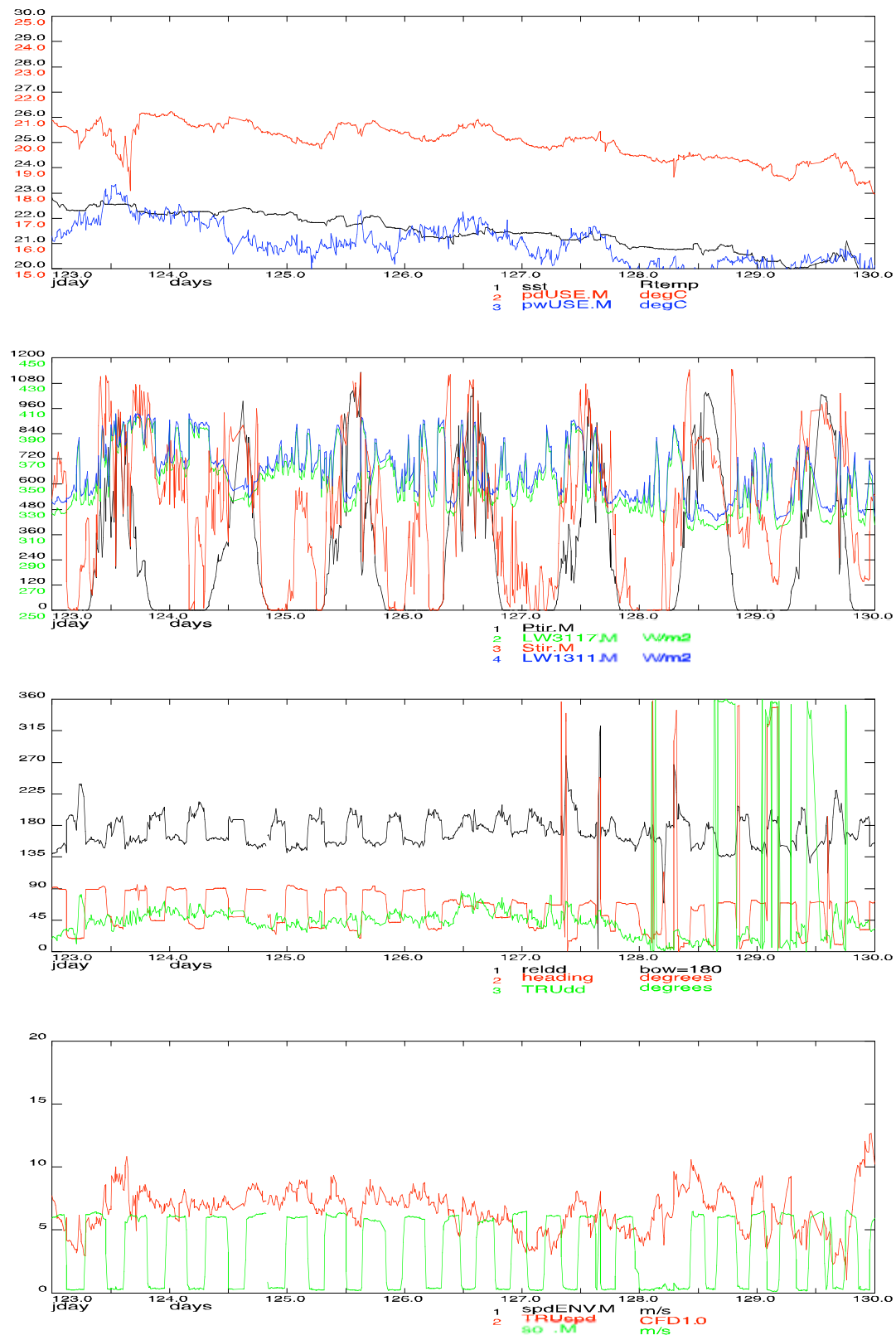


Figure 22.B.5: Mean meteorological data for days 123 to 130.

## 23. SURFACE MET DATA

Rachel Hadfield, Margaret Yelland, Robin Pascal

The meteorological data was processed by the following execs:

Smtexec0	transfers the underway surfmet data from RVS to PSTAR format.
Smtexec1a	changes surfmet absent data values of 99999 to -999, computes the surface salinity and merges in bestnav positions.
Smtexec1b	merges the underway data with the heading files, gyro and ash-gyro.
Smtexec2	computes vessel speed and subtracts this from relative winds to get true wind speed and direction.
Pikexec	copies the time in seconds and converts it to a jday time variable.
Multiplot	produces daily and weekly plots of the data.

For cruise 279, this processing was done on a daily basis, while data from cruises 277 and 278 were processed in one go at the start of cruise 279. During cruise 279, there were problems with the starboard incoming radiation sensor, with large spikes evident in the data, even during night time. On day 116, the cables for the port and starboard sensors were switched to check if the problem was due to the sensor malfunctioning or the cable. After the switch, the starboard sensor continued to give poor data, indicating that the problem was with the sensor itself, and on day 117, the cables were swapped back again.

### 23.1 Surfmet Sensor Information

The surfmet sensor information, which remained unchanged for cruises 277 through 279, is shown Table 23.1 below. All sensors, with the exception of the conductivity sensor are calibrated.

Table 23.1: Surfmet sensor information.

<b>Manufacturer</b>	<b>Sensor</b>	<b>Serial No</b>	<b>Remarks</b>
FSI	OTM (Temperature)	1340	Housing
FSI	OTM (Temperature)	1348	Remote
WetLabs	Fluorometer	W53S-248	
SeaTech	Transmissometer	CST-113R	
FSI	OCM (conductivity)	1376	

## 24. SALINITY CALIBRATION OF UNDERWAY DATA

Rachel Hadfield

For calibration of underway salinity data, bottle salinities were collected from the uncontaminated water supply at roughly four hour intervals. Throughout cruise 277, sampling frequency was typically much less than this, with an average of one sample roughly every 10 hours. However, whilst crossing the Florida Straits, samples were taken every 1-2 hours. During cruise 279, samples were drawn from the contaminated water supply due to low water pressure in the uncontaminated supply, with sample frequency varying between 2 and 8 hours.

The collected bottle salinities were analysed in the usual way and the results were entered into Excel CSV files, ftp'd onto the UNIX system and converted into PSTAR format. To remove any heat dependence, bottle salinities were converted to conductivity using the PSTAR routine `peos83`. The bottle conductivities were then merged with 5 minute binned underway data. The merged file was exported into Matlab, where a 6 point running mean of the conductivity offset was calculated. This running mean was then applied as a calibration curve to the original 2-minute averaged underway data file. The first and last points of the calibration curve were taken to be the first and last conductivity offsets. Where the end points appeared to be an outlier from the mean trend, the mean trend was extrapolated to provide start and end points. This analysis was carried out using four main execs – `time.exec`, `merg.exec`, `condsur.exec` and `smtcornnn.exec` (where *nnn* is the cruise number). Table 24.1 shows the processing sequence.

Results of the calibration applied are summarised in Table 24.2. The standard deviation for cruise 278 is quite high due to a couple of spikes remaining in the underway data despite binning of the data into 5 minute time periods. The calibrated underway salinities were also compared to the gridded 10m CTD station salinities (Figure 24.1). Mean differences between the CTD and underway salinities were -0.003, 0.009 and 0.002 with standard deviations of 0.009, 0.010 and 0.012 for cruises 277, 278 and 279 respectively.



Table 24.1: Processing sequence

Process	File(s) In	File(s) Out
time.exec – converts csv to pstar and cales time in seconds	surnnn001.csv	surnnn001.time
papend – appends all bottle salinity files together	surnnn001.time, surnnn002.time...	surnnn.time
pavrge – bins underway data into 5 min bins	smtnnn99.met	smtnnn99.bin
merg.exec – merges bottle salinity files with underway data files, and calculates offset between the two.	smtnnn99.bin surnnn.time	smtnnn99.bin.pik surnnn.dif smtnnn_bin.mat
Condsur.exec – calculates bottle conductivities and offsets between underway and bottle conductivity	surnnn.dif	surnnn_bin.mat
Smtnnn.m – a matlab file which calculates the correction curve	surnnn_bin.mat smtnnn_bin.mat	cornnn.mat cor_curve.ps
pmatlb – converts matlab file to pstar	cornnn.mat	cornnn.p
smtcornnn.exec – applies the correction and outputs file with calibrated salinities	cornnn.p smtnnn99.pik	smtnnn99.cor
merg.exec2 – calculates the difference between calibrated and bottle salinities	smtnnn99.cor surnnn.time	surnnn_cor.mat

Table 24.2: The mean offset between calibrated and uncalibrated salinities (i.e. calibrated minus uncalibrated) and the standard deviation of corrected salinities against bottle salinities.

Cruise	Mean Offset	Standard Deviation
277	-0.13648	0.009
278	-0.07080	0.021
279	-0.11361	0.009

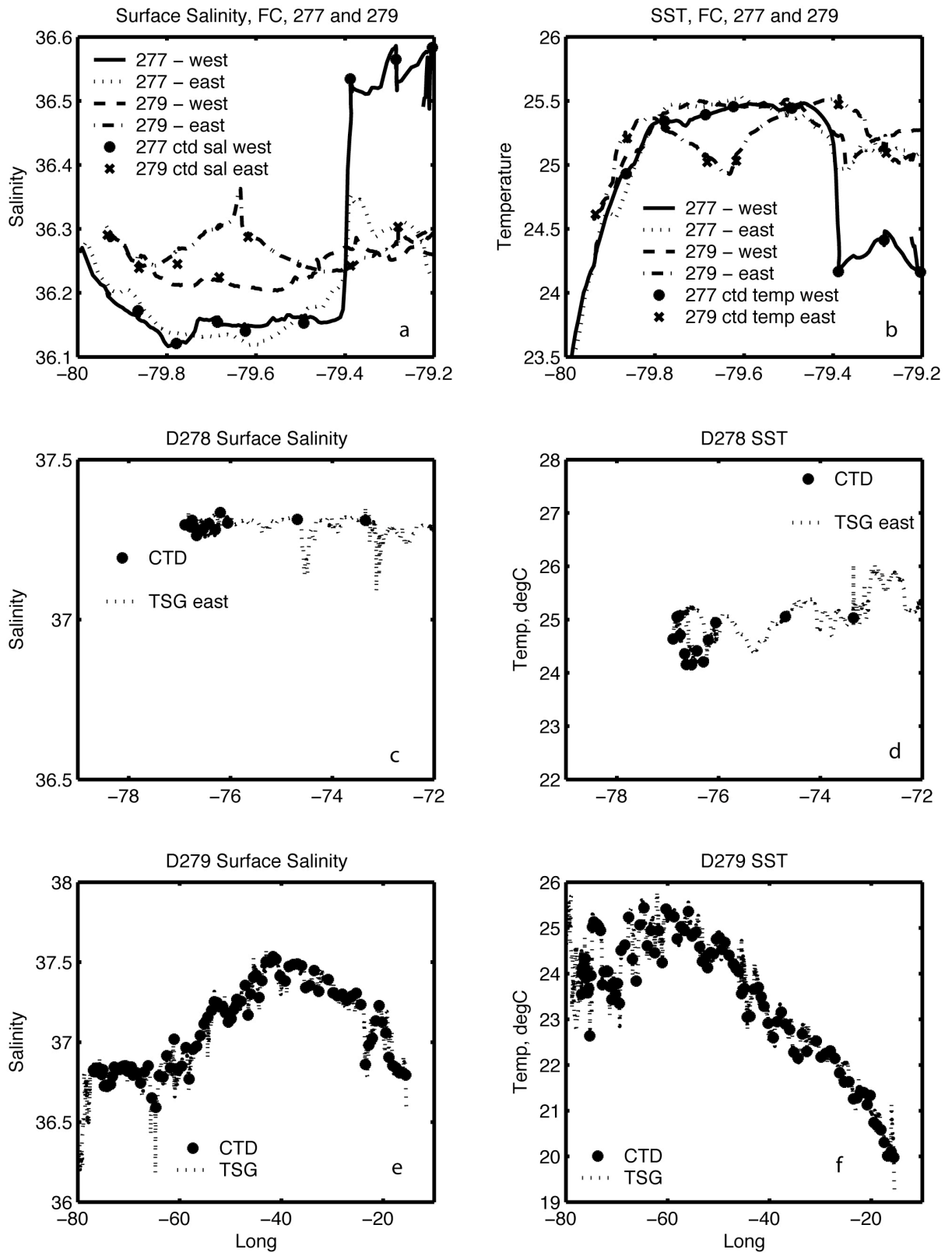


Figure 24.1: Surface (TSG) and 10m (CTD) readings of (a) salinity across the Florida Current, (b) temperature across the Florida Current, (c) salinity, cruise D278, (d) temperature, cruise D278, (e) salinity, cruise D279 and (f) temperature, cruise D279.

## 25. BATHYMETRY

Amanda Simpson

The RRS *Discovery* is equipped with a hull mounted transducer, Precision Echosounding (PES) ‘fish’ transducer and Simrad EA500 Hydrographic Echosounder. The PES fish transducer was deployed shortly after leaving Freeport and was used in preference to the hull transducer for the duration of the cruise. During the cruise, the Simrad Echosounder was used continuously for bottom detection.

The Simrad control screen and monitor showed a visual display of the return echo. A secondary monitor and control screen was slaved to the main system and positioned at the back of the main lab for use when on station. A hard copy output of the screen’s display was also produced using a colour HP paint jet printer. This paper output was marked with the position of the stations and filed. Watchkeepers were required to check on an hourly basis that the echosounder was functioning correctly, that the visual display was set to a sensible range and that the printer was working normally.

The depth values logged by the echosounder were passed via a RVS level A interface to the level C system for processing. A constant sound speed of  $1500 \text{ ms}^{-1}$  was used by the echosounder throughout the cruise. The first level of processing was to correct the raw data for variations in the speed of sound. This was done using Carter tables by RVS level C stream *prodep*.

Data were then converted from RVS format into PSTAR files using *simexec0*, which prompts the user to enter the start and end times of the data to be processed. This was done daily, producing the PSTAR file *sim279nn.cal* (nn refers to the number of the file) which contains the time, uncorrected depth, corrected depth and the carter table area at intervals of around 6s. *Simexec1* was then run, which uses *pintrp* to interpolate for missing data and then *pmerg2* to merge the bathymetry data with the navigational data (*abnv27901*). The main output file used was *sim279nn.nav*, which contains the fields: time, latitude, longitude, uncorrected depth, corrected depth, carter table area, distance and speed made good. A 5 minute averaged file was also produced at this stage containing the same fields (*sim279nn.5min*).

It was then necessary to edit the corrected depth variable for spikes and erroneous data, especially on station. The merged *sim279nn.nav* file was copied to file *sim279nn.naved*, in preparation for editing. This was done using the PSTAR routine *plxied*, which allows the user to manually select and remove data from an interactive plot. The speed made good was also displayed on the plot, to facilitate identification of station sections.

There appeared to be substantial interference between the CTD pinger and the echosounder transducer. Also, on a few occasions, the loss of accurate bottom detection was apparent whilst steaming and, where obvious, this was also removed.

After editing, the output file `sim279nn.naved` was then averaged into 5 minute intervals using *pavрге* to generate the file `sim279nn.ed5min`.

Four master files were created from the daily files. These were:

<b><code>sim279il.nav</code></b>	This is the appended file of all the daily .nav files and contains the unedited corrected depth data.
<b><code>sim279j1.naved</code></b>	This is the appended file of all the daily .naved files for which the corrected depth has been edited to remove spikes and anomalous on station data.
<b><code>sim279k1.ed5min</code></b>	This is the appended file containing the edited data averaged into 5 minute intervals.

Finally, the corrected depth in `sim279k1.ed5min` was interpolated to provide a continuous estimate of depth along the cruise track. This is found in file **`sim279m1.int5min`**.

As the intended cruise tracks for D279 and D277 were identical, it was interesting to compare the echosounder data for the two cruises. In order to do this, the 5 minute average files for both cruises were first sorted in terms of longitude and then the two files were merged using *pmрг2*. On merging, the D277 depths were interpolated onto the longitude data of D279. The difference between the two depth estimates was then calculated for each longitude using *parith*.

The top plot in Figure 25.1 shows the bathymetry for D279 and D279 and the bottom plot shows the difference between the two depth estimates.

Some of the discrepancy can be accounted for by differences in latitude between the two cruise tracks. This accounts for the large differences seen at the start of D279, when a return trip to Freeport was taken over a different route from the main cruise track.

Away from the Mid-Atlantic ridge and ignoring the beginning and end sections where the cruise tracks diverge, the mean absolute difference between the two estimates is 15.3 m with a standard deviation of 10.8 m. This increases to a mean of 97.2 m and standard deviation of 173.29 m across the ridge. The echosounder may find it difficult getting accurate estimates of depth over such steep

bottom topography, accounting for the greater variation. Variations in latitude also have a greater impact on the depth recorded over the rough Mid-Atlantic ridge section.

There is significant divergence between the two estimates around 38W, which did not relate to a large latitude difference. When investigated on the hard copy output from D279, the strongest echoes do not relate to the bottom output on file. Although not obvious in editing, the bottom detection algorithm was unable to provide an accurate estimate of depth at this point.

Towards the end of D279, the D277 and D279 cruise tracks diverge in latitude and so the bathymetry also differs. The large spikes seen in the D279 bathymetry at this point were identified as seamounts.

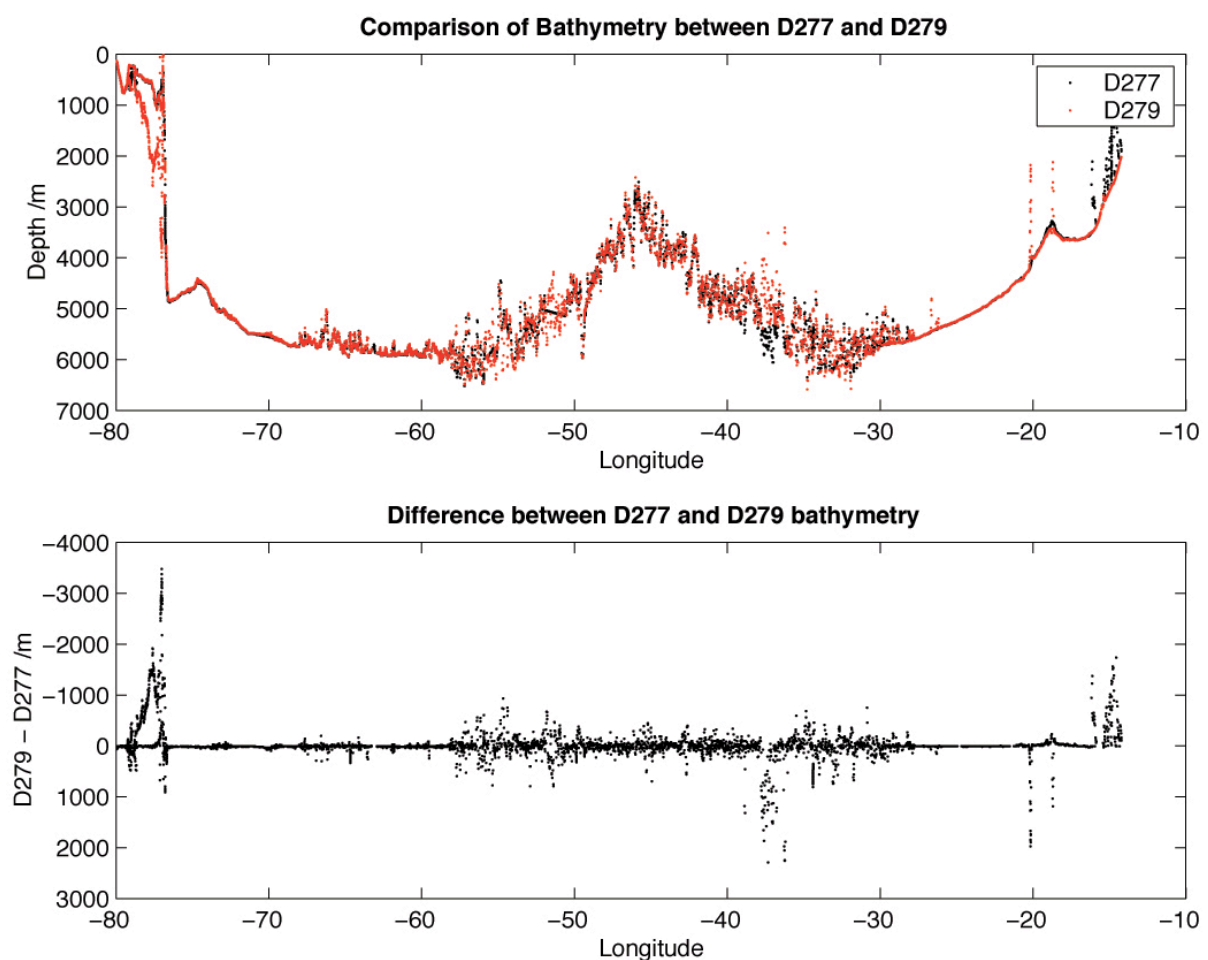


Figure 25.1: D277 and D279 bathymetry.

## 26. SHIPBOARD INSTRUMENTATION AND COMPUTING

### 26.1 Data Logging

Data were collected using the Level ABC data logging system.

Data Grabber	Instrument	
GPS_4000	Trimble GPS 4000	MkII Level A
GPS_ASH	Ashtec ADU	MkII Level A
GPS_GLOS	Glomass GPS	MkII Level A
GPS_G12	SeaStar G12 (DGPS)	MkII Level A
SURFMET	On board surfmet system	Direct to Level B
ADP	150Khz ADP	Direct to Level C
WINCH	CLAM system	Direct to Level B
LOG_CHF	Chernikeef Log	MkII Level A
GYRONMEA	Ships Gyro	MkII Level A

### 26.2 Logging Parameters

```
Fromlevb -t20 | parse -L &
```

```
FromADP -d /dev/ttya -t 180s | ADPin ADP &
```

The grabbers log these data files in /rvs/raw\_data in files with the same name.

### 26.3 Level C Data Files

In addition to the above data files, which are called raw data, there are processed data files, which are stored in /rvs/pro\_data and referred to as pro data. These are:

Rawdep                      An intermediate file created with the copyit command directly from ea500d1, and avoids problems with bad data and backward times.

Pro\_dep                      Depth corrected to Carter Area, using the prodep program.

Relmov	Required by bestnav, stands for relative motion, and uses gyronmea and log_chf to calculate the relative motion
Bestnav &bestdrf	Are generated by the bestnav program, and use up to 3 gps input files, in this case gps_4000 (1), gps_g12 (2), and gps_glos (3), in order of their priority. It also takes in the relmov data, and outputs a 10 second 'best of what's available from navigation'. It automatically calculates position in case of gps failure.
Pro_wind	Absolute wind direction and speed calculated using the windcalc command, takes in bestnav and surfmet data streams.

## 26.4 Master Clock Jump

Occurred at midnight on day 120, time offsets were observed between gps\_ash and gyronmea. After the level As were reset, these offsets vanished. Prior to the master clock jump, the offset was in the region of 16 seconds. Further investigation showed that the gyronmea level A was not synchronising with the external clock correctly, and running on the internal clock only. The internal clock was drifting by about 0.5 seconds per day and it was agreed to manually reset the level A, meaning the maximum error would be less than 1 second. A record of manual resets was kept and passed to Steve Alderson.

## 26.5 Level B

No problems were experienced with the Level B data logger throughout the cruise.

## 26.6 ADP

The 150kHz ADP was logged directly to the Level C workstation. The ADP data files were accessed directly by the scientific party using datapup.

## 26.7 GPS Systems

GPS positioning was logged from a variety of receivers. Ashtec 4000 (gps\_4000) was the main receiver, Ashtec G12 being the secondary receiver. Both these receivers were fed differential corrections from the Fugro Seastar differential receiver from the AM-SAT. For a few hours, these differential corrections were not being received - the effect was temporary and was not caused by being outside the AM-SAT satellite footprint. During the cruise, and before we reached the limit of the AM-SAT footprint, the Seastar receiver was allowed to autoscan to the EA-SAT. Once it was

tuned and checked to ensure correct operation, the autoscan option was disabled, effectively locking the receiver to the EA-SAT.

## **26.8 Processed Data Fields**

The data files were processed during the cruise: bestnav (using gps\_4000), prodep, protsg and pro\_wind. The raw data file (rawdep) used for prodep was not edited for bad data during the cruise at the request of the Principal Scientific Officer, as on the previous cruise. However, it was processed for carter area correction, and the wind was processed, resulting in absolute values for direction and speed.

## **26.9 Winch**

Winch data were logged directly to the Level B, and as long as the CLAM system was not powered down totally and the Stop Logging button was pressed on, the screen returned to the wire settings menu. On several occasions near the start of the cruise, the CLAM system stopped logging several times to the Level B after a write error message appeared. This was resolved by pressing the “Continue” button on the error message box, which started logging again.

## **26.10 General Computing**

Several computers were attached to the ships network during the cruise. At the moment, there is no DHCP service on board and so IP numbers were issued as normal, entries were made in /etc/hosts on Discovery2. The wireless network gave full coverage to all laboratories on the main working deck, with a limited signal quality to the port accommodation, however, it was not used to great effect at this point due to the lack of wireless capable computers onboard.

## **26.11 CTD Processing and Data Archiving**

CTD cast data were transferred to the Black Translation PC in the computer room, either by zip (this proved unreliable), memory stick (slightly more reliable) or via the network (quick and easy). Seabird processing was carried out on the Translation PC, and processed files stored locally, with an archive on Discovery 5 /data51/rvsD279/.

/data51/rvsD279/RAW contained \*.CON, \*.DAT, \*.BL, \*.HDR, and ASCII digital thermometer files

/data51/rvsD279/Processed/ contained the \*.cnv and \*.ros files (binary data conversion and rosette)



Further CTD processing was performed by the scientists using pstar/pexec suite.

## 26.12 Email

A similar email schedule to the previous cruise was adopted, to best coincide with working hours in the UK and US. As the cruise progressed, the schedule was altered to allow for the advancing ships clock. Between the days 114-116, the HSD system suffered with problems obtaining and maintaining a reliable connection with SOC. This was wholly due to the satellite antenna being obscured by the main mast. The combination of constant easterly heading, and I would guess a low elevation of satellite position and angle, at that particular location in the ocean led to this temporary problem. As soon as the ship turned or we left the area, comms were back to normal.

## 26.13 Backup Options

Backup to CD, DVD, and DLT were available for final archiving. Daily backups were made to DLT on a 2-day odd/even rotation using the following command from Discovery 2.

```
Cd /
```

```
Tar cvf /dev/rmt/3 ./data51 ./rvs/raw_data ./rvs/pro_data  
./rvs/def7/control
```

## 26.14 Level B Tape Archive

```
echo reading.. ; cat /dev/rmt/0 > tape_`jday` ; echo compressing.. ;  
compress tape_`jday`
```

```
echo lb_tape_ini-ing.. ; lb_tape_ini -b4 -f /dev/rmt/0 -v ; echo  
checking initialisation.. ; cat /dev/rmt/0 ; echo All Done
```

As level B tapes last longer than 24 hours, it was possible to have automatic daily naming of tapes. Archive of Level B tapes is for internal use only, and is only used to restore lost data in case of a catastrophic loss of level C data and backups.

This would be done by decompressing the data files

```
Uncompress tape112.Z
```

Then 'cat'ing the tape into the parse command to rebuild the rvs data files.

```
Cat tape112 | parse &
```

### **26.15 CTD Computing Facilities**

The two CTD logging computers were, in my opinion, not a suitable choice for use in such a critical job as Seabird logging. The Windows 98 equipped desktop machines were, at best, just about satisfactory, and at worst, unsuitable. After only a few days, one broke down and refused to work any more, requiring an older CTD computer to substitute it, which was just about OK and only crashed a few times. Careful nursing was required to avoid loss of important cast data.

## 27. CARBON

Ute Schuster, Gareth Lee, Maria Nielsdottir

The CO<sub>2</sub> parameter analytical equipment was set up in the seagoing laboratory container of the Laboratory for Global Marine and Atmospheric Chemistry (LGMAC), University of East Anglia (UEA), Norwich, UK. Four instruments were set up for the analysis of discrete total inorganic carbon (TCO<sub>2</sub>), discrete total alkalinity (TA), discrete partial pressure of CO<sub>2</sub> (discrete pCO<sub>2</sub>) and, continuous partial pressure of CO<sub>2</sub> (continuous pCO<sub>2</sub>) and oxygen. The discrete instrumentation was used to analyse seawater samples collected from the Niskin bottles of the CTD, the continuous pCO<sub>2</sub> was analysing sea surface pCO<sub>2</sub> and oxygen was continuously measured in the non-toxic seawater supply. Due to the length of time needed for the analyses, particularly the TIC (30 min per sample), every second station was sampled for the three discrete analyses, apart from the beginning of the cruise (Florida Straits), where almost every station was sampled. TA could not be analysed at the beginning of the cruise due to the instrument not being operational. It was a new system and delivered one week before transport to the cruise, hence setting up this system took until station 15; samples sampled prior to that had been fixed and stored, and were run later during the cruise.

Discrete seawater samples were taken according to Standard Operating Procedure (SOP) 1 outlined in DOE (1994). Reagent bottles of 250ml volume were used for TCO<sub>2</sub> and TA samples, and 500ml volumetric flasks were used for discrete pCO<sub>2</sub>. They were drawn from the Niskin bottles immediately after the oxygen samples were taken. All seawater samples were taken with Tygon tubing into pre-cleaned bottles and flasks. They were rinsed once, filled from the bottom, and overflowed once. Bottles and flasks were stoppered without any gas bubbles entrapped. The samples were fixed by creating a headspace and adding saturated mercuric (II) chloride (HgCl<sub>2</sub>) solution according to DOE (1994). Samples were fixed and stored at room temperature and run within 16 hours of sampling, except for those TCO<sub>2</sub> samples which were stored at 12°C until post-cruise analysis back at the UEA laboratory.

Replicate samples were taken for all discrete analyses from random Niskin bottles at several stations, and run on board for all TA and discrete pCO<sub>2</sub>. TIC replicates of Niskin bottles were analysed on board or stored for analysis back at UEA. Additional replicates were taken from the ship's non-toxic seawater supply and analysed on board.

Table 27.1 lists number of samples taken and analysed on board from either CTD Niskins or the ship's non-toxic seawater supply, including replicates. A total of 4672 samples were taken, 1623 for pCO<sub>2</sub>, 1526 for TA and 1523 for TCO<sub>2</sub>. A total of 4280 samples were analysed on board, 1563 for

pCO<sub>2</sub>, 1501 for TA and 1216 for TCO<sub>2</sub>. A total of 297 fixed TCO<sub>2</sub> samples were stored for analysis back at UEA.

### **27.1 Discrete Total Inorganic Carbon (TCO<sub>2</sub>)**

Total inorganic carbon was analysed by coulometry. The instrument consisted of a coulometer (model 5100, UIC Inc, USA) and a CO<sub>2</sub> extraction unit based on the Single Operator Multiparameter Metabolic Analyzer (SOMMA), developed by Kenneth Johnson (Johnson et al. 1985, 1987, 1993) and modified at UEA.

In this system, all inorganic carbonate is converted to CO<sub>2</sub> (gas) by addition of excess phosphoric acid (1 M, 8.5%) to a calibrated volume of seawater sample. OfN nitrogen gas passed through soda lime to remove any traces of CO<sub>2</sub> is used to carry the evolving CO<sub>2</sub> to the coulometer cell. In the coulometer cell, all CO<sub>2</sub> is quantitatively absorbed forming an acid, which is coulometrically titrated. The coulometer is set to integrate the titration as counts (CTS) and the titration endpoint are set to within 25 CTS per 60 min.

The accuracy of the analysis on board was determined regularly by measuring certified reference material (CRM), supplied by Dr. A. Dickson of Scripps Institution of Oceanography (SIO), Batch #62 (certified TCO<sub>2</sub> value: 2126.46±0.56µmol/kg). A total of 66 CRMs were run (Figure 27.1). The cruise-length average of CRM analyses was 2126.65±2.3µmol/kg.

Standard deviation of replicate TCO<sub>2</sub> analysis is plotted in Figure 27.2 (station 1 was a test station, and station 11 was repeated as station 12, hence used for replicate analysis). The cruise-length standard deviation of Niskin replicate analyses was ±0.5µmol/kg (n=33) and for replicates of the non-toxic supply was ±1.1µmol/kg (n=23).

Post-cruise work will involve the analysis of the stored samples, which could not be analysed on board. A post-cruise calibration of the temperature sensor and the pipette volume will also be done, and the sample results recalculated if necessary.

### **27.2 Discrete Total Alkalinity (TA)**

Total alkalinity was determined by the titration of a calibrated volume of seawater, equilibrated to 25°C, with a strong acid (HCl). The s-shaped titration curve produced by potential of a proton sensitive electrode shows two inflection points, characterizing the protonation of carbonate and bicarbonate, respectively. The acid consumption up to the second point is equal to the titration alkalinity. From this value, the carbonate alkalinity is calculated by subtracting the contributions of

other ions present in the seawater. These concentrations can be derived from the pH and salinity of the sample.

For this analysis, the VINDTA (Versatile INstrument for the Determination of Titration Alkalinity, Marianda, Kiel, Germany) was used. It is an open cell titration system, with sample delivery via a thermostated calibrated pipette. Sample handling and titration is program controlled. The titration is carried out using a Titrino (Model 719 S, Metrohm, Switzerland). The results are calculated using a non-linear curve fitting approach, comparing a calculated curve to the data points and making use of the best-fit coefficients for alkalinity calculation.

A 0.1M solution of hydrochloric acid was made up for the titrations. This acid was made up on board and a sub-sample taken for post-cruise analysis to determine the exact concentration. The correct concentration will then be used to recalculate the results.

The accuracy of the analysis was determined twice daily by measuring Certified Reference Materials (CRM), supplied by Dr. A. Dickson of Scripps Institution of Oceanography (SIO), Batch #62 (certified TA value:  $2338.2 \pm 0.46 \mu\text{mol/kg}$ ). A total of 43 CRMs were run (Figure 27.3). The cruise-length average of CRM analyses was  $2337.8 \pm 1.8 \mu\text{mol/kg}$ .

Alkalinity data was calibrated with CRMs. However, the calculation method is dependent on a realistically estimated ratio of acid factor and pipette calibration, and since the same calibration factor can also be obtained with various combinations of these two parameters, the quality of the curve fit will be different. Therefore a re-calibration of the pipette and exact calculation of the acid factor will be processed post cruise. Changes that would exceed the mean standard deviation of the method are not likely. A number of early stations were analysed using an inaccurate acid factor. These stations have an incorrect concentration at the end of the cruise. Recalculation is required post cruise to enter the correct acid factor and thus obtain a corrected result. The nutrient and salinity data will also be included in the post cruise processing, together with back calculation of rejected samples.

Analysis of replicates taken from Niskin bottles or the ship's non-toxic supply have a standard deviation of  $\pm 1.1 \mu\text{mol/kg}$  and  $\pm 1.5 \mu\text{mol/kg}$  respectively (Figure 27.4).

For the calculation of carbon alkalinity from total alkalinity, the phosphate and silicate alkalinity has to be known. This can be done using the separately determined nutrient concentrations. However, the contribution is low for phosphate about equal to the phosphate concentration (i.e.  $0-3 \mu\text{mol/kg}$  for open ocean waters), and a factor of 10 lower for silicate. Nutrient data was not available immediately during this cruise and therefore not included in the calculations. This will be part of the post-cruise recalculation.

A problem of system blockages was encountered during the mid phase of the cruise. This resulted in pipette emptying problems and incorrect sample volumes. Tubing was renewed to overcome the problem, but a number of stations were affected and the samples were rejected. Stations rejected were 73, 75, 77, 79, 81, 83, 85, and 87. Although these samples have been rejected, back calculation is possible from the values of  $p\text{CO}_2$  and  $\text{TCO}_2$ . This will be carried out in post-cruise reprocessing.

### **27.3 Discrete Partial Pressure of $\text{CO}_2$ (Discrete $p\text{CO}_2$ )**

The partial pressure of  $\text{CO}_2$  in seawater was determined by infrared absorption of  $\text{CO}_2$  in a gas stream that was equilibrated with  $\text{CO}_2$  in a seawater sample at  $15^\circ\text{C}$ . The system was built new at UEA prior to this cruise, its design based on the one described by Waninkhof & Thoning (1993).

A headspace was created in the 500ml volumetric flasks by replacing a volume of seawater with a gas of a  $\text{CO}_2$  concentration close to that of the seawater. Six gas standards (10 litre, BOC, UK) were available with different  $\text{CO}_2$  concentrations: 267.43ppm, 357.35ppm, 479.27ppm, 696.49ppm, 890.54ppm and 1150.11ppm, which had been calibrated against primary NOAA gas standards prior to the cruise. Headspace volumes created in sample flasks ranged from 62 to 84ml, and were measured for each sample. The headspace gas was circulated through the seawater sample and the IR detector (LiCor model 6262, LiCor, Inc., USA) until equilibrium was reached, generally after 20 min, whilst maintaining close to atmospheric pressure within the loop.

The system had two loops, which were used alternatively, saving analysis time by equilibrating one sample, whilst preparing the next. On 02 May 2004, loop 2 failed, and remaining samples were analysed only on loop 1.

All gas standards were run after each 12 to 15 samples, in order to calibrate the LiCor detector. The precision of the analysis was determined by running replicate samples, taken either from Niskin bottles or the ship's non-toxic seawater supply.

### **27.4 Continuous Partial Pressure of $\text{CO}_2$ (Continuous $p\text{CO}_2$ )**

The partial pressure of  $\text{CO}_2$  in surface seawater was determined by infrared absorption of  $\text{CO}_2$  in a gas stream being continuously equilibrated with the  $\text{CO}_2$  of surface seawater. The system used was built new at UEA prior to this cruise, its design based on the one described by Cooper et al (1998).

Seawater from the continuous non-toxic supply of RRS *Discovery* was tee-ed off from a high flow (>50 litres/min) bypass, passed through a strainer and housing containing an oxygen/temperature sensor (Aanderaa model 3930, Aanderaa Instruments AS, Norway), and into a perculator type equilibrator at 5 litres/min. A coulterflow of air was continuously circulated through the equilibrator

and the detector (LiCor model 6262, LiCor, Inc., USA). At least once per hour, the system analysed CO<sub>2</sub> in air, pumped in from the foremast. Gas standards of 267.43ppm, 357.35ppm, and 479.27ppm CO<sub>2</sub> in air were measured throughout the cruise, in order to calibrate the LiCor detector.

Under controlled conditions in the laboratory, and during a pool side international intercomparison in Japan in 2003, the type of instrument used for this cruise gave a precision of  $\pm 0.7$ ppm CO<sub>2</sub>.

Table 27.1: Number of samples taken and analysed during the cruise for the three discrete carbon parameters pCO<sub>2</sub>, TA, and TIC, from either CTD Niskins or the RRS *Discovery*'s non-toxic seawater supply. Numbers sampled include replicates. TIC samples not analysed were stored to be analysed back at UEA.

Station	Samples taken from		pCO <sub>2</sub>		TA		TIC	
	CTD Niskins	non-tox. supply	Sampled	Analysed on board	Sampled	Analysed on board	Sampled	Analysed on board
1	24		20	8			20	13
2	3		3	3	3	2	3	0
3	4		4	4	4	2	4	4
4	5		5	5	5	5	5	5
5	6		6	6	6	5	6	6
6	6		6	6	6	6	6	5
7	7		8	8	7	7	8	8
8	7		7	7	7	7	7	7
9	6		6	6	6	6	6	6
10	5		5	5	5	5	5	5
11	12		12	12			12	10
12	5		5	5	5	5	5	5
13	14		14	14	14	14	14	14
14	16		16	16	16	16	16	16
15	20		20	19	20	0	20	20
16	22		22	22	22	22	22	22
17	23		23	22			23	0
18	24		24	23	24	24	24	24
19	24		24	0			24	0
20	24		24	24	24	24	24	24
22	24		24	24	24	24	24	24
24	24		24	24	24	24	24	24
26	22		22	22	22	22	22	0
29		X	6	6				
29	24		24	24	24	24	24	24
31	23		23	23	23	23	23	23



Station	Samples taken from		pCO <sub>2</sub>		TA		TIC	
	CTD Niskins	non-tox. supply	Sampled	Analysed on board	Sampled	Analysed on board	Sampled	Analysed on board
33		X	6	6				
33	24		24	24	24	24	24	0
35	23		23	22	25	25	23	23
37		X	6	6				
37	24		24	24	24	24	24	24
39		X	6	6				
39	24		24	24	24	24	24	24
41	24		24	24	24	24	24	24
43		X	6	6				
43	24		24	23	24	24	24	24
45		X	12	10	10	9		
45	24		24	24	24	24	24	24
47		X	6	6	5	5		
47	24		24	24	24	24	24	24
49		X	6	6				
49	24		24	24	24	24	24	24
51		X	6	6	10	10		
51	24		24	24	24	24	24	24
53		X	6	6	8	8		
53	24		24	24	24	24	24	24
54		X			15	15		
55		X	6	6				
55	24		24	24	24	24	24	24
57		X			15	15		
57	24		24	23	24	24	24	24
58		X	6	6				
58	1		1	1				
59	23		23	22	23	23	23	23
60		X	6	6				
60	1		1	1				

Station	Samples taken from		pCO <sub>2</sub>		TA		TIC	
	CTD Niskins	non-tox. supply	Sampled	Analysed on board	Sampled	Analysed on board	Sampled	Analysed on board
61		X					4	4
61	24		24	24	28	28	28	26
62		X	6	6				
63	24		24	24	24	24	24	24
65		X	6	6	6	6		
65	24		24	24	24	24	24	24
66		X	6	6				
66	1		1	1				
67	24		24	23	24	24	24	24
69	24		24	23	24	24	24	24
71	24		24	23	24	24	24	24
72		X					10	10
73	24		24	23	24	24	24	24
75	24		24	24	24	24	24	24
77	24		24	24	24	24	24	0
79	24		29	29	29	29	24	24
81	24		24	23	24	24	24	0
83	24		24	24	24	24	24	24
85	24		24	24	24	24	24	0
87	24		24	24	24	24	24	24
89		X	2	2	2	2	2	2
89	24		26	26	26	26	26	26
90		X	5	4	4	4	4	4
91	24		24	24	24	24	24	24
93		X	5	3	5	5		
93	24		26	26	26	26	26	26
95		X			5	5	5	3
95	24		26	26	26	26	26	0
97	24		26	26	26	26	26	24
99	24		26	25	26	26	26	26

Station	Samples taken from		pCO <sub>2</sub>		TA		TIC	
	CTD Niskins	non-tox. supply	Sampled	Analysed on board	Sampled	Analysed on board	Sampled	Analysed on board
101		X	10	9	10	10		
101	24		26	25	26	26	26	26
103	24		26	26	26	26	26	25
105		X			10	10	10	10
105	24		26	26	26	26	27	26
107	24		26	25	26	26	26	25
109	24		26	26	26	26	26	2
111	24		26	26	26	26	26	26
113		X	10	10	10	10		
113	24		26	26	27	27	26	0
115	20		22	20	22	22	22	20
117	21		23	23	21	21	23	22
119	19		21	21	21	21	22	20
121	15		17	16	17	17	17	0
123	12		13	13	13	13	14	0
125	7		8	8	8	8	8	0
Total			1623	1563	1526	1501	1523	1216

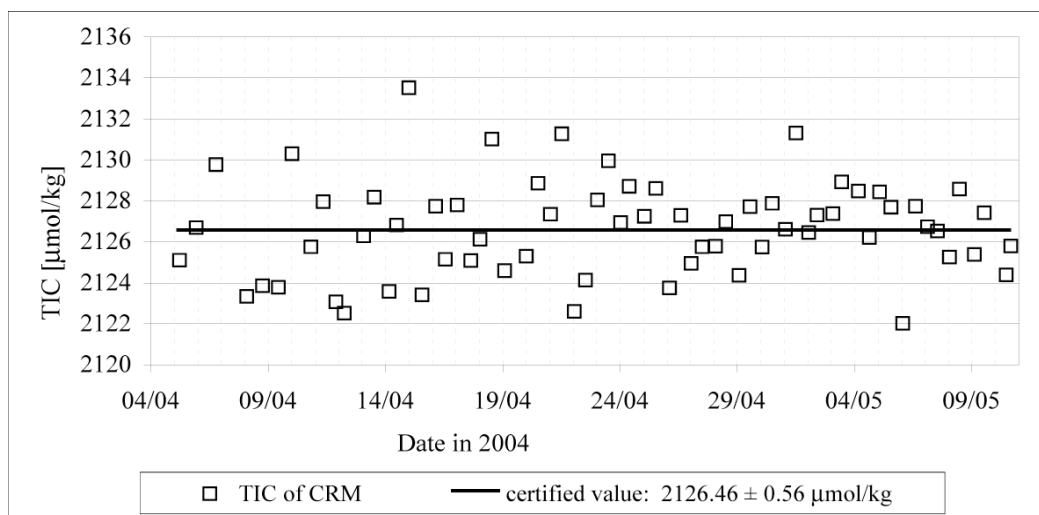


Figure 27.1: Results of the TIC analysis of CRM batch 62 throughout the cruise.

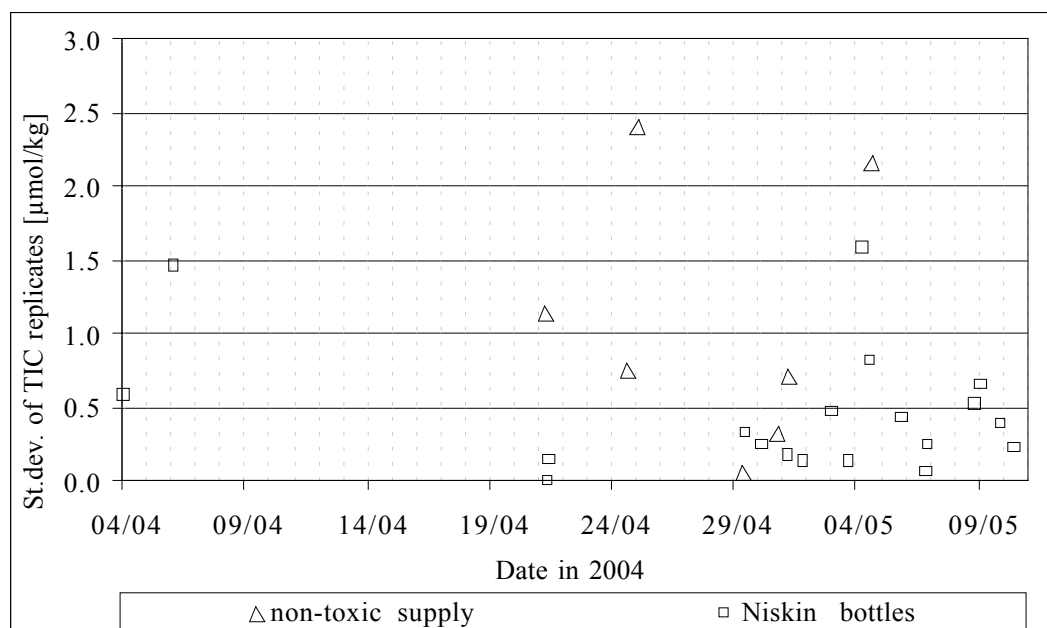


Figure 27.2: Standard deviation of TIC analysis of replicate samples taken from Niskin bottles or the non-toxic seawater supply.

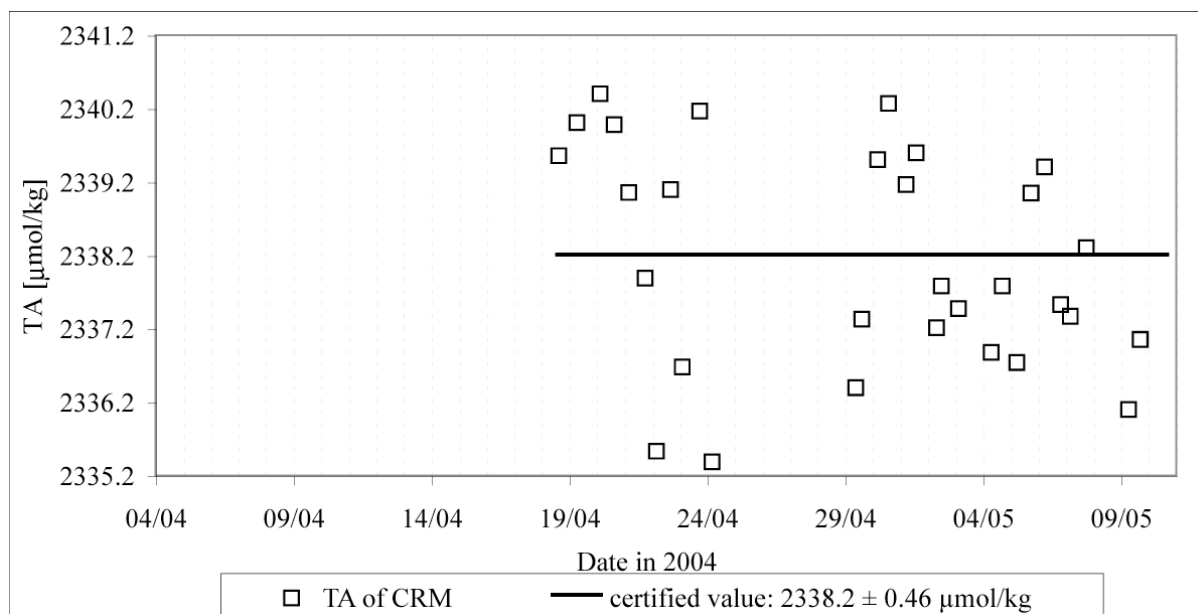


Figure 27.3: Results of the TA analysis of CRM batch 62 from 18 April 2004 onwards. Prior to 18 April, the acid factor used was not correct, and CRM as well as sample values need to be recalculated.

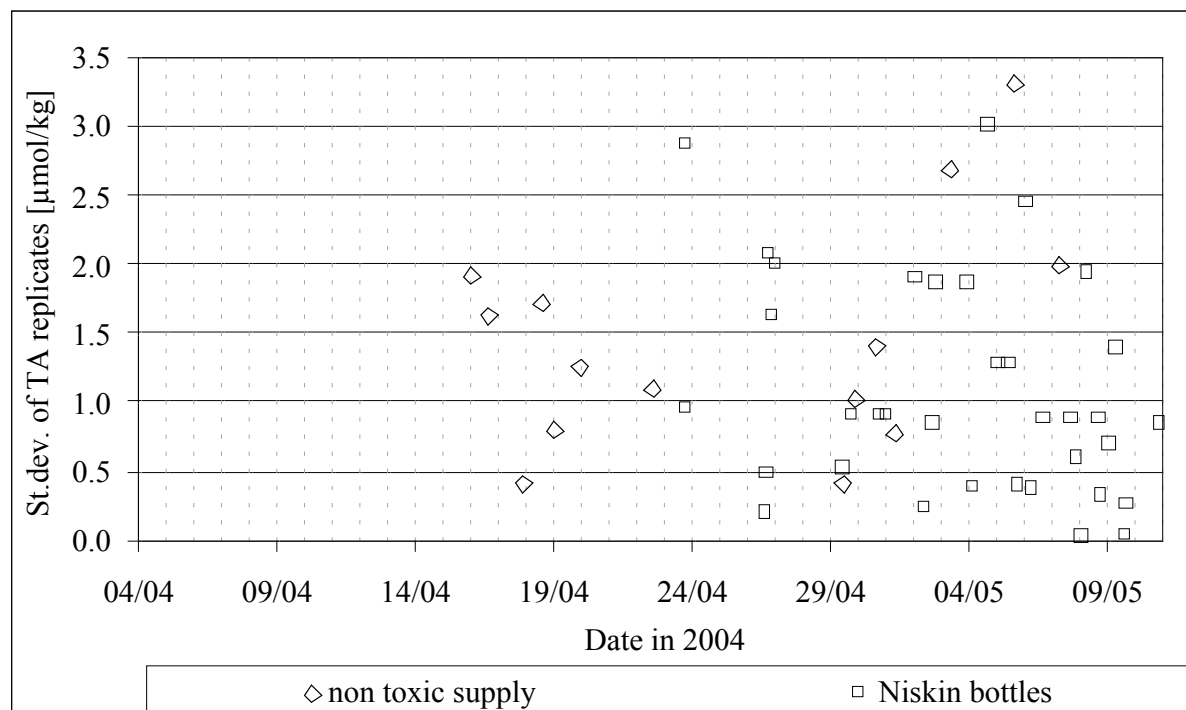


Figure 27.4: Standard deviation of TA analysis of replicate samples taken from Niskin bottles or the non-toxic seawater supply.

## 28. HALOCARBONS

David Cooper and Charlene Grail

Cruise D279 presents an excellent opportunity to measure concentrations of CFC-12, CFC-11, CFC-113, and carbon tetrachloride ( $\text{CCl}_4$ ) from the WOCE reoccupation transect 26-24.5°N (A05). The objective is to provide a high quality data set, and make it available nearly immediately to the community as required by the Global Repeat program. The program is in support of CLIVAR and the Carbon Science Programs, and is a component of a global observing system for the physical climate/ $\text{CO}_2$  system. The data will contribute to documenting and understanding how ventilation and ocean carbon change over time. A number of alternative, although still indirect, means of estimating anthropogenic  $\text{CO}_2$  use CFC data. These will contribute to quantifying the inventory and flux of anthropogenic  $\text{CO}_2$  in the oceans, and to understanding its variability. The 26-24.5° N CFC data from this cruise occupation will fill a zonal gap in a region where CFC inventories are relatively large, and in the west increasing rapidly throughout the water column. Our intention was to sample as extensively as possible.

### 28.1 Sample Collection

Samples were collected from 10 litre Niskin bottles attached to a 24 bottle rosette. The Niskin bottles were refitted with o-rings specially made without grease or solvents to avoid any chance of halocarbon contamination. A water sample was collected directly from the Niskin bottle petcock using a 100ml ground glass syringe which was fitted with a three-way stopcock that allowed flushing without removing the syringe from the petcock. The syringes were stored in a flow-through seawater bath and analyzed within 8 -10 hours after collection.

### 28.2 Analysis

Halocarbon analyses were performed on a gas chromatograph (GC) equipped with an electron capture detector (ECD). Samples are introduced into the GC-EDC via a purge and dual trap system. The samples are purged with nitrogen and the compounds of interest are trapped on a main Porapak N trap held at  $\sim -20^\circ\text{C}$  with a Vortec Tube cooler. After the sample has been purged and trapped for several minutes at high flow, the gas stream is stripped of any water vapor via a magnesium perchlorate trap prior to transfer to the main trap. The main trap is isolated and heated by direct resistance to  $140^\circ\text{C}$ . The desorbed contents of the main trap are backflushed and transferred with helium gas, over a short period of time, to a small volume focus trap in order to improve chromatographic peak shape. The focus trap is also Porapak N and is held at  $\sim -20^\circ\text{C}$  with a Vortec Tube cooler. The focus trap is flash heated by direct resistance to  $155^\circ\text{C}$  to release the compounds of

interest onto the analytical pre-column. The analytical pre-column is held in-line with the main analytical column for the first 3 minutes of the chromatographic run. After 3 minutes, all of the compounds of interest are on the main column and the pre-column is switched out of line and backflushed with a relatively high flow of nitrogen gas. This prevents later eluting compounds from building up on the analytical column, eventually eluting and causing the detector baseline signal to increase.

In total, measurements were made on 129 stations, most of which contained 24 samples, plus one duplicate taken randomly. Every ten measurements were followed by a purge blank and a standard, gas2.09ml. Time permitting, the surface sample was held after measurement and was sent through the process in order to “restrip” it to determine the efficiency of the purging process. In all cases, the restripped sample contained no more concentration of targeted halocarbons than the purge blanks.

### **28.3 Calibration and Precision**

For accuracy, the standard, S43, was cross-calibrated to the SIO-98 absolute calibration scale. A 19 point calibration curve was run every 7-10 days for all four halocarbons. Estimated accuracy is  $\pm 2\%$ . Precision for CFC-12, CFC-11 and CFC-113 is less than 1%; precision for  $\text{CCl}_4$  was approximately 1-2%.

### **28.4 Final Comments**

For the most part, sample collection and measurement were very successful. The three-way stopcock on the syringes made sample collection a simple and rapid procedure. The integration of the computer software with the GC-EDC system hardware made the procedure almost completely automated. A few problems were encountered initially. The analytical column had to be replaced with the spare due to some unknown source of contamination. The focus trap failed and was replaced by a spare trap. The humidity and temperature were a little high in the chemistry lab, thus necessitating daily replacement of the magnesium perchlorate trap, which removed any water vapour from the nitrogen gas stream after purging.

## 29. ATMOSPHERIC SAMPLING

Rhiannon Mather

### 29.1 Aerosol Collection

During this cruise, aerosol samples were collected over roughly a 24-hour period using a high volume aerosol sampler placed on the monkey island of the ship. Filters were changed during the morning, usually between the hours of 8 and 9:30 ship time (ST), corresponding with between 11:00 and 14:00 GMT. The sampler was generally left to run continuously, as the ship was positioned head to wind when on station, therefore reducing the risk of contamination from the chimney stack.

The sampler was switched off each morning for the changing of the filter paper. The filter paper was changed in the fume cupboard of the chemistry lab, as no laminar flow hood was available on the ship. The fume cupboard was rarely used for any other purposes. Filter papers were changed wearing plastic gloves to avoid the risk of sample contamination. Once removed from the cartridge, the filter paper was sealed in a zip lock bag, which was subsequently placed in two further plastic bags (one other sealed) in the freezer. These were stored at -25°C for the remainder of the cruise. Transport of the filter papers between the monkey island and the fume cupboard was carried out in the sampler cartridge covered with an aluminium plate, and subsequently placed into a large plastic zip lock bag. Samples were collected onto Whatman 41 filters.

At the start and end of each sample, the time, position, date, air temperature, pressure, wind direction, wind speed, ship direction, and ship speed were all noted down (Table 29.1). A counter reading within the sampler was unable to be recorded as this failed to work for the entire cruise. As a back up, circular chart recorders were also used. Samples failed to be taken at the start of the cruise on the 5<sup>th</sup> and 6<sup>th</sup> of April. On these days, the aerosol sampler failed to work due to an electrical problem within the instrument. This problem was resolved to commence sampling on the 7<sup>th</sup> April.

Two blanks were also run during the cruise: a cassette blank and an exposure blank. The cassette blank was performed whilst docked in Freeport, Grand Bahama. For this, a filter paper was loaded into the sampler cartridge with the aluminium cover in place, and subsequently placed in a large zip lock bag for 24 hours. This sample was performed in the chemistry lab of the ship. The exposure blank was treated in exactly the same manner as the running of normal samples, with the exception that the sampler was not switched on for the 24 hour duration within which the sample was loaded. The exposure blank was performed on the 4<sup>th</sup> of April on the first leg out of Freeport.



## **29.2 Sample Analysis**

Aerosol samples collected throughout this cruise will be delivered to the University of East Anglia (UEA) Environmental Sciences department for analysis. The samples are expected to be analysed for a number of nutrients, including nitrate, ammonia, silica, phosphate, and sulphate. The concentrations of trace metals such as lead, copper, zinc, nickel, cobalt and cadmium will also be investigated with graphite furnace atomic absorbance spectrometry (GFAAS). This technique has the low detection limits that are required to measure the expected low concentrations. The filter papers are finally to be analysed for the presence of chloride. This is likely to have originated from sea spray, and the potential contamination of the paper can therefore be assessed.

Table 29.1: Aerosol deposition sample start and end location and dates.

Sample Name	Date	Sampling Start		Date	Sampling End	
		Longitude (°W)	Latitude (°N)		Longitude (°W)	Latitude (°N)
Cassette Blank 1	03/04/04			04/04/04		
Exposure Blank	04/04/04	26 54.08	79 09.78	05/04/04	27 00.84	79 23.28
Sample 1	07/04/04	26 02.56	77 50.34	08/04/04	26 29.91	76 40.90
Sample 2	08/04/04	26 29.99	76 40.90	09/04/04	26 29.67	76 26.17
Sample 3	09/04/04	26 29.60	76 25.77	10/04/04	26 30.12	75 56.06
Sample 4	10/04/04	26 29.83	75 53.92	11/04/04	26 31.04	75 04.47
Sample 5	11/04/04	26 31.18	75 04.44	12/04/04	26 30.04	73 55.60
Sample 6	12/04/04	26 29.97	73 55.29	13/04/04	26 29.97	72 29.17
Sample 7	13/04/04	26 29.94	72 29.27	14/04/04	26 29.91	70 59.88
Sample 8	14/04/04	26 29.77	70 59.76	15/04/04	25 21.97	69 54.03
Sample 9	15/04/04	25 21.08	69 52.45	16/04/04	24 31.24	68 21.82
Sample 10	16/04/04	24 30.95	68 18.67	17/04/04	24 29.67	65 53.79
Sample 11	17/04/04	24 29.72	65 49.71	18/04/04	24 30.50	63 25.53
Sample 12	18/04/04	24 30.33	63 21.54	19/04/04	24 29.71	61 28.48
Sample 13	19/04/04	24 29.68	61 24.53	20/04/04	24 29.93	59 25.49
Sample 14	20/04/04	24 29.99	59 21.41	21/04/04	24 30.34	56 58.64
Sample 15	21/04/04	24 30.09	56 54.36	22/04/04	24 29.89	56 54.36
Sample 16	22/04/04	24 29.71	54 43.11	23/04/04	24 30.21	52 38.32
Sample 17	22/04/04	24 3.25	52 38.24	23/04/04	24 30.16	50 49.17
Sample 18	23/04/04	24 30.08	50 45.64	24/04/04	24 29.77	48 46.35

Sampling Start				Sampling End		
Sample Name	Date	Longitude (°W)	Latitude (°N)	Date	Longitude (°W)	Latitude (°N)
Sample 19	24/04/04	24 29.76	48 46.37	25/04/04	24 29.96	46 07.73
Sample 20	26/04/04	24 29.99	46 03.07	27/04/04	24 29.93	43 50.45
Sample 21	27/04/04	24 29.95	43 50.48	28/04/04	24 31.28	41 38.89
Sample 22	28/04/04	24 31.14	41 31.29	29/04/04	24 30 06	39 01 36
Sample 23	29/04/04	24 29 98	38 57 58	30/04/04	24 29 52	36 25 07
Sample 24	30/04/04	24 29 81	36 20 95	01/05/04	24 29 58	33 54 12
Sample 25	01/05/04	24 29 63	33 50 88	02/05/04	24 30 30	31 19 29
Sample 26	02/05/04	24 30 27	31 16 14	03/05/04	24 30 44	28 49 31
Sample 27	03/05/04	24 30 35	28 44 09	04/05/04	24 98 98	25 58 71
Sample 28	04/05/04	24 30 05	25 55 33	05/05/04	24 37 41	23 11 03
Sample 29	05/05/04	24 38 44	23 07 10	06/05/04	25 27 28	20 48 10
Sample 30	06/05/04	25 27 17	20 47 86	07/05/04	25 55 86	19 28 87
Sample 31	07/05/04	25 55 84	19 28 81	08/05/04	26 45 55	16 57 74
Sample 32	08/05/04	26 46 80	16 54 15	09/05/04	27 35 45	14 19 91

## **30. TRIAL FLOAT DEPLOYMENT**

Robin Pascal

Instruments on Argo floats are severely limited by the low data capacity of the standard Argos satellite link. The advent of the Iridium and Orbcomm systems based on low orbit satellite constellations offer the possibility of increasing the data capacity by several orders of magnitude. There is also some interest in recoverable Argo floats. The chances of successfully recovering these would be greatly enhanced by an on-board GPS receiver with a near real time data link to the mother ship.

The float deployed on this cruise is intended to investigate the behaviour of GPS and Iridium on the far from ideal platform of an Argo float using a newly developed marinised and pressure resistant antenna assembly. The float has a plastic body designed to mimic the dynamic behaviour of a surfaced Argo float but cannot dive - the latter restriction enables a very large battery capacity sufficient for many months of transmission every four hours. Initial indications are that the Iridium transmitter is performing well but the GPS much less so, probably because the GPS is unable to receive digital data with sufficient continuity.

### **30.1 Deployment Details**

The float was deployed immediately following a CTD cast with the ship steaming slowly forwards. No problems were experienced during the deployment and the float appeared to be floating at the expected level just below the end cap. Deployed on day 120 at 15:30 hrs GMT, 24° 30' N, 38° 32' W.

## 31. DISSOLVED OXYGEN MICROELECTRODE SENSOR

Robin Pascal

A new dissolved oxygen sensor is being developed within OED. The sensor is based on a platinum microdisc (25  $\mu\text{m}$  diameter) working electrode and a copper counter electrode. The advantage of this type of sensor compared to those commercially available is that it has the potential to have a very fast response time (fractions of a second) and should not suffer from hysteresis due to temperature and pressure effects.

Previous experience with the sensor has shown that it is sensitive to fluctuations in the flow across the head. A new head arrangement has been designed so that the electrode sits within a chamber through which water is pumped periodically. Oxygen measurements are made while there is no flow. Due to the pumps construction it is mounted in a separate oil filled pressure balanced housing. A major objective of the current trial was to ascertain that the new flow head and pump arrangement was robust enough to work under pressure and to withstand depths down to 5000 m. If so, it was hoped that the new arrangement would reduce the noise in the data caused by the motion of the CTD through the water.

### 31.1 CTD Deployments

The sensor was installed within the CTD frame prior to cast 93. Unfortunately, on power-up it became clear that it had been incorrectly wired. This resulted in the pump circuit being damaged, which resulted in only 2 pumps per cycle rather than the usual 5 being performed from then on. With the wiring corrected, subsequent tests on deck showed the sensor to be working correctly and that data were being successfully acquired by the Seabird CTD. However, as soon as the CTD entered the water the sensor output went full scale and stayed there for the entire profile. Different sensor setups and gains were tried but with little improvement. It was concluded that the various metals (e.g. zinc) contained in the CTD frame and in the other instruments were pulling the oxygen sensor's measurement potential away from its correct setting. Adjustments were made for this and significant improvements were seen. The sensor was removed from the CTD frame for the deep stations (greater than 5000 m) and was later re-installed on CTD cast 109. For this and subsequent casts the sensor was mounted on the fin, rather than within the frame, to try to minimise unwanted electropotential effects. This resulted in significant improvement but the measurement potentials still needed to be shifted significantly from their design settings. Despite this, after some minor modifications to the inlet, the sensor performed very well and produced encouraging profiles (Figure 31.1). The calibration for the sensor was based on the bottle sample data (below). The profiles in Figure 31.2 have been adjusted to

allow for an approximate 2 minute delay in the sensor response. This delay may be partly due to the reduced number of pumping cycles not completely flushing the flow head in one cycle.

### 31.2 Bottle Sample Measurements

During the deep stations, when deployment of the sensor on the CTD was not possible, a second sensor was used to measure the dissolved oxygen levels in the water bottle samples. A suitable head was chosen which could be fully inserted into a standard oxygen water sample jar. Samples from the CTD bottles were then measured and the results compared to those of the independent oxygen titrations. Initially, the oxygen results were calculated using the temperatures recorded for the titrations. However, these temperatures proved rather inaccurate and the errors in temperature resulted in large apparent errors in the calculated oxygen values. A thermometer was therefore obtained in order to make direct measurements: this significantly improved the quality of the oxygen results.

The main aim of performing the bottle sample measurements was to detect any drift in the sensor calibration. In 3 out of 12 of the casts sampled the sensor showed temporary calibration jumps. The reason for this is not yet known but intermittent use of the sensor in this fashion is far from ideal. Despite this, the results were generally in very good agreement with the oxygen titration results (Figure 32.2) and no calibration drift was detected between casts.

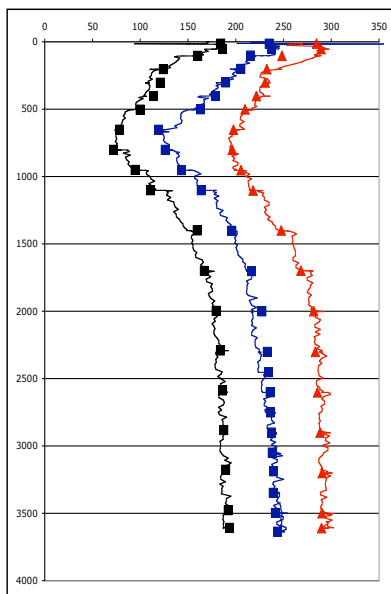


Figure 31.1: Three up casts from the microelectrode oxygen sensor plotted with oxygen titration values. The same calibration is applied to all three profiles. Black cast 115 (offset  $-50 \mu\text{moles}$ ). Blue cast 116. Red Cast 117 (offset  $+50 \mu\text{moles}$ ).

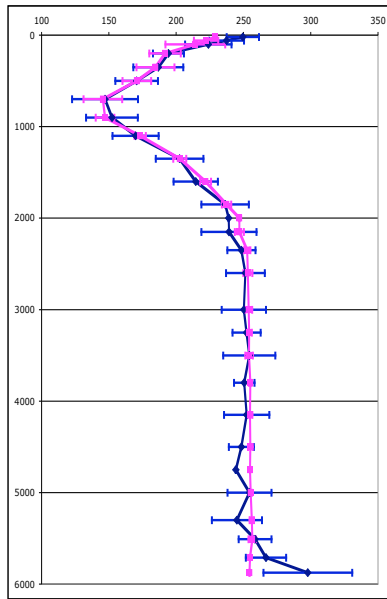


Figure 31.2: The average of 5 profiles (blue) made up from discrete samples taken from the CTD water bottles are plotted with the average of the same 5 profiles of oxygen titrations (pink). Error bars indicate the standard deviation of the data.

## 32. REFERENCES

- Arbic, B.K. & Owens, W.B. 2001. Climate warming of Atlantic Intermediate waters. *Journal of Climate* **14** (20): 4091-4108.
- AutoFlux group. 1996. AutoFlux - an autonomous system for monitoring air-sea fluxes using the inertial dissipation method and ship mounted instrumentation. Proposal to MAST research area C - Marine Technology, 38 pp. + appendices.
- Broecker, W.S. & Denton, G.H. 1989. The role of ocean-atmosphere reorganizations in glacial cycles. *Geochim Cosmochim Acta* **53**: 2465-2501.
- Bryden, H.L. 2003. RRS Charles Darwin Cruise 139, 01 MAR - 15 APR 2002, Trans-Indian Hydrographic Section across 32°S, pp. 122, Southampton Oceanography Centre, Southampton.
- Bryden, H.L., Griffiths, M.J., Lavin, A.M., Millard, R.C., Parrilla, G. & Smethie, W.M. 1996. Decadal changes in water mass characteristics at 24°N in the subtropical North Atlantic Ocean. *Journal of Climate* **9** (12): 3162-3186.
- Bryden, H.L. & Imawaki, S. 2001. Ocean Heat Transport, in *Ocean Circulation & Climate: Observing and Modelling the Global Ocean*. (eds) Siedler, G., Church, J. & Gould, J. pp. 715, Academic Press, San Diego, San Francisco, New York, Boston, London, Sydney, Tokyo.
- Bryden, H.L., Johns, W.E. & Saunders, P.M. 2004. Deep Western Boundary Current east of Abaco: Mean structure and transport. *J. Mar. Res.*, submitted.
- Cooper, D.J., Watson, A.J. & Ling, R.D. 1998. Variation of pCO<sub>2</sub> along a North Atlantic shipping route (UK to the Caribbean): A year of automated observations. *Marine Chemistry* **60**: 147-164.
- Cunningham, S.A. 2005. RRS *Discovery* Cruises 277 (26 MAR - 16 APR 2004) and 278 (19 MAR - 30 MAR 2004): RAPID Mooring Cruise Report, pp. 150, Southampton Oceanography Centre, Southampton.
- Dansgaard, W. 1993. Evidence for general instability of past climate from a 250-kyear ice-core record. *Nature* **364**: 218-220.
- Dickson, A.G. 1994. Determination of dissolved oxygen in seawater by Winkler titration. WOCE operations manual, WOCE Report 68/91 Revision 1 November 1994.
- DOE. 1994. Handbook of methods for the analysis of the various parameters of carbon dioxide system in sea water; version 2, (eds) Dickson, A.G. & Goyet, C. ORNL/CDIAC-74.



- Fillenbaum, E.R., Lee, T.N., Johns, W.E. & Zantopp, R.J. 1997. Meridional heat transport variability at 26.5°N in the North Atlantic. *J. Phys. Oceanography* **27** (1): 153-174.
- Fuglister, F.C. 1960. Atlantic Ocean atlas of temperature and salinity profiles and data from the International Geophysical Year of 1957-1958, 209 pp., Woods Hole Oceanographic Institution, Woods Hole.
- Ganachaud, A. 2003. Large-scale mass transports, water mass formation, and diffusivities estimated from World Ocean Circulation Experiment (WOCE) hydrographic data. *J. Geophys. Res.* **108** (C7): 3213, doi: 10.1029/2002JC001565.
- Ganachaud, A. & Wunsch, C. 2000. Improved estimates of global ocean circulation, heat transport and mixing from hydrographic data. *Nature* **408** (6811): 453-457.
- Hall, M.H. & Bryden, H.L. 1982. Direct estimates and mechanisms of ocean heat transport. *Deep Sea Research* **29** (3A): 339-359.
- Johnson K.M., King, A.E. & Sieburth, J.M. 1985. Coulometric TCO<sub>2</sub> analyses for marine studies; an introduction. *Marine Chemistry* **16**:61-82.
- Johnson, K.M., Williams, P.J.leB., Brändström, L. & Sieburth, J.M. 1987. Coulometric TCO<sub>2</sub> analysis for marine studies: automation and calibration. *Marine Chemistry* **21**: 117-133.
- Johnson, K.M., Wills, K.D., Butler, D.B., Johnson W.K. & Wong, C.S. 1993. Coulometric total carbon dioxide analysis for marine studies: maximising the performance of an automated continuous gas extraction system and coulometric detector. *Marine Chemistry* **44**: 167-187.
- Josey, S.A., Pascal, R.W., Taylor, P.K. & Yelland, M.J. 2002. A new formula for determining the atmospheric longwave flux at the ocean surface at mid-high latitudes. In press JGR-Oceans.
- Kirkwood, D.S. 1995. Nutrients: Practical notes on their determination in seawater. ICES Techniques in Marine Environmental Science report 17, International Council for the Exploration of the Sea, Copenhagen. 25p. ISSN 0903-2606.
- Lee, T.N., Johns, W., Schott, F. & Zantopp, R. 1990. Western boundary current structure and variability east of Abaco, Bahamas at 26.5°N. *J. Phys. Oceanography* **20**: 446-466.
- Lee, T.N., Johns, W.E., Zantopp, R.J. & Fillenbaum, E.R. 1996. Moored observations of western boundary current variability and thermohaline circulation at 26.5°N in the subtropical North Atlantic. *J. Phys. Oceanography* **26**: 962-983.

- Mantyla, A.W. 1994. The treatment of inconsistencies in Atlantic deep water salinity data. *Deep Sea Research* **41(9)**: 1387-1405.
- McTaggart, K.E., Johnson, G.C., Fleurant, C.I., Baringer, M.O. 1999. CTD/O<sub>2</sub> measurements collected on a Climate and Global Change cruise along 24°N in the Atlantic Ocean (WOCE Section A6) during January-February 1998, Pacific Marine Environmental Laboratory, Seattle.
- Parilla, G., Garcia, M., Bryden, H. & Millard, R. 1994. Informe de la Campana HE06 (A-5, WOCE, 1992), pp. 110p, Inst. Esp. de Oceanog., Madrid.
- Pascal, R.W. & Josey, S.A. 2000. Accurate radiometric measurement of the atmospheric longwave flux at the sea surface. *J. Atmos. Oceanic Technol.* **17(9)** : 1271-1282.
- Rahmstorf, S. & Ganopolski, A. 1999. Long-term global warming scenarios computed with an efficient coupled climate model. *Climatic Change* **43(2)**: 353-367.
- Roemmich, D. & Wunsch, C. Two transatlantic sections: meridional circulation and heat flux in the subtropical North Atlantic Ocean. *Deep Sea Research* **32(6)**: 619-664.
- Saunders, P.M., 1986. The accuracy of measurement of salinity, oxygen and temperature in the deep ocean. *J. Phys. Oceanography* **16**: 189-195.
- Sea-Bird. 2004. SBE 35 Temperature Sensor, Deep Ocean Standards Thermometer, Configuration and Calibration Manual, SEA-BIRD ELECTRONICS, INC., Bellevue, Washington 98005, USA.
- Smith, S. D. 1988. Coefficients for Sea Surface Wind Stress, Heat Flux and Wind Profiles as a Function of Wind Speed and Temperature. *J. Geophys. Res.* **93**: 15467-15474.
- Tavener, J.P. 2001. Gallium Apparatus Model 17402B Includes Gallium Cell Model 17401, pp. 18, Isothermal Technology Limited, Southport.
- Vellinga, M. & Wood, R.A. 2002. Global climate impacts of a collapse of the Atlantic thermohaline circulation. *Climatic Change* **54(3)**: 251-267.
- Visbeck, M. 2002. Deep velocity profiling using lowered acoustic doppler current profilers: bottom track and inverse solutions. *J. Atmos. Oceanic Technol.* **19(5)**:794-807.
- Wanninkhof, R. & Thoning, K. 1993. Measurement of fugacity of CO<sub>2</sub> in surface water using continuous and discrete methods. *Marine Chemistry* **44**: 189-204.

- Yelland, M.J., Moat, B.I., Taylor, P.K., Pascal, R.W. Hutchings, J. & Cornell, V.C. 1998. Wind stress measurements from the open ocean corrected for airflow disturbance by the ship. *J. Phys. Oceanography* **28**: 1511 - 1526.
- Yelland, M.J., Moat, B.I., Pascal, R.W. & Berry, D.I. 2002. CFD model estimates of the airflow distortion over research ships and the impact on momentum flux measurements. *J. Atmos. Oceanic Technol.* **19**: 1477-1499.
- Yelland M.J. & Pascal, R.W. 2003. Measurement and parameterisation of the air-sea fluxes of CO<sub>2</sub> and H<sub>2</sub>O. Proposal to the Southampton Oceanography Centre Technology Innovation Fund.